

Individualized conditional independence testing under model-X with heterogeneous samples and interactions

Matteo Sesia*, Tianshu Sun*

May 19, 2022

Abstract

Model-X knockoffs and the conditional randomization test are methods that search for conditional associations in large data sets, controlling the type-I errors if the joint distribution of the predictors is known. However, they cannot test for interactions nor find whether an association is only significant within a latent subset of a heterogeneous population. We address this limitation by developing an extension of the knockoff filter that tests conditional associations within automatically detected subsets of individuals, provably controlling the false discovery rate for the selected hypotheses. Then, under the additional assumption of a partially linear model with a binary predictor, we extend the conditional randomization test as to make inferences about quantiles of individual effects that are robust to sample heterogeneity and interactions. The performances of these methods are investigated through simulations and with the analysis of data from a randomized blood donation experiment with several treatments.

1 Introduction

1.1 Background and motivation

Many contemporary data sets, whether observational or collected from randomized experiments, gather numerous variables, many of which may be irrelevant or redundant. Making sense of such information is challenging, especially if reliable models for the outcome of interest are a-priori unavailable and the samples are heterogeneous, either because the individuals have diverse covariates or because their outcomes follow different underlying models. For instance, genome-wide associations studies measure hundreds of thousands of genetic variations across the genomes of many people [1], who may follow opposite lifestyles and descend from various ancestral groups [2], with the goal of gaining a better understanding of the genetic roots of heritable diseases or explaining observed variations in medically relevant traits. In those applications, it is useful to cull the observed variables to a subset of promising predictors that are likely to have a meaningful and potentially causal association with a phenotype of interest, while controlling the rate of false positives [3]. Similar problems arise in many other fields; for example, e-commerce and social media companies have access to a vast trove of data [4], and they may be able to observe customer behaviour in response to randomized interventions [5, 6]. Careful statistical analyses can convert these data into valuable knowledge, and the framework proposed by [7] provides two powerful and versatile methods—the model-X knockoff filter and the conditional randomization test (CRT)—that address this challenge by rigorously seeking significant conditional associations. However, the interpretation of their findings is complicated by possible sample heterogeneity and unknown interactions, and addressing those issues requires novel tools.

*Department of Data Sciences and Operations, University of Southern California, Marshall School of Business.

The attractiveness of model-X inference mainly stems from its ability to leverage powerful machine learning algorithms and provide finite-sample guarantees under the sole assumption that the distribution of the explanatory variables is known. This assumption is not always easily justified, and some applications may demand substantial approximations for model-X techniques to be deployed [7, 8], but there are examples for which their framework fits very well. In particular, the joint distribution of genotypes in genetic association studies is realistically approximated by hidden Markov models that lend themselves well to model-X testing [9]. In the case of familial studies involving both parents and their offspring, the genetic data can be seen as obtained from a well-understood randomized experiment carried out by nature, and this even allows a rigorous causal interpretation to be conferred to model-X inferences [10]. Further, the model-X framework is also intuitive in other contexts, including in the analysis of data from complex randomized experiments.

Modern randomized experiments sometimes involve many treatment variables whose joint distribution is complex and may depend on high-dimensional covariates [11–15]. An example involving social networks is the display of “things in common” to encourage friendship formation [15]. There, users who hover on the profile of another user are randomly shown some of their shared features (e.g. attended the same school, expressed similar interests, etc.), with the goal to discover which interventions promote new connections. In e-commerce, customers may be recommended products among those that are similar to their past purchases or consistent with their browsing histories. In healthcare, various combinations of different medications may exist, but the viable options for each patient are constrained by their particular symptoms, clinical history, and other factors. Therefore, *marginal* associations derived from univariate analyses of these data may be misleading. At the same time, classical multivariate analyses rely on parametric models that may be difficult to justify if the phenomena under study are poorly understood. By contrast, the model-X framework does not require unrealistic assumptions in this setting to discover associations with a precise causal meaning [10].

An open challenge is to account for sample heterogeneity. Existing model-X methods are designed to test whether an outcome is independent of a predictor, conditional on the other available variables, *at the population level*, but this is not always fully satisfactory. In fact, even assuming the possibility of assigning a causal meaning to a conditional association, not everyone in the population may be equally impacted by that variable. Imagine that only people with a rare genetic variant respond to a medication intended to lower blood pressure. As long as the sample size is sufficiently large, a statistical test may detect this medication is associated with changes in blood pressure. Yet, such findings may not be very helpful if the interaction with the genetic variant is ignored. Similarly, marketing researchers may be pleased to discover that an online advertisement for replacement iPhone screens influences the sales of said product, but it would also be valuable for them to know this advertisement only affects the behaviour of users who recently visited the Apple App Store. The ability to discover such *individualized* associations would be especially useful when dealing with heterogeneous populations in which subsets of individuals have disparate features and may respond incongruously to a treatment. For example, people with diverse ancestries do not all have the same allele frequencies, and even if the likelihood of the phenotype given all relevant variables is assumed to be universal [16], interactions can result in some variants having large effects for some groups while being practically useless for others.

A second open challenge related to sample heterogeneity in model-X inference involves the *estimation* of the direction and strength of conditional associations. Estimates of this kind may carry useful information in addition to that produced by *tests* of independence, but the problem is difficult to even define clearly in a fully non-parametric setting. If one focuses on a single variable of interest (i.e., the “treatment”) and accepts the relatively mild additional assumption of a partially linear model [17] for the outcome, the CRT of [7] can be adapted and inverted to construct intuitive confidence intervals for the linear “treatment” effect. Unfortunately, confidence intervals thus obtained are generally delicate [18] and may lead to very unreliable estimates if the individual treatment effects are heterogeneous.

1.2 Preview of our contributions and related work

First, this paper builds upon model-X [7] knockoffs [19]. Prior work studied the construction of knockoffs [8, 9, 20], robustness to model mis-specification [21], and power [22–25], while we address sample heterogeneity: aiming to automatically identify relatively homogeneous groups of individuals among which a variable is conditionally associated with the outcome, controlling the false discovery rate for the hypotheses thus selected. Our solution is flexible and can take advantage of any machine learning model without naive data splitting, which would unnecessarily reduce power. Although the idea is versatile, we focus concretely on discovering interactions. There are numerous other works dealing with interactions [26–28] and sample heterogeneity [29–31] in regression and causal inference, but they tend to rely on different assumptions and provide different guarantees compared to our model-X finite-sample framework. Of particular interest are the models and algorithms designed to estimate individual treatment effects [32–40]; our proposal can leverage any of those while producing rigorous finite-sample inferences. This paper is more closely related to [41], which utilizes knockoffs to analyze data collected from different sources, or *environments*, arguing that robust conditional associations are relatively good proxies for causal inferences. However, [41] considers each individual as preassigned to a distinct and *known* population, and it cannot test for interactions. By contrast, we output selective inferences for suitable data-driven hypotheses. While we analyze data from a randomized experiment in this paper, the methodology is general and relevant to many other applications [42–48].

Second, this paper extends the CRT [7] to make inferences about quantiles of individual effects that are robust to sample heterogeneity, in a partially linear model with a binary “treatment” variable. In particular, our modified CRT can be inverted to construct confidence bounds for quantiles of individual effects. On top of the novel emphasis on sample heterogeneity, this research is original in that it extends the CRT from the domain of non-parametric conditional independence testing to that of semi-parametric estimation. Indeed, prior work on the CRT did not explore the estimation of “treatment” effects, partly due to the need for additional assumptions. Further, inverting a randomization test can be problematic [18, 49], and we confirm empirically the limitations of a naive approach to this task in the presence of heterogeneity. Our solution is inspired by the recent work of [50], which studied univariate permutation tests and Fisher’s exact test [51]. Finally, this work is related to [52], which studied the computation of fast and powerful CRT statistics.

1.3 Basic notation and setup

Consider a data set with n individual samples of $(X^{(i)}, Y^{(i)}, Z^{(i)})$, where $X^{(i)} = (X_1^{(i)}, \dots, X_p^{(i)}) \in \mathbb{R}^p$ describes p variables, $Y^{(i)} \in \mathcal{Y}$ is an outcome of interest, taking values in some continuous or discrete set $\mathcal{Y} \subset \mathbb{R}$, and $Z^{(i)} = (Z_1^{(i)}, \dots, Z_m^{(i)}) \in \mathbb{R}^m$ contains m covariates. Depending on the application, X may be a vector of randomized treatments or a subset of the observational covariates. In any case, the joint distribution of X conditional on the other covariates is known, or at least assumed to be well-approximated, and the goal is to discover distinct association between the variables in X and the outcome of interest. In general, the model-X framework of [7] is concerned with testing conditional independence in a non-parametric setting, but if the data are collected from a randomized experiment with fully known design and perfect compliance, its output can also provide rigorous causal inferences [10], as we shall discuss in more detail later. Throughout this paper, we let $\mathbf{X} \in \mathbb{R}^{n \times p}$, $\mathbf{Y} \in \mathbb{R}^{n \times 1}$, and $\mathbf{Z} \in \mathcal{Y}^{n \times m}$ be the matrices collecting the data for all individuals. Their joint distribution can be factored as $P_{X,Y,Z}(\mathbf{X}, \mathbf{Y}, \mathbf{Z}) = P_Z(\mathbf{Z}) \cdot P_{X|Z}(\mathbf{X} \mid \mathbf{Z}) \cdot P_{Y|X,Z}(\mathbf{Y} \mid \mathbf{Z}, \mathbf{X})$, where P_Z is irrelevant because \mathbf{Z} will be treated as fixed, $P_{X|Z}$ is assumed to be known, and $P_{Y|X,Z}$ is the target of inference, which may be arbitrary and completely unknown. Finally, we imagine different individuals are independent of one another, but this simplifying assumption could be relaxed at the cost of more involved calculations if the sample dependencies are known [16].

2 Individualized conditional testing

2.1 A review of conditional testing with knockoffs

The original conditional testing problem in [7] can be thought of as testing, for any $j \in [p]$, the hypothesis of no association between Y and X_j given X_{-j}, Z , where X_{-j} denotes all explanatory variables excluding X_j :

$$\mathcal{H}_{0,j} : Y \perp\!\!\!\perp X_j \mid X_{-j}, Z. \quad (1)$$

If the values of X and Z are determined before that of Y , and X is a randomized treatment conditionally independent of any relevant unmeasured variables, then rejecting (1) is equivalent to making a causal inference; see Appendix A1.1 and Figure A1 for details. In any case, the rejection of (1) can be informative even without causal inferences. For example, if one assumed (which we do not do here) a generalized linear model for $Y \mid X, Z$, then (1) would essentially amount to stating the linear coefficient for X_j is zero [7].

The methodology of model-X knockoffs [7] is designed to simultaneously test $\mathcal{H}_{0,j}$ in (1) for all variables $j \in [p]$ while controlling the false discovery rate [53] below any desired level $\alpha \in (0, 1)$. Recall that the false discovery rate is the expected proportion of true null hypotheses among those rejected:

$$\text{FDR} = \mathbb{E} \left[\frac{|\{j \in [p] : \mathcal{H}_{0,j} \text{ is rejected}\} \cap \{j \in [p] : \mathcal{H}_{0,j} \text{ is true}\}|}{|\{j \in [p] : \mathcal{H}_{0,j} \text{ is rejected}\}| \vee 1} \right] \leq \alpha, \quad (2)$$

where $a \vee b = \max\{a, b\}$. This is a particularly meaningful error rate if the number of tested variables is large and many of them are expected to be non-null.

Model-X knockoffs, which we denote as \tilde{X} , are synthetic variables created by the statistician as a function of X and Z , without looking at Y . By design, knockoffs are conditionally independent of Y given X, Z , but they are exchangeable with X in the joint distribution of $(X, \tilde{X}) \perp\!\!\!\perp Z$. That is, if $[\mathbf{X}, \tilde{\mathbf{X}}] \in \mathbb{R}^{n \times 2p}$ is the matrix obtained by concatenating $\mathbf{X} \in \mathbb{R}^{n \times p}$ with the corresponding $\tilde{\mathbf{X}} \in \mathbb{R}^{n \times p}$ and, for any $j \in \{1, \dots, p\}$, the matrix $[\mathbf{X}, \tilde{\mathbf{X}}]_{\text{swap}(j)}$ is obtained by swapping the j -th column of \mathbf{X} with the j -th column of $\tilde{\mathbf{X}}$, then

$$[\mathbf{X}, \tilde{\mathbf{X}}]_{\text{swap}(j)} \mid \mathbf{Z} \stackrel{d}{=} [\mathbf{X}, \tilde{\mathbf{X}}] \mid \mathbf{Z}, \quad \forall j \in [p]. \quad (3)$$

Hence, swapping any X_j with \tilde{X}_j does not alter the joint distribution of $[\mathbf{X}, \tilde{\mathbf{X}}]$ given \mathbf{Z} . In fact, the only meaningful difference between X_j and \tilde{X}_j may be the lack of conditional association of the latter with Y , and this is what makes knockoffs useful to test (1). Constructing knockoffs that satisfy (3) requires knowing $P_{X|Z}$, but it is a well-studied problem for which exact solutions are available [7–9, 20].

Knockoffs serve as negative control variables within a model predicting Y given X, \tilde{X} and Z , from which one computes importance measures T_j and \tilde{T}_j for each X_j and \tilde{X}_j , respectively. Any model can be employed for this purpose, as long as swapping X_j with \tilde{X}_j only results in T_j being swapped with \tilde{T}_j [7]. A popular choice is to fit a sparse generalized linear model (e.g., the lasso [54]) and define the importance measures as the absolute values of the (scaled) regression coefficients for X and \tilde{X} , respectively, after tuning the regularization via cross-validation. Then, T_j and \tilde{T}_j are combined pairwise for each j into an anti-symmetric statistic W_j , such as $W_j = T_j - \tilde{T}_j$. This ensures the signs of the W_j 's are mutually independent coin flips for all j corresponding to a true $\mathcal{H}_{0,j}$, while larger and positive values provide evidence against the null in (1). More precisely, letting $\epsilon \in \{-1, +1\}^p$ be a random vector such that $\epsilon_j = +1$ if $\mathcal{H}_{0,j}$ is false and otherwise $\mathbb{P}[\epsilon_j = +1] = 1/2$, independently of everything else, then W satisfies a *coin-flip* property [7]:

$$W \mid \mathbf{Z} \stackrel{d}{=} W \odot \epsilon \mid \mathbf{Z}, \quad (4)$$

where \odot indicates element-wise multiplication. Intuitively, the sign of each W_j may be seen as a conservative p-value for $\mathcal{H}_{0,j}$: $p_j = 1/2$ if $W_j > 0$ and $p_j = 1$ otherwise [19]. Finally, a rejection rule for the hypotheses in (1) can be obtained by applying a sequential testing procedure to these independent p-values, in the order given by the absolute values of W [19]. As each of these p-values only contains a single bit of information, an appropriate sequential testing procedure is the knockoff filter (or selective SeqStep+ test) of [19], which computes an adaptive significance threshold for W_j controlling the false discovery rate in finite samples.

2.2 Individualized conditional hypotheses for heterogeneous populations

Conditional testing as described above can be a useful first step to identify interesting variables among a large number of candidates, but it is not fully satisfactory. In fact, rejecting $\mathcal{H}_{0,j}$ in (1) informs us that X_j may have *some* conditional association with Y in the population, but it sheds no light on the possible heterogeneity of this relation across different individuals. Consider for example a population following a simple mixture distribution, in which approximately half of the individuals have $Z_1 = 1$ while the others have $Z_1 = 0$. Suppose X_1 has a positive effect β_1 on Y , following a linear model with standard Gaussian noise, but only if it interacts with $Z_1 = 1$; otherwise, it has no effect whatsoever. That is, $Y \sim \mathcal{N}(Z_1 X_1 \beta_1, 1)$. For simplicity, imagine all other variables are independent standard Gaussian noise. Then, the hypothesis in (1) is true if and only if $\beta_1 = 0$; see [7]. Thus, testing $\mathcal{H}_{0,j}$ may be helpful to distinguish X_1 from the other variables, but it informs us about neither the specific interaction between X_1 and Z_1 , nor the general presence of population heterogeneity. This motivates a more flexible testing methodology that can reliably discover associations holding for more specific subsets of the population. Continuing with the previous example, our method will be able to report that X_1 is associated with Y if $Z_1 = 1$, and that no evidence of association is found if $Z_1 = 0$. Crucially, there will be no need to know in advance that X_1 interacts with Z_1 .

As in the previous section, let \mathbf{X} , \mathbf{Y} , and \mathbf{Z} indicate the data matrices whose rows contain the observations of X , Y , Z , respectively. Let $\tilde{\mathbf{X}} \in \mathbb{R}^{n \times p}$ indicate a matrix of valid knockoffs for \mathbf{X} , which we assume to have been generated with existing techniques [7–9, 20]. For convenience, we will sometimes refer to the knockoff-augmented data as $\mathcal{D} = (\mathbf{X}, \tilde{\mathbf{X}}, \mathbf{Y}, \mathbf{Z})$. Fix any $j \in [p]$ and take any given partition ψ_j of the covariate space \mathbb{R}^m into G disjoint regions, each identifying a distinct *group* of individuals. Note that the number of regions G may in principle also depend on j , but for now we ignore that eventuality as it would complicate the notation. Consider testing whether Y is conditionally independent of $X_j \mid Z, X_{-j}$, within the sub-population mapped into a specific group $g_j \in [G]$. In other words, we will test the conditional hypothesis

$$\mathcal{H}_{0,j}^{(g_j)} : Y^{(g_j)} \perp\!\!\!\perp X_j^{(g_j)} \mid X_{-j}^{(g_j)}, Z^{(g_j)}, \quad (5)$$

for some $j \in [p]$ and $g_j \in [G]$. Above, $(X^{(g_j)}, Y^{(g_j)}, Z^{(g_j)})$ denotes a sample from $P_{X,Y,Z}^{(g_j)}$: the conditional distribution obtained by restricting $P_{X,Y,Z}$ on $\{z \in \mathbb{R}^m : \psi_j(z) = g_j\}$. If we look at (5) for all possible $j \in [p]$ and $g_j \in [G]$, we find ourselves with a multiple testing problem with mG hypotheses, for which we wish to control the false discovery rate. If $G = 1$, this reduces to the original conditional testing problem in (1). In general, however, a rejection of (1) is not as informative as one of (5), because the latter null hypothesis is implied by the former but the converse is not true. In particular, rejecting (5) can narrow down the effect of X_j to the individuals in group g_j and, as discussed below, it can help us discover significant interactions.

Before explaining how to utilize knockoffs to test (5) with false discovery rate control, we begin by discussing the choice of grouping functions ψ_j . Note that the hypotheses in (5) are more informative than those in (1) only if they are based on a partition of the individuals into meaningful groups that internally are sufficiently homogeneous, with respect to their associations with a variable. But it is not clear how to define such partitions a priori if no external information is available about $P_{Y \mid X, Z}$. Therefore, ψ_j must be allowed to be data-driven, which makes the tested hypotheses in (5) random. To address this task, useful information about sample heterogeneity can be extracted from the available data using existing tools, for example by fitting a sufficiently flexible multivariate model for predicting $Y \mid X, Z$. However, if the same data were naively used twice, first to define the hypotheses in (5) and then to test them, the false discovery rate would not be controlled, as previewed by Figure 1. Data splitting would provide a simple patch to retain the test validity after selecting the random hypotheses, but it is a wasteful approach, as also previewed in Figure 1. Therefore, we propose a more efficient solution that makes it possible to safely re-use most of the data to first define and then test the individualized hypotheses in (5), while provably controlling the false discovery rate in finite samples.

2.3 A selective knockoff filter

For any $j \in [p]$, let $\hat{\psi}_j$ be a data-driven partition of the covariate space: a function of $z \in \mathbb{R}^m$ whose parameters may depend on the knockoff-augmented data \mathcal{D} and that can be written as $\hat{\psi}_j(z; [\mathbf{X}, \tilde{\mathbf{X}}], \mathbf{Y}, \mathbf{Z}) \in \mathbb{N}$. Note that $\hat{\psi}_j$ is random mapping from \mathbb{R}^m to \mathbb{N} because its parameters depend on \mathcal{D} . In the following, we focus on $\hat{\psi}_j$ that are invariant under permutations of any variable with its own knockoff.

Definition 1 (Knockoff-invariant partition). *Let $\mathbf{V} \in \{0, 1\}^{n \times p}$ be i.i.d. Bernoulli random variables, independent of anything else, and $[\mathbf{X}, \tilde{\mathbf{X}}]_{\text{swap}(\mathbf{V})}$ be the matrix obtained concatenating \mathbf{X} and $\tilde{\mathbf{X}}$ column-wise and then swapping the i -th observation of X_j with the corresponding knockoffs if and only if $V_{ij} = 1$. A random function $\hat{\psi}(z; [\mathbf{X}, \tilde{\mathbf{X}}], \mathbf{Y}, \mathbf{Z}) : \mathbb{R}^m \rightarrow \mathbb{N}^p$ induces knockoff-invariant partitions of \mathbb{R}^m if*

$$\hat{\psi}_j(z; [\mathbf{X}, \tilde{\mathbf{X}}], \mathbf{Y}, \mathbf{Z}) = \hat{\psi}_j^0(z; [\mathbf{X}, \tilde{\mathbf{X}}]_{\text{swap}(\mathbf{V})}, \mathbf{Y}, \mathbf{Z}),$$

for all $j \in [p]$, $z \in \mathbb{R}^m$, and any fixed function $\hat{\psi}^0 : \mathbb{R}^m \rightarrow \mathbb{N}^p$ whose parametrization may depend on the data with swapped knockoffs in \mathcal{D} . Above $\hat{\psi}_j$ and $\hat{\psi}_j^0$ indicate the j -th components of $\hat{\psi}$ and $\hat{\psi}^0$.

In other words, invariant partitions may depend on the data, but they cannot make use of any knowledge about which variables are real and which are knockoffs, as the identities of the latter are masked by random swapping. Consequently, for any $\hat{\psi}$ satisfying Definition 1, the conditional distribution of $\hat{\psi}(z; [\mathbf{X}, \tilde{\mathbf{X}}], \mathbf{Y}, \mathbf{Z})$ given \mathcal{D} is the same as that of $\hat{\psi}(z; [\mathbf{X}, \tilde{\mathbf{X}}]_{\text{swap}(\mathbf{V}')}, \mathbf{Y}, \mathbf{Z})$, for any fixed $\mathbf{V}' \in \{0, 1\}^{n \times p}$ and any $z \in \mathbb{R}^m$:

$$\hat{\psi}(z; [\mathbf{X}, \tilde{\mathbf{X}}], \mathbf{Y}, \mathbf{Z}) \mid [\mathbf{X}, \tilde{\mathbf{X}}], \mathbf{Y}, \mathbf{Z} \stackrel{d}{=} \hat{\psi}(z; [\mathbf{X}, \tilde{\mathbf{X}}]_{\text{swap}(\mathbf{V}')}, \mathbf{Y}, \mathbf{Z}) \mid [\mathbf{X}, \tilde{\mathbf{X}}], \mathbf{Y}, \mathbf{Z}.$$

Despite the random swapping, $\hat{\psi}$ can capture useful information because the columns of $[\mathbf{X}, \tilde{\mathbf{X}}]_{\text{swap}(\mathbf{V})}$ contain on average $n/2$ real variables. Thus, approximately half of the original data remain intact. Any method may be employed to define $\hat{\psi}^0$, and an example designed to detect pairwise interactions is discussed in Section 2.4. For now, we assume $\hat{\psi}$ is already available and focus on testing the corresponding random hypotheses in (5).

For any $\hat{\psi}$ and $j \in [p]$, let $\hat{G}_j([\mathbf{X}, \tilde{\mathbf{X}}], \mathbf{Y}, \mathbf{Z}) = \sup_{z \in \mathbb{R}^m} \hat{\psi}_j(z) \in \mathbb{N}$ denote the cardinality of $\hat{\psi}_j$; that is, the number of disjoint regions into which $\hat{\psi}_j$ partitions the covariate space. Further, let $\hat{G} = \sum_{j=1}^p \hat{G}_j$. To lighten the notation, the data dependence of $\hat{\psi}(x)$, \hat{G}_j , and \hat{G} will not be shown explicitly hereafter unless needed to avoid ambiguity. Define $[\mathbf{T}, \tilde{\mathbf{T}}] \in \mathbb{R}^{2\hat{G}}$ as the vector of importance measures for all variables and knockoffs in each region of the covariate space determined by $\hat{\psi}$. More precisely, \mathbf{T} (resp. $\tilde{\mathbf{T}}$) is the concatenation of p sub-vectors $T_j^{g_j}$ (resp. $\tilde{T}_j^{g_j}$) for all $j \in [p]$ and $g_j \in [\hat{G}_j]$, whose elements quantify the importance of X_j (resp. \tilde{X}_j) in predicting Y conditional on all other variables, looking only at the observations in group g_j . In general, $[\mathbf{T}, \tilde{\mathbf{T}}]$ can be written as the output of a randomized function τ applied to the full data set:

$$[\mathbf{T}, \tilde{\mathbf{T}}] = \tau([\mathbf{X}, \tilde{\mathbf{X}}], \mathbf{Y}, \mathbf{Z}) = [t([\mathbf{X}, \tilde{\mathbf{X}}], \mathbf{Y}, \mathbf{Z}), \tilde{t}([\mathbf{X}, \tilde{\mathbf{X}}], \mathbf{Y}, \mathbf{Z})]. \quad (6)$$

Above, \mathbf{t} (resp. $\tilde{\mathbf{t}}$) are defined in terms of τ , as its first (resp. last) \hat{G} elements. For any $\mathcal{S} \subseteq \{1, \dots, \hat{G}\}$, whose elements uniquely identify pairs (j, g_j) for $j \in [p]$ and $g_j \in [\hat{G}_j]$, let $[\mathbf{X}, \tilde{\mathbf{X}}]_{\text{swap}(\mathcal{S})}$ be the matrix obtained from $[\mathbf{X}, \tilde{\mathbf{X}}]$ after swapping the sub-column $\mathbf{X}_j^{(g_j)}$, which contains all observations of X_j in group g_j , with the corresponding knockoffs, for all $(j, g_j) \in \mathcal{S}$. Note the slight change of notation compared to (3): there, the swapping was simultaneous for an entire column. The function τ may be anything, as long as swapping the true variables and knockoffs in any one group of samples has the only effect of swapping the corresponding importance measures in that group, leaving all other elements of τ unchanged:

$$\tau(\mathbf{Y}, [\mathbf{X}, \tilde{\mathbf{X}}]_{\text{swap}(\mathcal{S})}) \mid [\mathbf{X}, \tilde{\mathbf{X}}]_{\text{swap}(\mathbf{V})}, \mathbf{Y}, \mathbf{Z} \stackrel{d}{=} [t(\mathbf{Y}, [\mathbf{X}, \tilde{\mathbf{X}}]), \tilde{t}(\mathbf{Y}, [\mathbf{X}, \tilde{\mathbf{X}}])]_{\text{swap}(\mathcal{S})} \mid [\mathbf{X}, \tilde{\mathbf{X}}]_{\text{swap}(\mathbf{V})}, \mathbf{Y}, \mathbf{Z}. \quad (7)$$

Importantly, the above equality only needs to hold in distribution, as τ may involve additional sources of independent randomness; e.g., it may involve cross-validation to tune some hyper-parameters. A concrete

example of τ satisfying (7) is presented in Section 2.5. In general, for our method to be powerful, τ should be such that a larger value in position (j, g_j) of \mathbf{T} indicates evidence from group g_j that Z_j is conditionally associated with Y , while a larger value in position (j, g_j) of $\tilde{\mathbf{T}}$ points to a corresponding association of \tilde{Z}_j with Y , which must be spurious because knockoffs have no conditional association with Y .

Given any importance measures $[\mathbf{T}, \tilde{\mathbf{T}}]$ satisfying (7), the statistics $\mathbf{W} \in \mathbb{R}^{\hat{G}}$ are assembled with the standard pairwise anti-symmetric approach reviewed in Section 2.1:

$$W_j^{g_j} = T_j^{g_j} - \tilde{T}_j^{g_j}. \quad (8)$$

This ensures the signs of statistics corresponding to true nulls $\mathcal{H}_{0,j}^{(g_j)}$ in (5) are independent coin flips conditional on the absolute values of all entries in \mathbf{W} , extending the result in (4) from [7] and allowing the application of the standard knockoff filter to compute an adaptive significance threshold that controls the false discovery rate. Figure A2 in Appendix A1.2 provides a schematic representation of this procedure.

Theorem 1. *Given \mathbf{V} and $[\mathbf{X}, \tilde{\mathbf{X}}]_{\text{swap}(\mathbf{V})}, \mathbf{Y}, \mathbf{Z}$, let $\hat{\psi}$ be a knockoff-invariant partition with total size $\hat{G} = \sum_{j=1}^p \hat{G}_j$. Assume $\mathbf{W}([\mathbf{X}, \tilde{\mathbf{X}}], \mathbf{Y}, \mathbf{Z}) \in \mathbb{R}^{\hat{G}}$ are statistics computed as in (8). Suppose $\mathbf{U} \in \{\pm 1\}^{\hat{G}}$ has random independent entries such that $U_j^{g_j} = \pm 1$ with probability 1/2 if $\mathcal{H}_{0,j}^{(g_j)}$ in (5) is true and $U_j^{g_j} = +1$ otherwise, for all $j \in [p]$ and $g_j \in [\hat{G}_j]$. Then, the knockoff filter [19] applied to \mathbf{W} controls the false discovery rate (2) for the hypotheses defined in (5), conditional on $\hat{\psi}$, because*

$$\mathbf{W} \mid \hat{\psi} \triangleq \mathbf{W} \odot \mathbf{U} \mid \hat{\psi}. \quad (9)$$

Figure 1 previews the performance of our method—the *selective knockoff filter* (SKF)—on synthetic data from a linear model with heterogeneous coefficients; see Section 4.1 for details. The performance is measured in terms of false discovery rate, power, and informativeness of the findings. Informativeness is quantified by two metrics: the average homogeneity of the rejected hypotheses, defined as the proportion of individuals in the reported group for which the variable of interest has a non-zero coefficient within the true data-generating model, and the corresponding heterogeneity of individual effects, defined as the standard deviation of the aforementioned coefficients. The first benchmark is the vanilla knockoff filter of [7]; this controls the false discovery rate but can only test population-wide hypotheses. The second one is a data-splitting version of the SKF, utilizing half of the samples to learn the partition and the other half to test the conditional hypotheses; this is not as powerful as our method. The third benchmark is a naive invalid version of the SKF that utilizes all data twice, first to select the partitions and then to test the conditional hypotheses, without randomly masking the identity of the knockoffs; this does not control the false discovery rate.

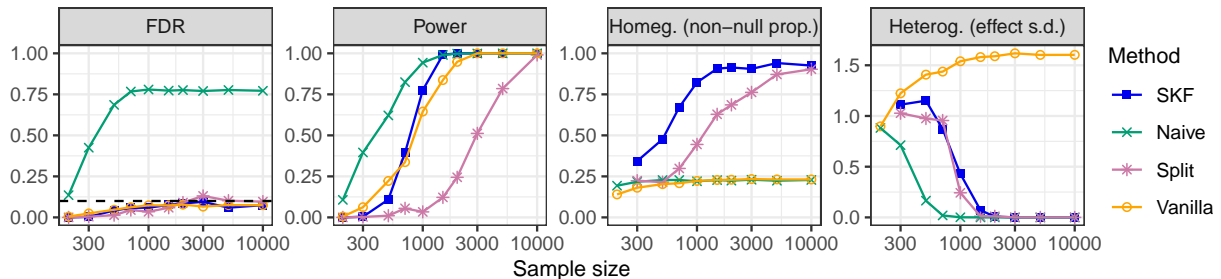


Figure 1: Performance of the SKF and benchmark methods for individualized conditional testing on synthetic data. The dashed horizontal line corresponds to the nominal false discovery rate level 0.1. The informativeness of the discoveries is quantified by the homogeneity of the corresponding groups (higher is better) and the heterogeneity of the underlying effects in the data-generating model (lower is better).

Before presenting further implementation details of the SKF, we note that statistics \mathbf{W} satisfying (9) can also be utilized to test hypotheses different from those in (5), by repurposing the multi-environment knockoff filter of [41]. This alternative approach outlined in Appendix A1.3 allows testing whether any variables have a robust association across the distinct groups of individuals identified by the adaptive partitions ϕ , which may be useful to find variables whose associations are *not* driven by interactions.

2.4 Partitioning the samples to detect pairwise interactions

The flexibility in the choice of data-driven partitions allows any model or machine learning algorithm to be leveraged by the SKF to group the samples. As a concrete example, consider the following approach designed to detect pairwise interactions between variables and covariates. Note that our method is easily extended to test for interactions between different variables in X , but the notation is simpler if we focus on interactions with the covariates in Z . For simplicity, imagine also that all covariates are binary and the conditional distribution of $Y | X, Z$ can be approximated by a generalized linear model with interactions. In this context, a reasonable approach to construct $\hat{\psi}^0$ starts by fitting a sparse generalized linear model (i.e., the lasso) to predict \mathbf{Y} given $[\mathbf{X}, \tilde{\mathbf{X}}]_{\text{swap}(\mathbf{V})}, \mathbf{Z}$, after augmenting the data matrix with all possible pairwise interactions between the variables in \mathbf{Z} and those in $[\mathbf{X}, \tilde{\mathbf{X}}]_{\text{swap}(\mathbf{V})}$. Algorithms have been developed to fit such models and variations thereof [26, 28, 55]. After tuning the regularization parameter by cross-validation, let $\hat{\beta}_j$ and $\hat{\beta}_{j+p}$ indicate the main effects estimated by this model for the (randomly swapped) variables X_j and \tilde{X}_j , for any $j \in [p]$. Let also $\hat{\gamma}_{l,j}$ and $\hat{\gamma}_{l,j+p}$ indicate the corresponding interaction coefficients involving Z_l and the (randomly swapped) variables X_j and \tilde{X}_j , respectively, for all $l \in [m]$ and $j \in [p]$. Given a constant upper bound G_{\max} on the number of interactions per variable (e.g., $G_{\max} = 2$), for all $j \in [p]$ let $\hat{\mathcal{I}}_j \subset [m]$ indicate the subset of G_{\max} covariates displaying the strongest (nonzero) interactions with X_j or \tilde{X}_j , with the understanding that ties are broken at random and $|\hat{\mathcal{I}}_j| < G_{\max}$ if the number of covariates with nonzero interaction coefficients is too small. In other words,

$$\hat{\mathcal{I}}_j := \{l \in [m] : |\hat{\gamma}_{l,j}| + |\hat{\gamma}_{l,j+p}| > 0, \sum_{l' \neq l} \mathbb{1} [|\hat{\gamma}_{l,j}| + |\hat{\gamma}_{l,j+p}| > |\hat{\gamma}_{l',j}| + |\hat{\gamma}_{l',j+p}|] > m - G_{\max}\}.$$

Thus, X_j is associated with at most G_{\max} potentially interacting covariates. Each $\hat{\psi}_j$ is defined as the mapping from the Cartesian space $\{0, 1\}^{\hat{\mathcal{I}}_j}$ to $\{1, \dots, 2^{|\hat{\mathcal{I}}_j|}\}$, indexing all possible configurations of the covariates in $\hat{\mathcal{I}}_j$. See Table 1 for a toy example with 3 variables and 3 binary covariates; here, the lasso selects Z_1, Z_2 as potentially interacting with X_1 , and Z_3 for X_2 . No interactions with X_3 are detected. The covariate space is thus partitioned into 4 groups for X_1 , 2 groups for X_2 , and 1 trivial group for X_3 , yielding a total of 7 hypotheses to be tested. The interpretation of the SKF findings is that X_1 is associated with Y for individuals with $Z_2 = 1$, while X_2 is associated with Y for individuals with $Z_3 = 1$, and X_3 is associated with Y at the aggregate level. No evidence of an association between X_1 and Y is detected among individuals with $Z_2 = 0$, and no evidence of association between X_2 and Y is detected among individuals with $Z_3 = 0$.

Table 1: Sample partition obtained by fitting the lasso with interactions on data with randomly swapped knockoffs, and corresponding SKF discoveries, in a toy example with 3 variables and 3 binary covariates. The term “influences” is utilized loosely here to indicate a (possibly non-causal) conditional association.

Variable	Covariates	Partition		Findings	
		Label	Definition	Rejected	Interpretation
X_1	$\{Z_1, Z_2\}$	1	$Z_1 = 0, Z_2 = 0$	No	
		2	$Z_1 = 0, Z_2 = 1$	Yes	X_1 influences Y if $Z_1 = 0$ and $Z_2 = 1$
		3	$Z_1 = 1, Z_2 = 0$	No	
		4	$Z_1 = 1, Z_2 = 1$	Yes	X_1 influences Y if $Z_1 = 1$ and $Z_2 = 1$
X_2	$\{Z_3\}$	1	$Z_3 = 0$	No	
		2	$Z_3 = 1$	Yes	X_2 influences Y if $Z_3 = 1$
X_3	\emptyset	1	All individuals	Yes	X_3 influences Y

The constant G_{\max} controls an important trade-off between the power of the SKF and the interpretability of its findings. A larger values G_{\max} tends to lead to more specific hypotheses, as the covariate space is partitioned into increasingly refined groups. Hypotheses defined over finer partitions, however, may be harder

to reject because they allow fewer samples to determine the sign of the test statistics, as explained in the next section. In fact, partitioning roughly reduces the effective number of samples by a factor of up to $2^{G_{\max}}$, in the case of binary covariates. Concretely, this paper utilizes $G_{\max} = 1$ or $G_{\max} = 2$, but the optimal G_{\max} may generally depend on the sample size as well as on the expected number of interactions in the data at hand. Finally, note that continuous covariates can be handled similarly after suitable discretization. Of course, the above lasso approach is only one among countless possible ways to define sample partitions satisfying Definition 1. Alternatively, one could take advantage of more sophisticated sample partitioning techniques, which may for example be based on Bayesian models [34], random forests [35], or neural networks [36].

2.5 Computing powerful test statistics for the selective knockoff filter

The SKF is flexible with respect to the choice of test statistics, as long as (7) is satisfied. Here, we present a relatively simple implementation of this method based on generalized linear models, continuing along the lines of Section 2.4. Recall that a popular method for computing model-X importance measures [7] utilizes the (generalized) lasso for predicting Y given X , \tilde{X} , and Z . Therefore, as (7) requires swapping X_j and \tilde{X}_j in group g_j to have the only effect of swapping the corresponding importance measures $T_j^{g_j}$ and $\tilde{T}_j^{g_j}$, an intuitive solution inspired by [41] is the following. First, a sparse generalized linear regression model (e.g., the lasso) is trained to predict \mathbf{Y} given $[[\mathbf{X}, \tilde{\mathbf{X}}]_{\text{swap}(\mathbf{V})}, \mathbf{Z}]$, tuning the regularization parameter by cross-validation. The absolute values of the regression coefficients serve as “prior” importance measures, T_j^{prior} and $\tilde{T}_j^{\text{prior}}$, for all variables and knockoffs indexed by $j \in [p]$. These are combined pairwise into a weight π_j for each j ; for example, as $\pi_j = \zeta(T_j^{\text{prior}} + \tilde{T}_j^{\text{prior}})$, where ζ is a positive and decreasing function such as $\zeta(t) = 1/(0.05 + t)$. Note that larger values of π_j suggest the j -th variable is more likely to have a significant effect among some individuals. Similar weights can also be defined for the covariates. Then, separately for each (j, g_j) , a new sparse generalized linear model is fitted using only the observations in the g_j -th group to predict $\mathbf{Y}^{(g_j)}$ given $[[\mathbf{X}^{(g_j)}, \tilde{\mathbf{X}}^{(g_j)}]_{\text{swap}(\mathbf{V})}, \mathbf{Z}^{(g_j)}]$, after taking care to restore the true variable and knockoff identities in the j -th and $(j + p)$ -th data columns. See Figure A3 for a schematic visualization of this algorithm.

The above model utilizes feature-specific regularization that depends on two hyper-parameters, $\lambda^{(j, g_j)} > 0$ and $\gamma^{(j, g_j)} \in [0, 1]$, both tuned by cross-validation, as well as on the weights π . Specifically, the penalty for the l -th variable is $\lambda_l^{(j, g_j)} = \lambda^{(j, g_j)}(1 - \gamma^{(j, g_j)}) + \gamma^{(j, g_j)}\pi_l$, for all $l \in [p]$. If $\gamma^{(j, g_j)} = 0$, this reduces to a standard lasso looking only at the samples in group g_j . But, in general, larger values of $\gamma^{(j, g_j)}$ can make our approach more powerful, as we gather strength from the data in all groups. In fact, null variables will tend to receive smaller values of π and will thus be less likely to be incorrectly selected by the final model, thereby reducing the noise in the test statistics. Of course, the weights π may not always be informative, hence why $\gamma^{(j, g_j)}$ is tuned by cross-validation. For that purpose, note that a two-dimensional grid search can be easily avoided by tuning first $\lambda^{(j, g_j)} > 0$ and then $\gamma^{(j, g_j)}$. Finally, the importance measures for the j -th variable and knockoff in group g_j are defined as the absolute values of the estimated regression coefficients for X_j and \tilde{X}_j , respectively. It is easy to prove this procedure satisfies (7). In fact, conditional on $\mathbf{Y}, [\mathbf{X}, \tilde{\mathbf{X}}]_{\text{swap}(\mathbf{V})}, \mathbf{Z}$, swapping all observations of X_j in group g_j with the corresponding \tilde{X}_j for any pair (j, g_j) simply results in swapping $T_j^{(g_j)}$ with $\tilde{T}_j^{(g_j)}$, as π remains unperturbed because it only depends on the fixed $[\mathbf{X}, \tilde{\mathbf{X}}]_{\text{swap}(\mathbf{V})}$.

Although it is convenient to think about the lasso, the main idea of the above procedure is generally applicable with any model. The key to ensuring (7) is that the importance measures indexed by (j, g_j) are computed by a predictive model that sees the other variables and the observations in other groups only through the lenses of the perturbed data set with randomly swapped knockoffs. Note that the weights π must be estimated based on $[[\mathbf{X}, \tilde{\mathbf{X}}]_{\text{swap}(\mathbf{V})}, \mathbf{Z}]$ to make the final test statistics mutually independent, which is required for false discovery rate control [19]; see the proof of Theorem 1 in Appendix A4. Further, revealing the identities of X_j and \tilde{X}_j within group g_j is essential to achieve non-trivial power—otherwise, it would be impossible to tell important variables apart from knockoffs. Of course, this is only one possible implementation of the SKF. A relatively straightforward generalization would involve estimating different sets of empirical prior weights in different groups, as sketched in Figure A3. That would still satisfy (7) if the models utilized to compute the priors only look at the randomly swapped data in $[\mathbf{X}, \tilde{\mathbf{X}}]_{\text{swap}(\mathbf{V})}$.

3 Quantile estimation of individual linear effects

3.1 A partially linear model with heterogeneous effects

This section focuses on the special case of a single *binary* variable, $X \in \{0, 1\}$, and further assumes the outcomes Y^i , for $i \in [n]$, are determined by a partially linear model [17] with heterogeneous effects:

$$Y^i = g(Z^i, C^i) + \tau^i X^i. \quad (10)$$

Above, g is an arbitrary *unknown* nuisance function, which we are not directly interested in estimating, and C is a vector of *unmeasured* covariates. The object of inference is the distribution of individual effects $\tau^i \in \mathbb{R}$. These parameters may be depend on both Z and C through completely unknown mechanisms; see Figure 2 for a graphical representation of this model. The goal is to estimate quantiles of τ^i , leveraging only our knowledge of $P_{X|Z}$. Note that the assumption of $p = 1$ is without loss of generality compared to the previous section, as one can always analyze one variable at a time, conflating the others into Z .

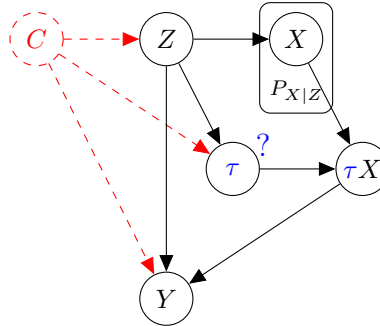


Figure 2: Graphical representation of a partially linear model with heterogeneous effects, linking the variable of interest (X), the outcome (Y), the measured covariates (Z), and other unmeasured variables (C). The goal is to estimate the individual linear effects of X , namely τ , leveraging our knowledge of $P_{X|Z}$.

3.2 The CRT for sharp hypotheses

The CRT [7] is a model-X alternative to knockoffs for testing the conditional hypothesis in (1). This test has complementary strengths and weaknesses relative to knockoffs. On the one hand, the CRT can compute a precise p-value for a single hypothesis, as opposed to being limited to controlling the false discovery rate over many variables [7]. On the other hand, the CRT tends to be computationally more expensive, but adjustments can be made to mitigate this issue [52]. It also produces p-values for different variables that generally have unknown dependencies with one another, and, without conservative precautions [56, 57], this may in theory invalidate certain multiple testing methods such as the Benjamini-Hochberg procedure [53].

While originally intended for a completely non-parametric model-X setting, the CRT can be easily adapted to work with a partially linear model. In particular, it can be repurposed to test a *sharp null* hypothesis that the individual effects τ in (10) are equal to an arbitrary fixed vector $\delta \in \mathbb{R}^n$:

$$\mathcal{H}_\delta : \tau^i = \delta^i, \quad \forall i \in [n]. \quad (11)$$

The most intuitive instance of \mathcal{H}_δ is that with $\delta = 0$, which reduces to the null hypothesis that X is conditionally independent of Y and is the case originally considered by [7]. In general, however, the sharp null hypothesis defined in (11) for different values of δ can also be useful to *estimate* τ , as explained below. Note that in the following we review the CRT of [7] while extending it to the more general case of $\delta \neq 0$.

As in the previous section, denote by $\mathbf{X} \in \mathbb{R}^{n \times 1}$, $\mathbf{Z} \in \mathbb{R}^{n \times m}$, $\mathbf{Y} \in \mathbb{R}^{n \times 1}$ the data matrices containing all n observations. For a fixed $K \in \mathbb{N}$ and each $k \in [K]$, let $\tilde{\mathbf{X}}^{(k)} \in \mathbb{R}^{n \times 1}$ be a column vector containing n observations of a *virtual* variable sampled by the statistician from $P_{X|Z}$, independently of the observed \mathbf{X} :

$$\tilde{\mathbf{X}}^{(k)} | \mathbf{Z} \stackrel{d}{=} \mathbf{X} | \mathbf{Z}, \quad \forall k \in [K]. \quad (12)$$

These virtual variables are related to knockoffs, but they are simpler to generate because (12) is strictly weaker than (3) whenever $p > 1$. The CRT utilizes K independent realizations of these virtual variables to compute a p-value as follows. Let $\bar{t} : \mathbb{R}^{n \times (m+2)} \rightarrow \mathbb{R}$ be any function taking as input $\mathbf{X}, \mathbf{Y}, \mathbf{Z}$ and returning a statistic designed to quantify the “importance” of X in predicting Y given Z . As for the knockoff filter, this statistic can take any form, including the absolute value of a regression coefficient for Z in a sparse generalized linear model for predicting Y given Z and X [7], for example. Other options for computing the test statistics will be discussed below. For any choice of t , the CRT p-value is then defined as

$$\hat{p}_{\delta}^{\text{CRT}}(\mathbf{X}, \mathbf{Y}, \mathbf{Z}) = \frac{1 + \sum_{k=1}^K \mathbb{1} \left[\bar{t}(\tilde{\mathbf{X}}^{(k)}, \mathbf{Y} - \mathbf{X} \odot \delta, \mathbf{Z}) \geq \bar{t}(\mathbf{X}, \mathbf{Y} - \mathbf{X} \odot \delta, \mathbf{Z}) \right]}{1 + K}. \quad (13)$$

Intuitively, this is the empirical fraction of virtual variable realizations leading to larger statistic values compared to the true variable. If \mathcal{H}_{δ} in (11) holds, then \mathbf{X} is exchangeable with each $\tilde{\mathbf{X}}^{(k)}$ conditional on \mathbf{Z} and $\mathbf{Y} - \mathbf{X} \odot \delta$, which implies the quantity in (13) is uniformly distributed on $\{1/(1+K), 2/(1+K), \dots, 1\}$.

Proposition 1. *If the partially linear model in (10) holds and \mathcal{H}_{δ} in (11) is true, the CRT p-value in (13) is uniformly distributed on $\{1/(1+K), 2/(1+K), \dots, 1\}$ conditional on \mathbf{Z} and \mathbf{Y} . In particular, for all $\alpha \in (0, 1)$, $\mathbb{P}[\hat{p}_{\delta}^{\text{CRT}}(\mathbf{X}, \mathbf{Y}, \mathbf{Z}) \leq \alpha | \mathbf{Z}, \mathbf{Y}] \leq \alpha$.*

Under the additional assumption of homogeneous effects in (10), i.e., $\tau^i = \tau$ for some $\tau \in \mathbb{R}$ and all i , it is possible to invert the CRT to estimate τ . More precisely, define the set $\hat{\mathcal{S}}(\alpha)$ of $\delta \in \mathbb{R}$ values such that \mathcal{H}_{δ} in (11) with $\delta = \delta \mathbf{1}$ is not rejected by the CRT at level α :

$$\hat{\mathcal{S}}(\alpha) = \{\delta \in \mathbb{R} : \hat{p}_{\delta \mathbf{1}}^{\text{CRT}}(\mathbf{X}, \mathbf{Y}, \mathbf{Z}) > \alpha\}. \quad (14)$$

This is a random set that depends on \mathbf{X} , \mathbf{Y} , and \mathbf{Z} , as well as on the K realizations of $\tilde{\mathbf{X}}$. The finite-sample validity of this confidence set is implied by Proposition 1 through the classical duality with hypothesis testing, as $\mathbb{P}[\tau \notin \hat{\mathcal{S}}(\alpha) | \mathbf{Z}, \mathbf{Y}] = \mathbb{P}[\hat{p}_{\delta \mathbf{1}}^{\text{CRT}}(\mathbf{X}, \mathbf{Y}, \mathbf{Z}) \leq \alpha | \mathbf{Z}, \mathbf{Y}] \leq \alpha$.

Unfortunately, confidence sets in (14) have limitations. Firstly, $\hat{\mathcal{S}}(\alpha)$ may be non-convex in general, which makes it difficult to interpret. Fortunately, many choices of statistics \bar{t} in (13) produce a confidence set (14) that approximately is an *interval*; see Appendix A1.4. Secondly, and more crucially, the CRT for a partially linear model relies heavily on the assumption of homogeneous effects in (10). This is likely an over-simplification of reality in many applications, and it is especially problematic because it may often lead to completely invalid inferences. In particular, if the partially linear model is misspecified, or if the true effects are heterogeneous, $\hat{\mathcal{S}}(\alpha)$ in (14) no longer has any guarantees, and it may turn out to be empty; see Figure 4 in Section 4 for examples. This is a known issue in causal inference [58], and it helps explain the reluctance of many in that field to adopt randomization testing more broadly [18, 49], at least for purposes other than preliminary discovery [59]. Therefore, we are motivated to extend the CRT as to test composite hypotheses that enable more robust estimates compared to those in (11); this work is inspired by [50], as explained next.

3.3 A quantile CRT for inference on individual effects

This section develops a quantile version of the CRT—the QCRT—to test whether the q -th largest individual effect in the sample is smaller than a constant c , for any fixed $q \in [n]$ and $c \in \mathbb{R}$. In other words, we will test

$$\mathcal{H}_{q,\leq,c} : \tau_{(q)} \leq c, \quad (15)$$

where $\tau_{(q)}$ is the q -th largest element in the vector $\boldsymbol{\tau}$ of true individual effects (10). The hypothesis in (15) is interesting because its rejection implies evidence of large effects in at least a certain subset of the observed samples. Further, inverting a test of (15) will lead to a one-sided confidence bound for the desired quantile of the individual effects that is naturally robust to heterogeneity, unlike the naive CRT confidence sets from Section 3.2. Of course, there is no need in general to focus only on right-tailed tests of the type in (15); in fact, one can also easily carry out left-tailed tests of $\mathcal{H}_{q,\geq,c} : \tau_{(q)} \geq c$, as explained later.

Before addressing $\mathcal{H}_{q,\leq,c}$ directly, it is convenient to consider the simpler but relevant problem of testing the null hypothesis $\mathcal{H}_{\leq\delta}$ of whether $\boldsymbol{\tau}$ is bounded from above by a fixed vector $\boldsymbol{\delta} \in \mathbb{R}^n$:

$$\mathcal{H}_{\leq\delta} : \tau^i \leq \delta^i, \quad \forall i \in [n]. \quad (16)$$

If $\boldsymbol{\delta} = c\mathbf{1}$, the hypothesis in (16) becomes a special case of that in (15) with $q = n$, although the two problems are generally distinct. The hypothesis $\mathcal{H}_{\leq\delta}$ in (16) can be tested with a modified CRT (13) in which the generic statistic \bar{t} is replaced by a more structured t that can be written as

$$\bar{t}(\tilde{\mathbf{X}}, \mathbf{Y} - \mathbf{X} \odot \boldsymbol{\delta}, \mathbf{Z}) = t(\tilde{\mathbf{X}}, \mathbf{Y} - \hat{g}(\mathbf{Z}; \mathbf{Z}, \mathbf{Y}) - (\mathbf{X} - \tilde{\mathbf{X}}) \odot \boldsymbol{\delta}). \quad (17)$$

Above, $\hat{g} : \mathbb{R} \rightarrow \mathbb{R}$ is a random function applied element-wise to \mathbf{Z} , whose parametrization may depend on \mathbf{Z} and \mathbf{Y} . Intuitively, one may think of \hat{g} as a data-driven function designed to approximate the expected value of g in the true underlying partially linear model (10). The \hat{g} is to be fitted on the data in \mathbf{Z} and \mathbf{Y} without looking at \mathbf{X} or $\tilde{\mathbf{X}}^{(k)}$. Meanwhile, $t : \mathbb{R}^{n \times 2} \rightarrow \mathbb{R}$ is a fixed function designed to measure the association between \mathbf{X} and the residuals $\mathbf{Y} - \hat{g}(\mathbf{Z})$, in such a way as to satisfy the following monotonicity property.

Definition 2. A statistic $t : \mathbb{R}^{n \times 2} \rightarrow \mathbb{R}$ is said to be effect-increasing if

$$t(\mathbf{X}, \mathbf{Y} + \mathbf{X} \odot \boldsymbol{\eta} + (\mathbf{1} - \mathbf{X}) \odot \boldsymbol{\xi}) \geq t(\mathbf{X}, \mathbf{Y}),$$

for all \mathbf{X}, \mathbf{Y} and $\boldsymbol{\eta}, \boldsymbol{\xi} \in \mathbb{R}^{n \times 1}$ such that $\boldsymbol{\eta} \geq 0 \geq \boldsymbol{\xi}$.

This states that $t(\mathbf{X}, \mathbf{Y})$ must not decrease if Y^i increases for individuals i receiving $X^i = 1$, and it must not increase if Y^i increases for individuals with $X^i = 0$. One example of a statistic t satisfying Definition 2 is $t(\mathbf{X}, \mathbf{Y}) = \sum_{i=1}^n X^i Y^i - \sum_{i=1}^n (1 - X^i) Y^i$, and a particularly interesting alternative will be discussed below. Now, with this setup in place, we are ready to write the modified the CRT p-value

$$\hat{p}_{\boldsymbol{\delta}}(\mathbf{X}, \mathbf{Y}, \mathbf{Z}) = \frac{1 + \sum_{k=1}^K \mathbb{1} \left[t(\tilde{\mathbf{X}}^{(k)}, \mathbf{Y} - \hat{g}(\mathbf{Z}; \mathbf{Z}, \mathbf{Y}) - (\mathbf{X} - \tilde{\mathbf{X}}^{(k)}) \odot \boldsymbol{\delta}) \geq t(\mathbf{X}, \mathbf{Y} - \hat{g}(\mathbf{Z}; \mathbf{Z}, \mathbf{Y})) \right]}{1 + K} \quad (18)$$

which is valid for testing $\mathcal{H}_{\leq\delta}$ in (16) as long as t is effect-increasing.

Theorem 2. Fix any $\boldsymbol{\delta} \in \mathbb{R}^{n \times 1}$ and assume the partially linear model in (10) holds. If the statistic t in (18) is effect-increasing and the bounded null hypothesis $\mathcal{H}_{\leq\delta}$ in (16) is true, then, for any $\alpha \in (0, 1)$,

$$\mathbb{P}[\hat{p}_{\boldsymbol{\delta}}(\mathbf{X}, \mathbf{Y}, \mathbf{Z}) \leq \alpha \mid \mathbf{Z}, \mathbf{Y}] \leq \alpha,$$

where $\hat{p}_{\boldsymbol{\delta}}(\mathbf{X}, \mathbf{Y}, \mathbf{Z})$ is the CRT p-value defined in (18).

From here, a p-value for testing $\mathcal{H}_{q,\leq,c}$ in (15) can be obtained quite easily. Define the subset of individuals receiving a positive true variable as $\mathcal{T} = \{i : X^i = 1\}$, as well as the corresponding set $\tilde{\mathcal{T}}^{(k)} = \{i : \tilde{X}^{(k)i} = 1\}$ for any fixed realization $\tilde{\mathbf{X}}^{(k)}$ of the virtual variable. Let $\tilde{m}^{(k)} \in [n]$ indicate the size of $\tilde{\mathcal{T}}^{(k)}$. Then, denote as $\tilde{\mathcal{I}}^{(k)} \subseteq [n]$ the set of individuals with the smallest $l^{(k)} = \min(\tilde{m}^{(k)}, n - q)$ values of Y^i among those in $\tilde{\mathcal{T}}^{(k)}$, for $i \in [n]$. Finally, define the vector $\boldsymbol{\eta}^{(k)} \in (\mathbb{R} \cup \{+\infty\})^n$ such that, for each $i \in [n]$,

$$\eta^{(k)i} = \begin{cases} +\infty, & \text{if } i \in \tilde{\mathcal{I}}^{(k)}, \\ c, & \text{otherwise.} \end{cases} \quad (19)$$

With this notation in place, let us define the QCRT p-value $\hat{p}_{q,c}(\mathbf{X}, \mathbf{Y}, \mathbf{Z})$ as

$$\hat{p}_{q,c}(\mathbf{X}, \mathbf{Y}, \mathbf{Z}) = \frac{1 + \sum_{k=1}^K \mathbb{1} \left[t(\tilde{\mathbf{X}}^{(k)}, \mathbf{Y} - \hat{g}(\mathbf{Z}; \mathbf{Z}, \mathbf{Y}) - (\mathbf{X} - \tilde{\mathbf{X}}^{(k)}) \odot \boldsymbol{\eta}^{(k)}) \geq t(\mathbf{X}, \mathbf{Y} - \hat{g}(\mathbf{Z}; \mathbf{Z}, \mathbf{Y})) \right]}{1 + K}. \quad (20)$$

Note that, above, the i -th element of the column vector $(\mathbf{X} - \tilde{\mathbf{X}}^{(k)}) \odot \boldsymbol{\eta}^{(k)}$ is understood to be equal to $+\infty$ if $(\mathbf{X} - \tilde{\mathbf{X}}^{(k)})^i = 0$ and $\boldsymbol{\eta}^{(k)i} = +\infty$. If t is a *monotone rank statistic*, a property defined below that is stronger than Definition 2, then $\hat{p}_{q,c}$ is a valid p-value for testing the quantile null hypothesis $\mathcal{H}_{q,\leq,c}$ in (15).

Definition 3. A statistic $t : \mathbb{R}^{n \times 1} \times \mathbb{R}^{n \times 1} \rightarrow \mathbb{R}$ is a *monotone rank statistic* if

$$t(\mathbf{X}, \mathbf{Y}) = \sum_{i=1}^n X^i \phi(r^i(\mathbf{Y})), \quad (21)$$

for some increasing function $\phi : \mathbb{R} \rightarrow \mathbb{R}$, where $r^i(\mathbf{Y})$ is the rank of the i -th element of \mathbf{Y} .

Theorem 3. Fix any $q \in [n]$, $c \in \mathbb{R}$, and assume the partially linear model in (10) holds. If t in (20) is a monotone rank statistic and the quantile null hypothesis $\mathcal{H}_{q,\leq,c}$ in (15) is true, then, for any $\alpha \in (0, 1)$,

$$\mathbb{P}[\hat{p}_{q,c}(\mathbf{X}, \mathbf{Y}, \mathbf{Z}) \leq \alpha \mid \mathbf{Z}, \mathbf{Y}] \leq \alpha,$$

where $\hat{p}_{q,c}(\mathbf{X}, \mathbf{Y}, \mathbf{Z})$ is the QCRT p-value defined in (20).

The QCRT p-values based on monotone rank statistics can be repurposed to make lower-bound inferences on the quantiles of individual effects in (10), specifically by testing the following hypothesis instead of $\mathcal{H}_{q,\leq,c}$:

$$\mathcal{H}_{q,\geq,c} : \tau_{(q)} \geq c. \quad (22)$$

Proposition 2. Fix any $q \in [n]$, $c \in \mathbb{R}$, and assume the partially linear model in (10) holds. If t in (20) is a monotone rank statistic and the quantile null hypothesis $\mathcal{H}_{q,\geq,c}$ in (22) is true, then, for any $\alpha \in (0, 1)$,

$$\mathbb{P}[\hat{p}_{n-q,-c}(\mathbf{X}, \mathbf{Z}, -\mathbf{Y}) \leq \alpha \mid \mathbf{Z}, \mathbf{Y}] \leq \alpha,$$

where $\hat{p}_{n-q,-c}(\mathbf{X}, \mathbf{Z}, -\mathbf{Y})$ is defined as in (20).

3.4 Change of treatment reference in the QCRT

The monotone rank statistics defined in (21) introduce some asymmetry into the testing procedure, as they only weigh the outcomes of ‘‘treated’’ individuals i with $X^i = 1$. Alternatively, one can compute the p-values in (20) after swapping all $X^i = 0$ with $X^i = 1$ for all $i \in [n]$ and flipping the signs of the corresponding outcomes Y^i . This still yields a valid QCRT p-value for testing $\mathcal{H}_{q,\leq,c}$ in (15), and it may be more powerful than the original approach if the individuals with $X = 0$ outnumber those with $X = 1$.

Proposition 3. Fix any $q \in [n]$, $c \in \mathbb{R}$, and assume the partially linear model in (10) holds. If t in (20) is a monotone rank statistic and the quantile null hypothesis $\mathcal{H}_{q,\leq,c}$ in (15) is true, then, for any $\alpha \in (0, 1)$,

$$\mathbb{P}[\hat{p}_{q,c}(\mathbf{1} - \mathbf{X}, \mathbf{Z}, -\mathbf{Y}) \leq \alpha \mid \mathbf{Z}, \mathbf{Y}] \leq \alpha,$$

where $\hat{p}_{q,c}(\mathbf{1} - \mathbf{X}, \mathbf{Z}, -\mathbf{Y})$ is defined as in (20).

In practice, one can decide whether to carry out this change of reference prior to applying the QCRT, based on whether the expected proportion of individuals with $X = 1$ is larger than $1/2$; and this is how we proceed in this paper. The reference change does not invalidate the QCRT as long as the choice of whether to carry it out only depends on the conditional distribution of $X \mid Z$, not on the observed X . Of course, the same argument can also be extended to the QCRT p-value of Proposition 2 for testing $\mathcal{H}_{q,\geq,c}$ in (22).

3.5 Computationally efficient inversion of the QCRT

The monotonicity of t implies the p-values $\hat{p}_{q,c}$ in (20) are monotone increasing in c , for any $\{\mathbf{X}^{(k)}\}_{k=1}^K$. This enables a computationally efficient inversion of the QCRT to construct one-sided confidence bounds for any quantile $\tau_{(q)}$ of the individual effects. For this purpose, consider the one-sided interval $[\hat{L}_q(\alpha), \infty)$ with

$$\hat{L}_q(\alpha) = \inf \{c \in \mathbb{R} : \hat{p}_{q,c} > \alpha\}. \quad (23)$$

This is a valid confidence interval for $\tau_{(q)}$ conditional on \mathbf{Z} and \mathbf{Y} because, by Theorem 3,

$$\mathbb{P} [\tau_{(q)} \notin [\hat{L}_q(\alpha), \infty) \mid \mathbf{Z}, \mathbf{Y}] \leq \mathbb{P} [\hat{p}_{q,c} \leq \alpha \mid \tau_{(q)} \leq c \mid \mathbf{Z}, \mathbf{Y}] \leq \alpha.$$

Note that it could be very expensive to compute $\hat{L}_q(\alpha)$ by brute force, evaluating $\hat{p}_{q,c}$ separately for each possible c , if K is large. However, $\hat{L}_q(\alpha)$ can be approximated using a Markov chain Monte Carlo procedure whose updates involve a single realization of $\tilde{\mathbf{X}}$, as in [60, 61]. This Markov chain is initialized at a sufficiently small starting point (a fixed known lower bound) and then it is updated until it converges to $\hat{L}_q(\alpha)$. The procedure is outlined in Algorithm 1. As explained in Section 3.4, this method is applied after swapping the X labels if the individuals with $X = 0$ are expected to outnumber those with $X = 1$.

Algorithm 1: QCRT lower confidence bounds for a quantile of individual linear effects

```

Input: data  $\mathbf{X}, \mathbf{Y}, \mathbf{Z}$ , distribution of  $P_{X|Z}$ , target quantile level  $q$ , decreasing sequence  $\{\lambda_k\}_{k=1}^K$ ,  

confidence level  $\alpha \in (0, 1)$ ;  

Compute  $E = \sum_{i=1}^n \mathbb{P} [X^i = 1 \mid Z^i]$ ;  

if  $E < n/2$  then  

| Define  $\mathbf{X}' = \mathbf{1} - \mathbf{X}$ ,  $\mathbf{Y}' = -\mathbf{Y}$ ;  

else  

| Define  $\mathbf{X}' = \mathbf{X}$ ,  $\mathbf{Y}' = \mathbf{Y}$ ;  

end  

Fit an estimate  $\hat{g}$  of  $g$  in (10), using the data in  $\mathbf{Y}', \mathbf{Z}'$ ;  

Initialize  $L^{(1)}$  to a sufficiently small value ensuring  $L^{(1)} < \tau_{(q)}$ ;  

Compute  $T = t(\mathbf{X}', \mathbf{Y} - \hat{g}(\mathbf{Z}; \mathbf{Z}, \mathbf{Y}'))$  ;  

for  $k = 1, \dots, K - 1$  do  

| Define  $\boldsymbol{\eta}^{(k)}$  as in (19), using  $c = L^{(k)}$ ;  

| Sample the knockoffs  $\tilde{\mathbf{X}}'^{(k)}$  given the observed  $\mathbf{Z}$  based on  $P_{X'|Z}$ ;  

| Compute  $\tilde{T}^{(k)} = t(\tilde{\mathbf{X}}'^{(k)}, \mathbf{Y} - \hat{g}(\mathbf{Z}; \mathbf{Z}, \mathbf{Y}') - (\mathbf{X}' - \tilde{\mathbf{X}}^{(k)}) \odot \boldsymbol{\eta}^{(k)})$  ;  

| if  $\tilde{T}^{(k)} \leq T$  then  

| | Update  $L^{(k+1)} \leftarrow L^{(k)} + \lambda_k \alpha$ ;  

| else  

| | Update  $L^{(k+1)} \leftarrow L^{(k)} - \lambda_k (1 - \alpha)$ ;  

| end  

| end  

end  

Output:  $\hat{L}_q(\alpha) = L^{(K+1)}$ .
```

Under weak regularity conditions, standard arguments [61, 62] establish the output of Algorithm 1 converges in probability to the desired lower confidence limit $\hat{L}_q(\alpha)$. The idea is that $\hat{L}_q(\alpha)$ is a stationary point because the expected increment at the $k + 1$ -th step is:

$$\begin{aligned} \mathbb{E} [L^{(k+1)} - L^{(k)} \mid \mathbf{Z}, \mathbf{Y}] &= \lambda_k \left[\alpha \left(1 - \mathbb{P} [\tilde{T}^{(k)} \geq T \mid \mathbf{Z}, \mathbf{Y}] \right) - (1 - \alpha) \mathbb{P} [\tilde{T}^{(k)} \geq T \mid \mathbf{Z}, \mathbf{Y}] \right] \\ &= \lambda_k \left[\alpha - \mathbb{P} [\tilde{T}^{(k)} \geq T \mid \mathbf{Z}, \mathbf{Y}] \right] \\ &= \lambda_k \left[\alpha - \hat{p}_{q, L^{(k)}}^{\infty} (\mathbf{X}, \mathbf{Y}, \mathbf{Z}) \right], \end{aligned}$$

where $\hat{p}_{q,L^{(k)}}^\infty(\mathbf{X}, \mathbf{Y}, \mathbf{Z})$ is the ideal QCRT p-value given by (20) in the limit of $K \rightarrow \infty$. Therefore, the expected increment is zero if and only if the current estimate $L^{(k)}$ is the target lower confidence bound $\hat{L}_q(\alpha)$ in (23). If $L^{(1)} < \tau_{(q)}$ and λ_k decay sufficiently fast (i.e., $\lambda_k \sim k^{-1}$), standard Markov chain Monte Carlo arguments guarantee the convergence of $L^{(k)}$ to $\hat{L}_q(\alpha)$ as $k \rightarrow \infty$; see [61, 62]. The same convergence also holds with the analogous Algorithm A2 for computing upper confidence bounds, in Appendix A1.5.

4 Numerical experiments with synthetic data

4.1 Individualized conditional testing

The empirical performance of the SKF from Section 2 is investigated here through numerical experiments. For this purpose we generate synthetic data with 20 binary variables and 80 covariates. The first 20 covariates are sampled from independent Bernoulli distributions with success probability equal to 0.5. The remaining 60 covariates follow a Gaussian autoregressive model of order one with correlation parameter 0.5. The outcome is generated from a linear model with heterogeneous effects and homoscedastic standard Gaussian noise. The linear coefficients in this model are zero for half of the variables, for all of the binary covariates, and for half of the 60 continuous covariates. That is, the expected outcome for the i -th individual is

$$\mathbb{E} \left[Y^{(i)} \mid X^{(i)}, Z^{(i)} \right] = \sum_{j=1}^p X_j^{(i)} \beta_j^{(i)} + \sum_{j=21}^m Z_j^{(i)} \gamma_j, \quad \beta_j^{(i)} = \bar{\beta}_j Z_{l_{j,1}}^{(i)} Z_{l_{j,2}}^{(i)}, \quad (24)$$

for $p = 20$ and $m = 80$. Above, the β coefficients are individual-specific, while the γ are constant. The constant non-zero $\bar{\beta}$ and γ are initialized with absolute value equal to 4 and independent random signs. Then, separately for each variable j and individual i , the individualized coefficient $\beta_j^{(i)}$ is set equal to the product of $\bar{\beta}_j$ and the two binary covariates $Z_{l_{j,1}}$ and $Z_{l_{j,2}}$, for some $l_{j,1}, l_{j,2} \in [20]$. Thus, each variable X_j has an effect on Y only within the sub-population with $Z_{l_{j,1}} = 1$ and $Z_{l_{j,2}} = 1$, which contains approximately 1/4 of all individuals if $l_{j,1} \neq l_{j,2}$. The indices $l_{j,1}, l_{j,2}$ are sampled with replacement from $\{1, \dots, 20\}$, independently for each j . Our goal is to discover which variables are non-null within which sub-populations, as powerfully (more numerous findings) and precisely (smaller sub-populations) as possible. Figure 1, previewed in Section 2.3, reports the performance of the SKF applied to these data over 100 independent experiments. The results confirm empirically the validity of our method and demonstrate its competitive performance compared to the naive, data-splitting, and vanilla knockoff filter benchmarks.

Next, we investigate the performance of the SKF in a “transfer learning” setting inspired by [41, 63]. The goal is complementary to that of the previous experiments: we wish to detect variables with a robust association across sub-populations with different covariate distributions. In other words, we want to find which variables maintain their association with Y within a future data set with covariate shift, in which the distribution of Z differs from the current one but the true model for $Y \mid X, Z$ is the same [63]. To simulate this scenario, we generate data from a model similar to that in (24), but now only half of the non-null variables interact with the covariates; i.e., $\beta_j^{(i)} = \bar{\beta}$ for half of the variables. Further, the data dimensions are increased to ensure sufficiently many discoveries can be made. Specifically, the number of variables is $p = 40$, while the number of covariates is $m = 160$, of which 120 are continuous. The covariate shift is imagined to be such that the 40 binary covariates are always equal to zero instead of following a symmetric Bernoulli distribution. Therefore, the goal is to identify the 20 variables whose association does not involve interactions, as the covariate shift would make the others irrelevant. These data are analyzed as in the previous experiments, with the only difference that the SKF from Section 2 is replaced by its robust version outlined in Appendix A1.3, which is designed to test partial conjunctions [64, 65] of the random conditional independence hypotheses in (5).

Figure 3 shows the results of 100 independent experiments in the transfer learning setup described above, as a function of the sample size. The performance of the robust version of the SKF is quantified in terms

of the empirical false discovery rate, the power, and the homogeneity of the reported findings, separately within the training population and under covariate shift. In the latter case, only the discoveries of variables with a direct conditional association with the outcome (i.e., not mediated by any covariate interactions) are counted as true, while the others are considered false positives. Therefore, neither the naive benchmark nor the vanilla knockoff filter control this notion of false discovery rate under covariate shift because they tend to report all associated variables, including those that are non-null only thanks to interactions. By contrast, our method empirically controls the false discovery rate even under covariate shift. The data-splitting benchmark here is a modified version of our robust SKF in which half of the observations are used for partitioning the covariate space, without randomly swapping the knockoffs, and the remaining half are utilized for testing the selected hypotheses. The results demonstrate data-splitting is valid under covariate shift but it is not as powerful as our method, especially if the sample size is moderately large.

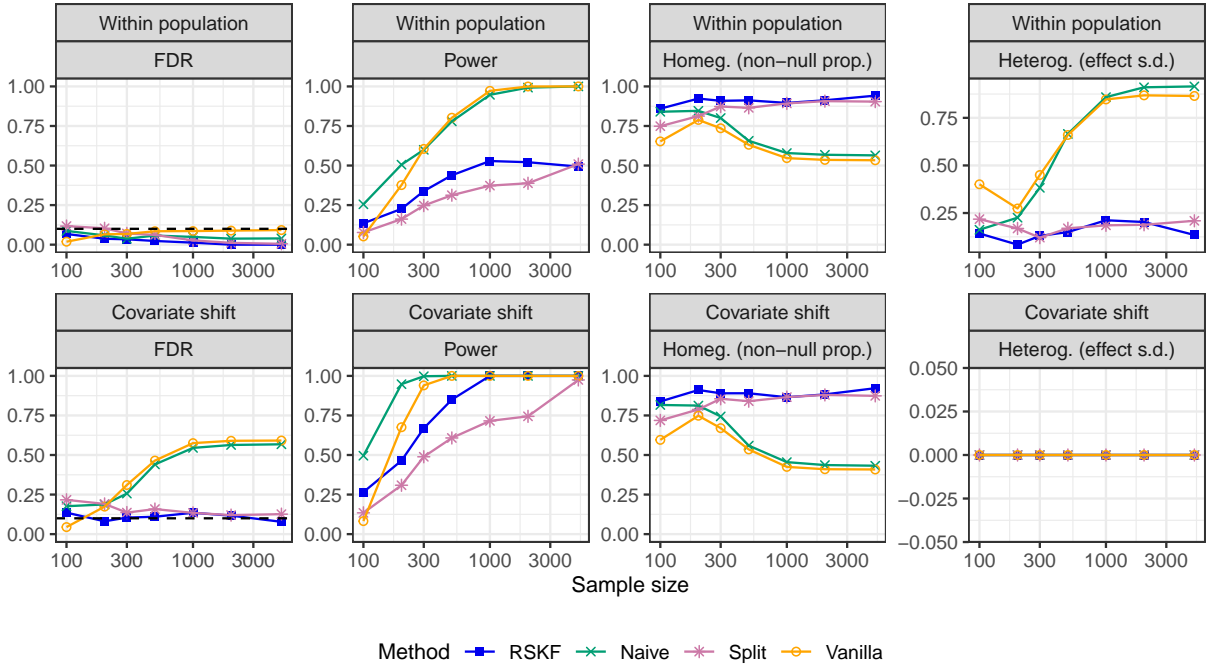


Figure 3: Performance of the robust SKF and alternative benchmarks for individualized conditional testing under covariate shift, in simulations with synthetic data. The findings summarized in the bottom panel are counted as true if and only if they report a variable whose conditional association with the outcome is robust to changes in the covariate distribution. Other details are as in Figure 1.

4.2 Lack of robustness of sharp CRT inferences

In this section, we demonstrate empirically that inverting the standard CRT for sharp hypotheses does not lead to reliable confidence intervals. In fact, these inferences are not robust to individual heterogeneity in the partially linear model effects. For this purpose, synthetic data with a continuous outcome, 2 binary variables, and 8 covariates are generated as follows. The first 2 covariates are sampled from independent Bernoulli distributions with success probability equal to 0.5. The remaining 6 covariates are independent standard Gaussian. The outcome is generated from a linear model with heterogeneous effects and homoscedastic standard Gaussian errors, as in the previous section. The linear coefficients in this model are zero for the one treatment variable, for all of the binary covariates, and for 3 of the 6 continuous covariates. Thus, the

expected value of the outcome for the i -th individual is

$$\mathbb{E} \left[Y^{(i)} \mid X^{(i)}, Z^{(i)} \right] = X_1^{(i)} \beta_1^{(i)} + \sum_{j=5}^{10} Z_j^{(i)} \gamma_j, \quad \beta_j^{(i)} = \bar{\beta}_1 Z_{l_1}^{(i)} Z_{l_2}^{(i)}. \quad (25)$$

Above, the β_1 coefficients are individual-specific, while the γ coefficients for the covariates are constant. The constant non-zero coefficients $\bar{\beta}_1$ and γ_j are initialized with absolute value equal to 2 and independent random signs. Then, separately for each individual i , the individualized coefficients $\beta_1^{(i)}$ is set equal to the product of $\bar{\beta}_1$ and the two binary covariates Z_{l_1} and Z_{l_2} , for some $l_1, l_2 \in [4]$. Thus, X_1 is effective within the sub-population with $Z_{l_1} = 1$ and $Z_{l_2} = 1$ (which contains approximately 1/4 of all individuals if $l_1 \neq l_2$), and only within it. The indices l_1, l_2 are sampled with replacement from $\{1, \dots, 4\}$. The goal is to construct a confidence interval for the average effect size, $\bar{\beta}_1 \cdot (1/n) \sum_{i=1}^n Z_{l_1}^{(i)} Z_{l_2}^{(i)}$ by inverting the sharp CRT.

Figure 4 reports the performance of the confidence intervals thus obtained in terms of empirical coverage and length, as a function of the sample size, averaging over 100 experiments. The results show inverting the sharp CRT yields confidence intervals with lower coverage than expected. In fact, their coverage may even be zero, depending on the choice of statistics. Statistics based on three alternative models are considered here: a standard lasso fitted on all variables [7]; a fast leave-one-out version of the latter inspired by [52], as detailed in Appendix A1.4; and a standard lasso as in [7] but fitted on all variables and all pairwise interaction terms with the covariates. The first two statistics lead to empirical coverage that steadily decreases as the sample size grows. Indeed, these statistics rely on models that cannot explain the underlying heterogeneity in the data, while the CRT becomes more and more likely to reject the false sharp null in (11) as the number of observations grows, thus leading to empty confidence intervals. By contrast, the coverage of intervals calculated based on the lasso model with interactions does not monotonically decrease with n ; instead, a sufficiently large sample size allows this model to partly explain away the effect size heterogeneity, thereby mitigating the implicit mis-specification in the tested sharp hypotheses (11). Nonetheless, the procedure remains generally invalid. The following additional results can be found in Appendix A2.1. Figure A4 reports on analogous simulations in which each variable interacts with only one covariate instead of two. Figure A5 shows the naive randomization confidence intervals are valid if the data follow a homogeneous partially linear model without interactions. Finally, Figure A6 confirms empirically the validity in this setting of the confidence bounds obtained with our proposed QCRT from Section 3, as anticipated by the theory.

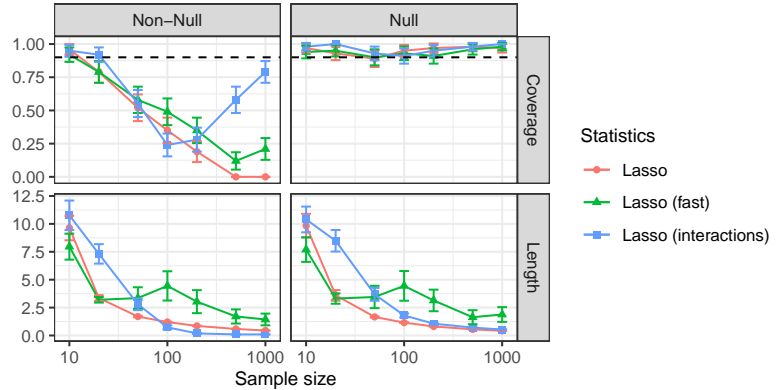


Figure 4: Performance of naive confidence intervals obtained by inverting the standard sharp CRT, on synthetic data following a partially linear model with interactions. The horizontal dashed line indicates the nominal 90% coverage level. Left: intervals for a non-null variable. Right: intervals for a null variable.

4.3 Quantile conditional randomization inferences

In this section, we investigate the performance of the QCRT and of its corresponding confidence bounds on synthetic data with a continuous outcome, p binary variables, and m covariates. The first p covariates are sampled from independent Bernoulli distributions with success probability equal to 0.5, while the remaining $m - p$ ones are from a Gaussian autoregressive model of order one with correlation parameter 0.5. The outcome is generated from a linear model with heterogeneous effects and homoscedastic standard Gaussian errors. The linear effects are zero for half of the variables, for the binary covariates, and for half of the $m - p$ continuous covariates. Thus, the expected outcome for the i -th individual is similar to (24):

$$\mathbb{E} \left[Y^{(i)} \mid X^{(i)}, Z^{(i)} \right] = \sum_{j=1}^p X_j^{(i)} \beta_j^{(i)} + \sum_{j=p+1}^m Z_j^{(i)} \gamma_j, \quad \beta_j^{(i)} = \bar{\beta}_j^{(i)} Z_{l_{j,1}}^{(i)} Z_{l_{j,2}}^{(i)}, \quad (26)$$

with the difference that $\bar{\beta}_j^{(i)}$ now depends on i . The $\bar{\beta}_j^{(i)}$ coefficients are independent Gaussian with mean ± 4 and unit variance for each individual and non-null variable. The signs of the Gaussian means are determined by independent coin flips for each j . As in Section 4.1, each $\beta_j^{(i)}$ is the product of $\bar{\beta}_j^{(i)}$ and two randomly chosen binary covariates $Z_{l_{j,1}}$ and $Z_{l_{j,2}}$, for some $l_{j,1}, l_{j,2} \in [20]$. Thus, X_j has a non-zero individual effect only within the sub-population with $Z_{l_{j,1}} = 1$ and $Z_{l_{j,2}} = 1$, which contains approximately 1/4 of all individuals if $l_{j,1} \neq l_{j,2}$. Our goal is to make inferences about quantiles of the distribution of $\beta_j^{(i)}$.

Figure 5 reports on 100 independent experiments in which the QCRT p-values from Section 3.3 are computed for the null hypothesis in (15) that the 90% quantile of individual effects is below 2. The performance of our method is quantified in terms of the probability of rejection at level $\alpha = 0.05$, separately for a null and a non-null variable; note that in the former case the type-I error rate is shown, while in the latter the power is shown. Here, $p = 2$, $m = 6$, and the sample size is varied from 10 to 5000. Two variations of the QCRT p-values are computed: with (multivariate approach) and without (univariate approach) estimating the nuisance function g in (10) through a cross-validated lasso fitted on all variables except the one currently tested. The results demonstrate the multivariate approach is more powerful, especially if the sample size is moderate. Both approaches control the type-I errors, as anticipated by the theory.

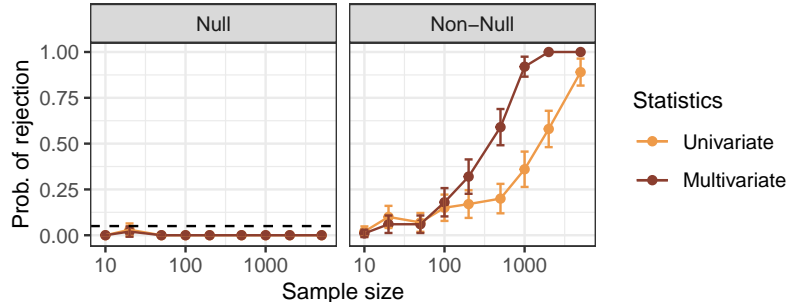


Figure 5: Rejection probability for the univariate and multivariate QCRT in simulations with synthetic data, as a function of the sample size. The tested hypothesis is that the 90% quantile of individual effects is below 2. Left: true null. Right: false null. The significance level is 5% (horizontal dashed line).

Figure A7 in Appendix A2.2 demonstrates the advantage of adaptively flipping the reference labels in the QCRT, as discussed in Section 3.4. Here, the experiments of Figure 5 are repeated with 1000 samples, varying the proportion of individuals with $X = 1$. The results demonstrate the QCRT always controls the type-I errors but its power is affected by the choice of reference labels. In particular, the power is maximized if the reference is set to the majority label (“treated” or “control”), as anticipated in Section 3.4. Figure A8 reports on experiments analogous to those in Figure 5, with the difference that the tested quantile q in $\mathcal{H}_{q,\leq,c} : \tau_{(q)} \leq c$, from (15), is now varied as a control parameter, for different target constant bounds c .

Again, the results confirm empirically the multivariate implementation of the QCRT is more powerful than its univariate version. This can also be seen in Figure A9, where the experiments are performed by varying the target constant bound c for the 90-th quantile of the individual effects, with different sample sizes.

Figure 6 visualizes confidence bounds obtained by inverting the QCRT as explained in Section 3.5. In these experiments, $p = 4$, $m = 16$, and the sample size is varied as a control parameter. The values of $\bar{\beta}_j^{(i)}$ in (26) for the non-null variables are sampled independently for each individual from a Gaussian distribution with mean ± 2 and unit variance; the signs of these means are determined as independent coin flips for each j . The confidence bounds are plotted separately for a null variable whose true quantile of interest is 0, and for a non-null one whose true quantile is positive. The results show our calculated lower and upper bounds approach the true target quantiles as the sample size increases, and the multivariate statistics are more powerful. Note that here the proportion of samples receiving $X = 1$ is 0.24; see Figure A10 in Appendix A2.2 for similar results from experiments in which the proportion of samples receiving $X = 1$ is 0.76. Finally, Figures A11–A12 visualize the empirical coverage and average distance from the true target quantile of the above lower bounds for the 90% quantile of individual effects in the partially linear model, as a function of the sample size. These results show the theoretical coverage holds in practice and the multivariate QCRT yields tighter bounds, regardless of the proportion of $X = 1$. Figures A13–A14 report analogous results separately for variables with positive and negative average effects.

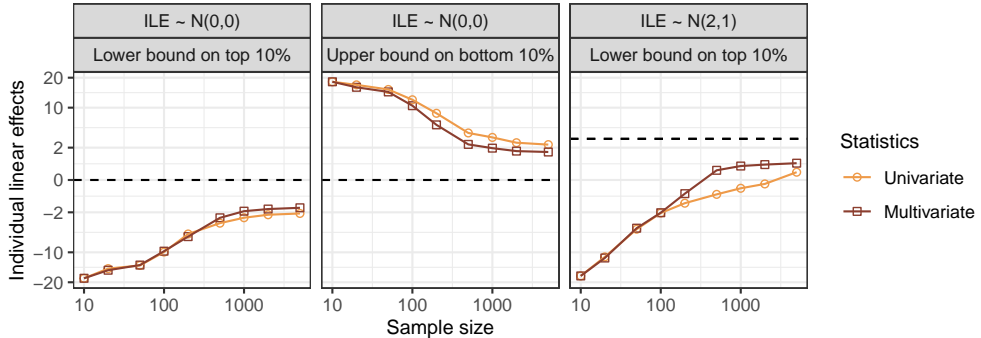


Figure 6: Bounds at confidence level 90% for quantiles of individual effects computed by inverting the QCRT in simulations with synthetic data. Left: lower bounds for the 90% quantile of individual linear effects (ILE) equal to 0. Center: upper bounds for the 90% quantile of individual linear effects equal to 0. Right: 90% lower bounds for the 10% quantile of individual linear effects following a normal distribution with mean 2 and variance 1. The dashed horizontal lines indicate the true quantiles. Other details are as in Figure 5.

5 Application

5.1 Data description

We consider a data set from a 2-week long randomized experiment involving 80,000 blood donors in China [13], which was designed to investigate the effectiveness of different interventions to incentivize past donors to make a new donation. At the beginning of the experiment, 80,000 individuals were randomly divided into 7 groups: a control group of size 14,000 and 6 treated groups of size 11,000 each. The treated groups received a text message with a reminder to donate, while the control group received nothing. The messages for treated groups 2–5 also contained further encouragement to donate: the promise of an individual monetary reward (equivalent to \$5.00–\$8.30, depending on the amount of blood donated) for group 2; a suggestion to bring a friend for group 3, both the individual monetary reward and the friend suggestion for group 4; a suggestion to bring a friend and the promise of a group reward (equivalent to the individual reward) for group 5; a suggestion to bring a friend, the promise of a group reward (as for the previous group), and the promise of

a small extra gift for group 6. See Table 2 for a summary of this experimental design. By the end of the experiment, 797 individuals donated blood (approximately 1%). In addition to the treatment assignments and observed binary outcomes (donate or not donate), this data set contains individual covariates including age, sex, weight, blood type, marital status, education level, occupation, residency status (local or non-local), and time since the last blood donation. Missing covariate values (less than 4%) are imputed with the corresponding sample median (or mode, for categorical covariates).

Table 2: Randomized treatment-control assignments in a field experiment conducted by [13] to investigate the effectiveness of different incentives for blood donors.

Assignment	Size	Treatments (X_1, \dots, X_5)				
		Reminder	Individual reward	Friend	Group reward	Group gift
Control group	14k	0	0	0	0	0
Treated group 1	11k	1	0	0	0	0
Treated group 2	11k	1	1	0	0	0
Treated group 3	11k	1	0	1	0	0
Treated group 3	11k	1	1	1	0	0
Treated group 4	11k	1	1	1	0	0
Treated group 5	11k	0	1	1	1	0
Treated group 6	11k	1	1	1	0	1

5.2 Data analysis

We begin by testing the conditional independence hypotheses that each treatment in Table 2 has no effect on the outcome, across the whole population, conditional on the other treatments and covariates. The standard model-X knockoff filter and the CRT [7] are applied utilizing synthetic treatments simulated as explained in the next paragraph. As discussed in Section 2.1, these methods yield causal inferences for randomized experiments; indeed, there can be no confounding here because the treatments are independent of any unobserved covariates. At the same time, our analysis does take advantage of the observed covariate information through the multivariate predictive model utilized to compute the test statistics. The latter are calculated as in Section 2.5, with sparse logistic regression including all pairwise interactions between the treatment and the covariates. Next, the SKF from Section 2 is applied to investigate possible interactions between the treatments and the covariates. In particular, we proceed as in Section 2.4, using sparse logistic regression on data with randomly swapped knockoffs to detect up to two possible interacting covariates for each treatment. For simplicity, we only consider interactions with the following eight binary features: age (< 25 or ≥ 25), sex (male or female), Rh negative (yes or no), married (yes or no), education (< 16 years or ≥ 16 years), student (yes or no), resident (local or not), recent donor (within 12 months or not).

To simplify the task of generating synthetic CRT treatments and knockoffs, we approximate the joint distribution of the binary treatment variables X_1, \dots, X_5 by imagining different individuals were assigned to one of the six possible groups in Table 2 independently of one another, with probability proportional to the observed group size. This model is not completely accurate since the group sizes were in truth fixed a priori, but the simplification is useful because it leads to a manageable joint treatment distribution for which exact knockoffs can be generated by the Metropolized algorithm of [20]. For example, note that our model implies $\mathbb{P}[(X_1, \dots, X_5) = (0, 0, 0, 0, 0)] = 14/80$, while other joint probabilities can be similarly computed from Table 2. Goodness-of-fit diagnostics for the knockoffs thus obtained are reported in Tables A1–A2, Appendix A3.1. Synthetic CRT treatments can be easily sampled based on analogous conditional probabilities computed from Table 2; e.g., $\mathbb{P}[X_1 = 1 | X_2, \dots, X_5] = 11/25$ if $(X_2, \dots, X_5) = (0, \dots, 0)$ and $\mathbb{P}[X_1 = 1 | X_2, \dots, X_5] = 1$ otherwise. In principle, it would also be possible to generate synthetic CRT treatments and knockoffs without the above independence assumption, as in [16], but that would require ad-hoc techniques which we do not discuss here for lack of space. In any case, the independence assumption should have little impact on the practical validity of our tests given that the sample size is quite large.

Table 3 summarises the results of our analyses. The vanilla knockoff filter is applied at the 10% level, without the conservative “+1” correction needed for theoretical false discovery rate control because the total number of tests is small [19]. As the findings are randomized, the analysis is repeated 100 times with independent realizations of the knockoff treatments, as in [7, 9]. Three treatments are consistently selected by the knockoff filter: the reminder, the individual reward, and the group reward. These are also selected by the Benjamini-Hochberg procedure applied to the CRT p-values based on 10,000 realizations of the synthetic treatments. Note that the CRT p-values for different treatments are not independent of one another, but the Benjamini-Hochberg procedure is practically quite robust to p-value dependencies [53, 56]. It is interesting to compare these findings to those obtained with classical multivariate logistic regression based on the same covariates but without interactions: in this case, only the reminder and the group reward are significant. This suggests our randomization methods are more powerful than the parametric approach despite the stronger assumptions of the latter, likely due to the relatively high dimensions. Unfortunately, including pairwise interactions in the logistic regression model would yield uninformative results due to perfect data separation. Table 3 also reports marginal p-values computed with Fisher’s exact test for each treatment. It must be emphasized that marginal p-values test completely different hypotheses than ours because they do not account for possible confounding across the mutually dependent treatment variables. In particular, the significance of the marginal p-value for the “friends request” may be solely due to that treatment being often applied in combination with the individual reward, and it does not imply that the “friends request” by itself has any effect whatsoever on the donation outcome. By contrast, conditional independence hypotheses speak directly as to the causal effectiveness of each distinct treatment, either at the population-wide level or within a specific sub-population. The SKF reports on average three such conditional associations involving the interaction of a treatments and a binary covariate; of these, one is consistent across most realizations of the knockoffs, while the other two are reported at least 20% of the time.

Table 3: Analysis of the blood donation randomized experiment data in Table 2. The percentages in the second and third columns indicate the frequency with which findings are reported over 100 sets of knockoffs. For the SKF, the parentheses indicate the sub-population in which the treatment is discovered. The p-values in parentheses are adjusted with the Benjamini-Hochberg procedure; asterisks mark those below 0.1.

Treatment	Discovered with knockoffs		P-value		
	Vanilla	SKF	CRT	Logistic regression	Marginal
Reminder	80%	70% (Married)	0.011 (0.032)*	0.026 (0.075)*	<0.001 (<0.001)*
Individual reward	59%	31% (Male)	0.031 (0.052)*	0.063 (0.106)	0.007 (0.019)*
Friends request	1%		0.701 (0.701)	0.600 (0.700)	0.024 (0.040)*
Group reward	74%	38% (Married)	0.013 (0.033)*	0.030 (0.075)*	0.049 (0.062)*
Small group gift	5%		0.455 (0.568)	0.680 (0.680)	0.134 (0.134)

Unfortunately, positive outcomes in this randomized experiment are relatively rare (fewer than 800) and this paucity of data constrains the number of discoveries that can be made. This limitation motivates additional semi-synthetic analyses in which the blood donations are replaced by artificial outcomes simulated from an imaginary causal model conditional on the treatments and covariates. This setup remains quite realistic, as it involves real explanatory variables, but it reduces the outcome imbalance and thus increases the effective sample size. Consequently, the analysis will provide a more informative demonstration of the potential effectiveness of the proposed methodology applied to large data sets. This is especially advantageous for knockoff-based methods, which perform best when applied to data for which more discoveries can be made [7, 48]. Further, as the ground truth is known exactly in such a controlled setting, we will have access to useful diagnostics such as the type-I errors.

5.3 Numerical experiments with synthetic outcomes

For each of the 80,000 individuals in the blood donation data, an imaginary binary outcome is simulated from a logistic model based on the m real covariates $Z \in \mathbb{R}^m$ and the treatment variables $X \in \mathbb{R}^5$:

$$\text{logit}(\mathbb{P}[Y = 1 | X, Z]) = -c + \sum_{j=1}^m Z_j b_j + a \sum_{j=1}^5 X_j \cdot g_j(Z), \quad (27)$$

where $c \in \mathbb{R}$ is an intercept, $b_1, \dots, b_m \in \mathbb{R}$ are linear coefficients for the m covariates, and each g_j is a binary-valued non-linear function of Z ; see Appendix A3.2 for details. The first treatment (text reminder) is effective for individuals who did not donate in the past 12 months and for those who are non-residents. The individual reward is effective for students, and twice as much for those who are male. The friends request is effective for female or unmarried individuals. The group reward is effective for males or students. The small gift is effective for individuals with fewer than 16 years of education. The goal is to discover which treatments are effective within which sub-populations, as powerfully and precisely as possible. The SKF is applied as in the previous section, but defining the selective hypotheses based on the top two (instead of one) candidate covariates selected by the lasso model fitted on the data with randomly swapped knockoffs.

Figure 7 summarizes the results of 100 experiments with independent knockoffs and imaginary outcomes, as a function of the sample size. An independent random subset of all 80,000 individuals is analyzed in each experiment. The performance of the SKF is quantified in terms of false discovery rate and power, as well as in terms of the relative homogeneity of the selected hypotheses, measured as in Section 4.1. The same benchmarks as in Section 4.1 are considered. The results confirm the SKF controls the false discovery rate, as predicted by the theory, while achieving higher power compared to data splitting. As expected, the naive benchmark does not control the false discovery rate, while the vanilla knockoff filter can only discover population-wide associations that completely ignore the underlying heterogeneity of the causal effects. The full list of discoveries obtained by the SKF in the first numerical experiment with sample size 80,000 is reported in Table 4. Among the 11 findings, that of the friends request among unmarried females has the largest test statistic; indeed, this treatment has a causal effect for all those individuals. Although no type-I errors are made in this case, not all findings are equally informative. For example, the reminder can be effective among both male and female residents, but the SKF does not tell us it is only causal for the 60% of them who are married. In fact, this interaction is not discovered by the SKF because the initial model fitted on the data with randomly swapped knockoffs did not select the corresponding covariate.

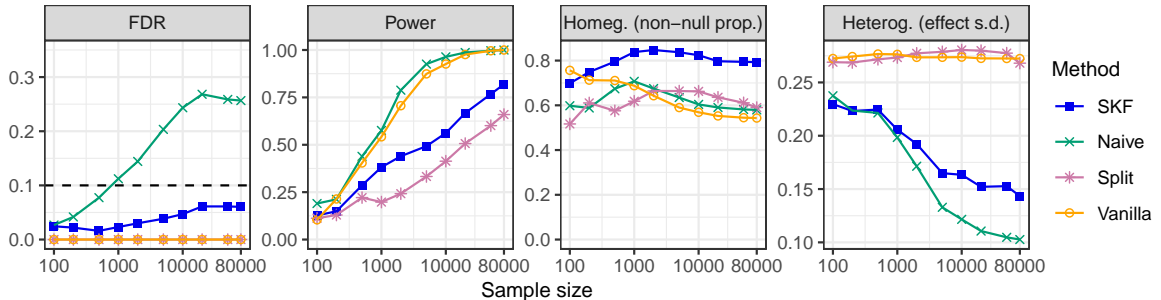


Figure 7: Performance of the SKF and benchmarks in simulations based on real covariates and treatment variables from the randomized blood donation experiment in Table 2. Other details are as in Figure 1.

Table 4: Discoveries reported by the SKF in the analysis of semi-synthetic blood donation data, as in Figure 7. The sample size here is equal to 80,000 and the nominal false discovery rate is 10%.

Treatment	Sub-population	Truth	W	Homeg.	Heterog.	Samples
Reminder	Resident : 0 and Male : 1	Non-null	5.94	1.00	0.19	32,550
	Resident : 0 and Male : 0	Non-null	5.47	1.00	0.19	19,866
	Resident : 1 and Male : 1	Non-null	2.55	0.63	0.19	16,037
	Resident : 1 and Male : 0	Non-null	2.24	0.64	0.19	11,547
Individual reward	Rh-negative : 1 and Student : 1	Non-null	7.81	1.00	0.20	142
	Rh-negative : 0 and Student : 1	Non-null	7.12	1.00	0.20	26,043
Friends request	Married : 0 and Male : 0	Non-null	8.54	1.00	0.00	22,547
	Married : 0 and Male : 1	Non-null	4.37	1.00	0.00	34,240
	Married : 1 and Male : 0	Non-null	3.83	1.00	0.00	8,866
Group reward	Student : 1 and Married : 0	Non-null	4.43	1.00	0.20	25,915

Finally, we turn to estimating the distribution of individual treatment effects. As the QCRT from Section 3 is limited to continuous outcomes, we replace the logit link in the data generating model (27) with a linear link, and we simulate continuous outcomes with Gaussian errors; see Appendix A3.2 for details. This setup is appropriate for the QCRT because the right-hand-side of (27) is a partially linear model with respect to each treatment. Figure 8 reports the results of 100 independent experiments as a function of the sample size. The QCRT is separately applied in its univariate version and in its multivariate version leveraging a lasso model as \hat{g} , with and without interactions. The goal is to estimate a lower bound for the 90-th quantile of the individual treatment effects of the reminder, at the 90% confidence level. The performance is quantified in terms of empirical coverage and mean absolute distance from the true quantile of interest. The results confirm the coverage is valid, while the distance of the calculated bound from the true quantile decreases as the sample size increases. Note that this problem is not easy because the CQRT makes no parametric assumptions beyond the relatively mild partially linear model. Yet, it discovers with relatively moderate sample sizes that at least 10% of the individuals have a quite large and positive response to the reminder. The ground truth here is the following: approximately 10,000 individuals have no response to this treatment, 35,000 have an individual treatment effect equal to 1, and 35,000 have an individual treatment effect equal to 2. Therefore, the true 90-th quantile is 2, while our lower bound is approximately 1 when the sample size is above 1000 and the test statistics are based on the lasso with interactions. Analogous results for the group reward treatment are reported in Figure A15, Appendix A3.3.

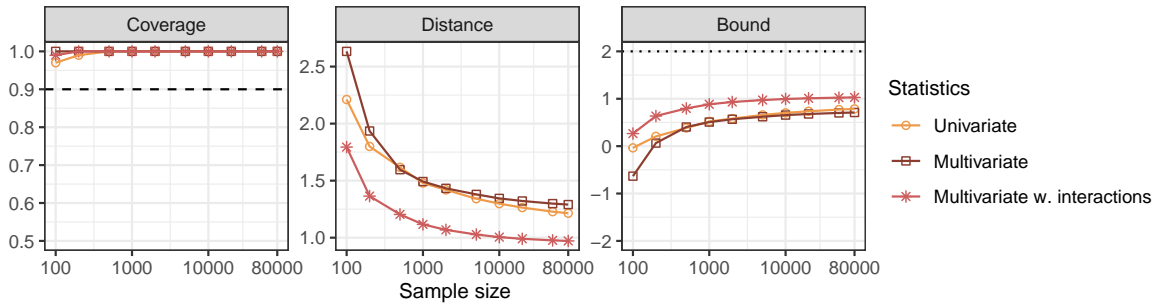


Figure 8: Confidence bounds for the 90% quantile of individual treatment effects in a simulation based on real covariates and treatments from the randomized blood donation experiment in Table 2. The QCRT is applied with three alternative test statistics. The dashed horizontal line marks the nominal 90% coverage level. The dotted horizontal line indicates the true quantile of interest.

6 Discussion

This paper has extended the model-X methodology of [7] to produce more informative inferences in the presence of unknown sample heterogeneity. This methodology is relevant within many applications in which data are gathered from mixture populations or involve unknown interaction effects. Flexibility is the key strength of our proposed SKF and QCRT: these methods can borrow strength from powerful multivariate models and sophisticated machine learning algorithms without having to rely on the validity of their assumptions about the unknown distribution of the outcome, or on the appropriateness of any asymptotic approximations. Instead, provably valid finite-sample inferences are derived under the sole assumption that the joint distribution of the explanatory variables is known. This model-X framework may not be well suited to all applications, but at least its assumptions are placed on measurable quantities and can sometimes be practically disproved [8, 66]. Further, the model-X framework is especially well-suited to the analysis of data from high-dimensional randomized experiments and genome-wide association studies [9].

Future research projects may investigate extensions of the QCRT beyond partially linear models with a continuous outcome and a binary treatment variable, or apply the methods developed in this paper to genome-wide association data, such as those collected by the UK Biobank [67] or the Million Veteran Program [68]. The populations sampled by modern genetic studies can be very heterogeneous [2], and the SKF may be particularly helpful to detect gene-gene and gene-environment interactions [69–73]. Further, the abundance of variables and observations in those studies will translate into further advantages for our methodology, which generally tends to perform better when applied to larger-scale data sets. Of course, computing powerful test statistics based on extremely big data sets raises additional computational challenges, but the model-X framework has already been demonstrated to be quite scalable [16, 48, 52, 74].

Software availability

A software implementation of the methods presented in this paper is available online at <https://github.com/msesia/i-modelx>, along with the code needed to reproduce our data analyses and simulations.

References

- [1] V. Tam, N. Patel, M. Turcotte, Y. Bossé, G. Paré, and D. Meyre. “Benefits and limitations of genome-wide association studies”. In: *Nat. Rev. Genet.* 20.8 (2019), pp. 467–484.
- [2] R. E. Peterson, K. Kuchenbaecker, R. K. Walters, C.-Y. Chen, A. B. Popejoy, S. Periyasamy, M. Lam, C. Iyegbe, R. J. Strawbridge, L. Brick, et al. “Genome-wide association studies in ancestrally diverse populations: opportunities, methods, pitfalls, and recommendations”. In: *Cell* 179.3 (2019), pp. 589–603.
- [3] D. Brzyski, C. B. Peterson, P. Sobczyk, E. J. Candès, M. Bogdan, and C. Sabatti. “Controlling the rate of GWAS false discoveries”. In: *Genetics* 205.1 (2017), pp. 61–75.
- [4] G. George, M. R. Haas, and A. Pentland. *Big data and management*. 2014.
- [5] R. Bapna and A. Umyarov. “Do your online friends make you pay? A randomized field experiment on peer influence in online social networks”. In: *Manag. Science* 61.8 (2015), pp. 1902–1920.
- [6] S. Aral and D. Walker. “Creating social contagion through viral product design: A randomized trial of peer influence in networks”. In: *Manag. Science* 57.9 (2011), pp. 1623–1639.
- [7] E. Candès, Y. Fan, L. Janson, and J. Lv. “Panning for Gold: Model-X Knockoffs for High-dimensional Controlled Variable Selection”. In: *J. R. Stat. Soc. B.* 80 (2018), pp. 551–577.
- [8] Y. Romano, M. Sesia, and E. Candès. “Deep Knockoffs”. In: *J. Am. Stat. Assoc.* 0.ja (2019), pp. 1–27.

[9] M. Sesia, C. Sabatti, and E. Candès. “Gene hunting with hidden Markov model knockoffs”. In: *Biometrika* 106 (2019), pp. 1–18.

[10] S. Bates, M. Sesia, C. Sabatti, and E. Candès. “Causal inference in genetic trio studies”. In: *Proc. Natl. Acad. Sci. U.S.A.* 117.39 (2020), pp. 24117–24126.

[11] S. Aral and D. Walker. “Identifying influential and susceptible members of social networks”. In: *Science* 337.6092 (2012), pp. 337–341.

[12] E. Bakshy, D. Eckles, R. Yan, and I. Rosenn. “Social influence in social advertising: evidence from field experiments”. In: *Proceedings of the 13th ACM conference on electronic commerce*. 2012, pp. 146–161.

[13] T. Sun, G. Gao, and G. Z. Jin. “Mobile messaging for offline group formation in prosocial activities: A large field experiment”. In: *Manag. Science* 65.6 (2019), pp. 2717–2736.

[14] T. Sun, S. Viswanathan, and E. Zheleva. “Creating social contagion through firm-mediated message design: Evidence from a randomized field experiment”. In: *Manag. Science* (2020).

[15] T. Sun and S. J. Taylor. “Displaying things in common to encourage friendship formation: A large randomized field experiment”. In: *Quantitative Marketing and Economics* 18 (2020), pp. 237–271.

[16] M. Sesia, S. Bates, E. Candès, J. Marchini, and C. Sabatti. “False discovery rate control in genome-wide association studies with population structure”. In: *Proc. Natl. Acad. Sci. U.S.A.* 118.40 (2021).

[17] P. M. Robinson. “Root-N-consistent semiparametric regression”. In: *Econometrica* (1988), pp. 931–954.

[18] A. Gelman. “Why it doesn’t make sense in general to form confidence intervals by inverting hypothesis tests”. In: *Statistical Modeling, Causal Inference, and Social Science (blog)*, August 25 (2011).

[19] R. F. Barber and E. Candès. “Controlling the false discovery rate via knockoffs”. In: *Ann. Stat.* 43.5 (2015), pp. 2055–2085.

[20] S. Bates, E. Candès, L. Janson, and W. Wang. “Metropolized knockoff sampling”. In: *J. Am. Stat. Assoc.* (2020), pp. 1–15.

[21] R. F. Barber, E. Candès, and R. J. Samworth. “Robust inference with knockoffs”. In: *Ann. Stat.* 48.3 (2020), pp. 1409–1431.

[22] J. Liu and P. Rigollet. “Power analysis of knockoff filters for correlated designs”. In: *Adv. Neural Inf. Process. Syst.* (2019).

[23] E. Katsevich and A. Ramdas. “On the power of conditional independence testing under model-X”. In: *preprint at arXiv 2005.05506* (2020).

[24] W. Wang and L. Janson. “A High-Dimensional Power Analysis of the Conditional Randomization Test and Knockoffs”. In: *Biometrika* (2021).

[25] A. Spector and L. Janson. “Powerful knockoffs via minimizing reconstructability”. In: *Ann. Stat.* 50.1 (2022), pp. 252–276.

[26] J. Bien, J. Taylor, and R. Tibshirani. “A lasso for hierarchical interactions”. In: *Ann. Stat.* 41.3 (2013), p. 1111.

[27] X. Wen and M. Stephens. “Bayesian methods for genetic association analysis with heterogeneous subgroups: from meta-analyses to gene-environment interactions”. In: *Ann. Appl. Stat.* 8.1 (2014), p. 176.

[28] M. Lim and T. Hastie. “Learning interactions via hierarchical group-lasso regularization”. In: *J. Comput. Graph. Stat.* 24.3 (2015), pp. 627–654.

[29] G. Verbeke and E. Lesaffre. “A linear mixed-effects model with heterogeneity in the random-effects population”. In: *J. Am. Stat. Assoc.* 91.433 (1996), pp. 217–221.

[30] R. Moore, F. P. Casale, M. Jan Bonder, D. Horta, L. Franke, I. Barroso, and O. Stegle. “A linear mixed-model approach to study multivariate gene–environment interactions”. In: *Nat. Genet.* 51.1 (2019), pp. 180–186.

[31] P. R. Hahn, J. S. Murray, and C. M. Carvalho. “Bayesian regression tree models for causal inference: Regularization, confounding, and heterogeneous effects (with discussion)”. In: *Bayesian Analysis* 15.3 (2020), pp. 965–1056.

[32] U. Shalit, F. D. Johansson, and D. Sontag. “Estimating individual treatment effect: generalization bounds and algorithms”. In: *Int. Conf. Mach. Learn.* PMLR. 2017, pp. 3076–3085.

[33] C. Louizos, U. Shalit, J. M. Mooij, D. Sontag, R. Zemel, and M. Welling. “Causal effect inference with deep latent-variable models”. In: *Adv. Neural Inf. Process. Syst.* 30 (2017).

[34] A. M. Alaa and M. van der Schaar. “Bayesian inference of individualized treatment effects using multi-task gaussian processes”. In: *Adv. Neural Inf. Process. Syst.* 30 (2017).

[35] S. Wager and S. Athey. “Estimation and inference of heterogeneous treatment effects using random forests”. In: *J. Am. Stat. Assoc.* 113.523 (2018), pp. 1228–1242.

[36] L. Yao, S. Li, Y. Li, M. Huai, J. Gao, and A. Zhang. “Representation learning for treatment effect estimation from observational data”. In: *Adv. Neural Inf. Process. Syst.* 31 (2018).

[37] J. Yoon, J. Jordon, and M. Van Der Schaar. “GANITE: Estimation of individualized treatment effects using generative adversarial nets”. In: *Int. Conf. Learn. Represent.* 2018.

[38] R. Guo, L. Cheng, J. Li, P. R. Hahn, and H. Liu. “A survey of learning causality with data: Problems and methods”. In: *ACM Computing Surveys (CSUR)* 53.4 (2020), pp. 1–37.

[39] X. Nie and S. Wager. “Quasi-oracle estimation of heterogeneous treatment effects”. In: *Biometrika* 108.2 (2021), pp. 299–319.

[40] I. Bica, A. M. Alaa, C. Lambert, and M. Van Der Schaar. “From real-world patient data to individualized treatment effects using machine learning: current and future methods to address underlying challenges”. In: *Clinical Pharmacology & Therapeutics* 109.1 (2021), pp. 87–100.

[41] S. Li, M. Sesia, Y. Romano, E. Candès, and C. Sabatti. “Searching for robust associations with a multi-environment knockoff filter”. In: *Biometrika* (2021).

[42] J. R. Gimenez, A. Ghorbani, and J. Zou. “Knockoffs for the mass: new feature importance statistics with false discovery guarantees”. In: *22nd International Conference on Artificial Intelligence and Statistics*. PMLR. 2019, pp. 2125–2133.

[43] C. Chia, M. Sesia, C.-S. Ho, S. S. Jeffrey, J. A. Dionne, E. Candes, and R. T. Howe. “Interpretable classification of bacterial Raman spectra with knockoff wavelets”. In: *IEEE J. Biomed. Health Inform.* (2021).

[44] Y. Fan, J. Lv, M. Sharifvaghefi, and Y. Uematsu. “IPAD: stable interpretable forecasting with knockoffs inference”. In: *J. Am. Stat. Assoc.* (2019), pp. 1–13.

[45] C.-M. Chi, Y. Fan, J. Lv, et al. “High-Dimensional Knockoffs Inference for Time Series Data”. In: *preprint at arXiv 2112.09851* (2021).

[46] E. Katsevich and C. Sabatti. “Multilayer knockoff filter: Controlled variable selection at multiple resolutions”. In: *Ann. Appl. Stat.* 13.1 (2019), p. 1.

[47] A. Shen, H. Fu, K. He, and H. Jiang. “False discovery rate control in cancer biomarker selection using knockoffs”. In: *Cancers* 11.6 (2019), p. 744.

[48] M. Sesia, E. Katsevich, S. Bates, E. Candès, and C. Sabatti. “Multi-resolution localization of causal variants across the genome”. In: *Nat. Commun.* 11.1 (2020), pp. 1–10.

[49] J. Neyman and K. Iwaszkiewicz. “Statistical problems in agricultural experimentation”. In: *Supplement to J. R. Stat. Soc.* 2.2 (1935), pp. 107–180.

[50] D. Caughey, A. Dafoe, X. Li, and L. Miratrix. “Randomization Inference beyond the Sharp Null: Bounded Null Hypotheses and Quantiles of Individual Treatment Effects”. In: *preprint at arXiv 2101.09195* (2021).

[51] R. Fisher. “Statistical methods for research workers, 13e”. In: *London: Oliver and Loyd, Ltd* (1925), pp. 99–101.

[52] M. Liu, E. Katsevich, L. Janson, and A. Ramdas. “Fast and powerful conditional randomization testing via distillation”. In: *Biometrika* (July 2021).

[53] Y. Benjamini and Y. Hochberg. “Controlling the false discovery rate: a practical and powerful approach to multiple testing”. In: *J. R. Stat. Soc. B*. 57 (1995), pp. 289–300.

[54] R. Tibshirani. “Regression shrinkage and selection via the lasso”. In: *J. R. Stat. Soc. Series B Stat. Methodol.* 58.1 (1996), pp. 267–288.

[55] R. Tibshirani and J. Friedman. “A pliable lasso”. In: *J. Comput. Graph. Stat.* 29.1 (2020), pp. 215–225.

[56] Y. Benjamini and D. Yekutieli. “The control of the false discovery rate in multiple testing under dependency”. In: *Ann. Stat.* (2001), pp. 1165–1188.

[57] W. Fithian and L. Lei. “Conditional calibration for false discovery rate control under dependence”. In: *preprint at arXiv 2007.10438* (2020).

[58] P. Ding. “A paradox from randomization-based causal inference”. In: *Stat. science* (2017), pp. 331–345.

[59] G. W. Imbens and D. B. Rubin. *Causal inference in statistics, social, and biomedical sciences*. Cambridge University Press, 2015.

[60] P. H. Garthwaite and S. T. Buckland. “Generating Monte Carlo confidence intervals by the Robbins–Monro process”. In: *J. R. Stat. Soc. Series C Appl. Stat.* 41.1 (1992), pp. 159–171.

[61] P. H. Garthwaite. “Confidence intervals from randomization tests”. In: *Biometrics* (1996), pp. 1387–1393.

[62] J. R. Blum et al. “Approximation methods which converge with probability one”. In: *Ann. Math. Stat.* 25.2 (1954), pp. 382–386.

[63] S. Li, Z. Ren, C. Sabatti, and M. Sesia. “Transfer learning in genome-wide association studies with knockoffs”. In: *preprint at arXiv 2108.08813* (2021).

[64] K. J. Friston, W. D. Penny, and D. E. Glaser. “Conjunction revisited”. In: *Neuroimage* 25.3 (2005), pp. 661–667.

[65] Y. Benjamini and R. Heller. “Screening for partial conjunction hypotheses”. In: *Biometrics* 64.4 (2008), pp. 1215–1222.

[66] L. B. Janson. “A model-free approach to high-dimensional inference”. PhD thesis. Stanford University, 2017.

[67] C. Bycroft, C. Freeman, D. Petkova, G. Band, L. T. Elliott, K. Sharp, A. Motyer, D. Vukcevic, O. Delaneau, J. O’Connell, A. Cortes, S. Welsh, A. Young, M. Effingham, G. McVean, S. Leslie, N. Allen, P. Donnelly, and J. Marchini. “The UK Biobank resource with deep phenotyping and genomic data”. In: *Nature* 562 (2018), pp. 203–209.

[68] J. M. Gaziano, J. Concato, M. Brophy, L. Fiore, S. Pyarajan, J. Breeling, S. Whitbourne, J. Deen, C. Shannon, D. Humphries, et al. “Million Veteran Program: A mega-biobank to study genetic influences on health and disease”. In: *J. Clin. Epidemiol.* 70 (2016), pp. 214–223.

[69] J. H. Moore, J. C. Gilbert, C.-T. Tsai, F.-T. Chiang, T. Holden, N. Barney, and B. C. White. “A flexible computational framework for detecting, characterizing, and interpreting statistical patterns of epistasis in genetic studies of human disease susceptibility”. In: *J. Theor. Biol.* 241.2 (2006), pp. 252–261.

[70] T. A. Manolio, F. S. Collins, N. J. Cox, D. B. Goldstein, L. A. Hindorff, D. J. Hunter, M. I. McCarthy, E. M. Ramos, L. R. Cardon, A. Chakravarti, et al. “Finding the missing heritability of complex diseases”. In: *Nature* 461.7265 (2009), pp. 747–753.

[71] M. D. Ritchie. “Using biological knowledge to uncover the mystery in the search for epistasis in genome-wide association studies”. In: *Ann. Hum. Genet.* 75.1 (2011), pp. 172–182.

[72] C. Niel, C. Sinoquet, C. Dina, and G. Rocheleau. “A survey about methods dedicated to epistasis detection”. In: *Frontiers in genetics* 6 (2015), p. 285.

- [73] D. S. Park, I. Eskin, E. Y. Kang, E. R. Gamazon, C. Eng, C. R. Gignoux, J. M. Galanter, E. Burchard, C. J. Ye, H. Aschard, et al. “An ancestry-based approach for detecting interactions”. In: *Genetic epidemiology* 42.1 (2018), pp. 49–63.
- [74] S. Li and E. J. Candès. “Deploying the Conditional Randomization Test in High Multiplicity Problems”. In: *arXiv preprint arXiv:2110.02422* (2021).
- [75] K. A. Bollen. *Structural Equations with Latent Variables*. Vol. 210. John Wiley & Sons, 2014.
- [76] J. Pearl. *Causality*. Cambridge University Press, 2009.
- [77] A. Li and R. F. Barber. “Accumulation tests for FDR control in ordered hypothesis testing”. In: *J. Am. Stat. Assoc* 112.518 (2017), pp. 837–849.
- [78] V. Chernozhukov, D. Chetverikov, M. Demirer, E. Duflo, C. Hansen, W. Newey, and J. Robins. “Double/debiased machine learning for treatment and structural parameters”. In: *J. Econom.* 21.1 (2018), pp. C1–C68.

A1 Additional methodological details

A1.1 From conditional testing to causal inference

In addition to the basic setup of Section 1.3, imagine the variables X are randomized treatments that may depend on the observed Z but are independent of anything else. Further, suppose the data distribution takes the form of a structural equation model [75, 76] in which Z and X may cause Y , but not the other way around, as visualized by the directed acyclic graph in Figure A1. It is easy to see this setup implicitly rules out confounding in a test of conditional independence between X and Z because the treatments are conditionally independent of any other unmeasured covariate C . Therefore, to test whether X_j has a causal effect on Y , it suffices to test whether the conditional independence hypothesis in (1).

Proposition A1 (From [10]). *Let C be any unmeasured covariate. If $X \perp\!\!\!\perp C \mid Z$, a valid test of the conditional independence null hypothesis $\mathcal{H}_{0,j}$ in (1) is also a valid test of the stronger null hypothesis*

$$\mathcal{H}_{0,j}^* : Y \perp\!\!\!\perp X_j \mid Z, X_{-j}, C. \quad (\text{A28})$$

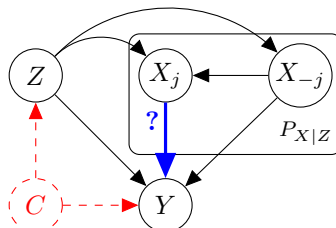


Figure A1: Graphical representation of a non-parametric causal model linking the treatment (X), the outcome (Y), the measured covariates (Z), and possibly also other unmeasured covariate (C). Our goal is to test whether a particular treatment X_j has any causal effect on the outcome. The joint distribution of $X \mid Z, C$ is assumed to be known and may depend only on Z , so that $X \perp\!\!\!\perp C \mid Z$.

A1.2 Schematics of the selective knockoff filter

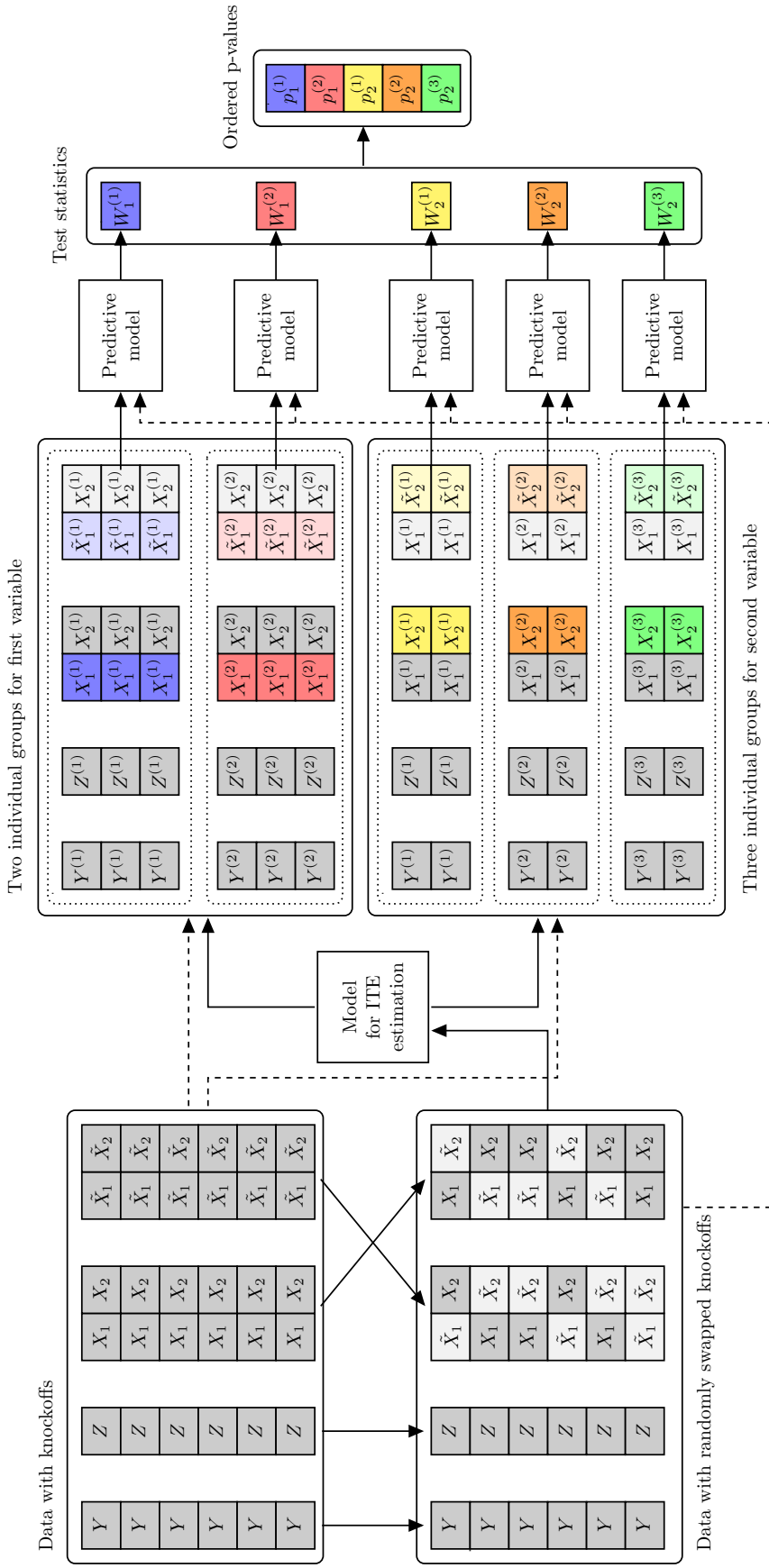
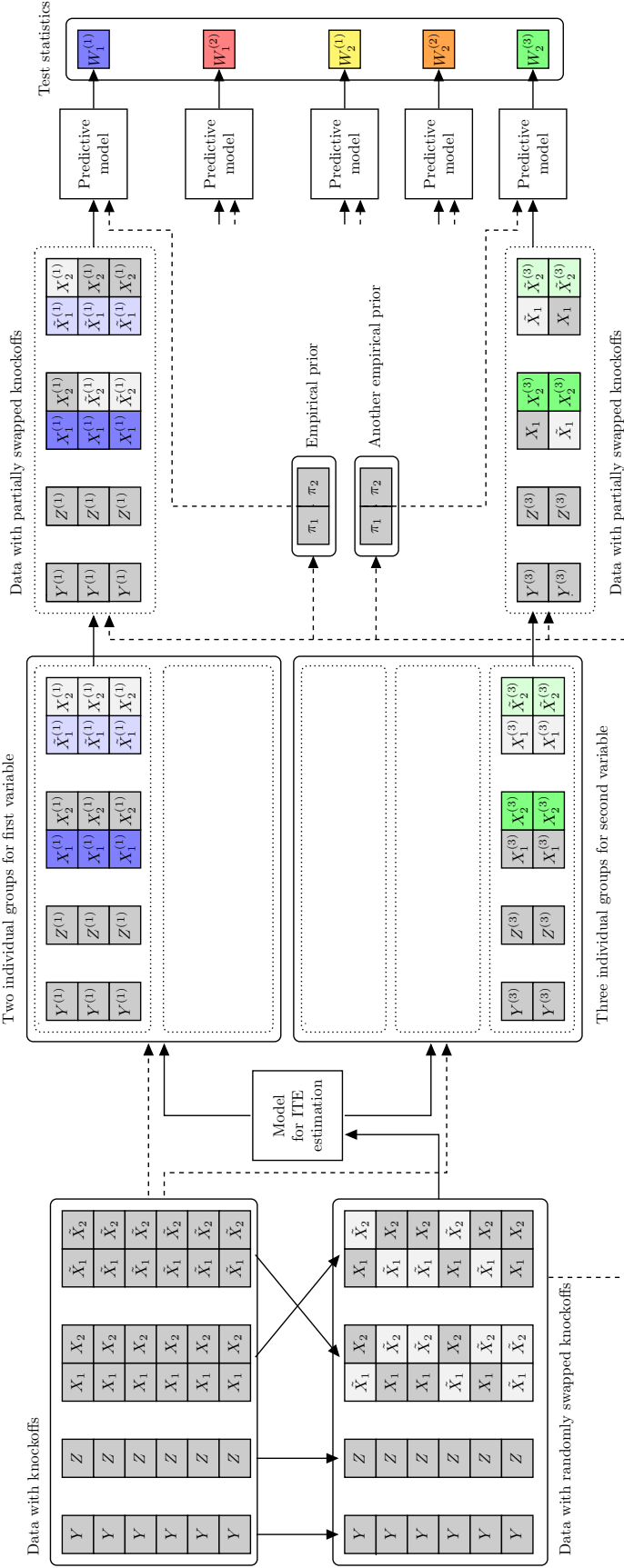


Figure A2: Schematic of the SKF for individualized conditional independence testing. The statistics for distinct combinations of variables and individual groups are shown in different colors.



A1.3 The robust selective knockoff filter

The SKF was presented in Section 2 for the purpose of testing the hypotheses defined in (5), namely

$$\mathcal{H}_{0,j}^{(g_j)} : Y^{(g_j)} \perp\!\!\!\perp X_j^{(g_j)} \mid X_{-j}^{(g_j)}, Z^{(g_j)},$$

for all variables j and individual groups g_j conditional on a random partition $\hat{\psi}$ based on the data with randomly swapped knockoffs. Here, we present an extension of the SKF that is inspired by the work of [41] and makes it possible to test the following *partial conjunction* [64, 65] hypotheses:

$$\mathcal{H}_{0,j}^{\text{pc},r} : \left| \left\{ g_j \in [G] : \mathcal{H}_{0,j}^{(g_j)} \text{ is true} \right\} \right| > G - r, \quad (\text{A29})$$

for any fixed $r \in \{1, \dots, G\}$. Intuitively, the partial conjunction hypothesis states that the number of groups for variable j in which $\mathcal{H}_{0,j}^{(g_j)}$ (5) is false is strictly smaller than r . Therefore, rejecting this null suggests X_j is associated with Y in at least r distinct groups of individuals. If $r = 1$, the partial conjunction hypothesis reduces to the original population-wide hypothesis of [7], in (1); in that case, rejecting $\mathcal{H}_{0,j}^{\text{pc},r}$ suggests the existence of least one sub-population in which X_j is conditionally associated with Y . By contrast, rejecting the hypothesis in (A29) for $r = G$ requires evidence of a conditional association between X_j and Y across *all* sub-populations. It can be interesting to test $\mathcal{H}_{0,j}^{\text{pc},r}$ because this hypothesis points towards the discovery of variables whose association with Y is *robust* to changes in the covariate distribution [41]. Intuitively, testing $\mathcal{H}_{0,j}^{\text{pc},r}$ can be seen as a way for discovering conditional associations that do *not* involve interactions, thus complementing the opposite point of view taken in Section 2. The p partial conjunction hypotheses defined in (A29) are relatively straightforward to test while provably controlling the false discovery rate, if one starts with a collection \mathbf{W} of SKF statistics satisfying (9). In fact, it suffices to apply the multi-environment knockoff filter of [41] to these statistics, as explained below.

For each $j \in \{1, \dots, p\}$, let n_j^- count the negative signs among the $W_j^{(g_j)}$ statistics for all groups g_j , and let n_j^0 be the number of zeros among them. For simplicity, assume $\hat{\psi}$ partitions the covariate space into G groups for each variable; this is without loss of generality, as it is otherwise sufficient to set the remaining undefined statistics to zero if $\hat{G}_j < G$ for some $j \in [p]$. Then, compute

$$p_j^{\text{pc},r} = \Psi \left(n_j^- - 1, (G - r + 1 - n_j^0) \vee 0, \frac{1}{2} \right) + U_j \cdot \Psi' \left(n_j^-, (G - r + 1 - n_j^0) \vee 0, \frac{1}{2} \right), \quad (\text{A30})$$

where $\Psi(\cdot, m, \pi)$ is the binomial cumulative distribution function, $\Psi'(\cdot, m, \pi)$ is the corresponding probability mass, and U_j is a uniform random variable on $[0, 1]$ independent of everything else. Further, define

$$|W_j^{\text{pc},r}| = \bar{w} \left(|W_j^{(1)}|, \dots, |W_j^{(G)}| \right), \quad (\text{A31})$$

for some symmetric function \bar{w} , such as that which multiplies the top r largest entries by absolute value:

$$w \left(|W_j^{(1)}|, \dots, |W_j^{(G)}| \right) = \prod_{g=1}^r |\bar{W}|_j^{(G-g+1)}.$$

Above, $|\bar{W}|_j^{(g)}$ are the order statistics for $\{|W_j^{(1)}|, \dots, |W_j^{(G)}|\}$. Then, the false discovery rate for (A29) can be controlled by applying the usual selective SeqStep+ sequential testing procedure of [19], thanks to a relatively simple extension of Theorem 1 in [41].

Theorem A1. *Selective SeqStep+ applied to the p-values (A30) ordered by (A31) controls the false discovery rate for (A29) if the statistics \mathbf{W} satisfy the flip-sign property in (9).*

Alternatively, the false discovery rate for (A29) could be (approximately) controlled by applying to the p-values (A30) ordered by (A31) the accumulation test [77] instead of SeqStep+; this can be proved with an analogous extension of Theorem 2 in [41], which we do not state explicitly here in the interest of space.

A1.4 Sharp confidence intervals from a specialized CRT

We discuss here a special case of the CRT [7] from Section 3.2 that can be inverted to give approximately convex confidence sets. The intervals thus obtained still do not explicitly account for sample heterogeneity, but at least they tend to be relatively more robust compared to their general counterparts. Further, these intervals can be useful to gain more understanding of the QCRT developed in Section 3.3.

Let \hat{g} be any data-dependent function of Z which can be utilized to predict Y ; ideally, we would like $\hat{g}(Z) \approx \mathbb{E}[g(Z, C) | Z]$, where g is the nuisance function in the partially linear model (10), although no assumptions are needed about the accuracy of this estimate. In fact, \hat{g} may be obtained by fitting on \mathbf{Z}, \mathbf{Y} any machine learning model, which we treat as a black box without statistical guarantees. Then, for $\mathbf{Y}' = \mathbf{Y} - \mathbf{X} \odot \boldsymbol{\delta}$ and any $\mathbf{X}' \in \mathbb{R}^n$, define the statistic $\bar{t}(\mathbf{X}', \mathbf{Z}, \mathbf{Y}')$ as the estimated regression coefficient obtained by regressing the residuals $\mathbf{Y}' - \hat{g}(\mathbf{Z})$ on \mathbf{X}' , where $\hat{g}(\mathbf{Z})$ denotes the column vector obtained by applying \hat{g} to each row of \mathbf{Z} . Concretely, this takes the form:

$$\bar{t}(\mathbf{X}', \mathbf{Z}, \mathbf{Y}') = \frac{1}{\sum_i (X'^{(i)} - \bar{X}')^2} \sum_i (X'^{(i)} - \bar{X}') \left[Y'^{(i)} - \hat{g}(Z^{(i)}) - \left(\bar{Y}' - \frac{1}{n} \sum_i \hat{g}(Z^{(i)}) \right) \right], \quad (\text{A32})$$

where $\bar{Z}' = (1/n) \sum_{i=1}^n Z'^{(i)}$ and $\bar{Y}' = (1/n) \sum_{i=1}^n Y'^{(i)}$. These statistics allow computing the CRT p-values without having to re-fit \hat{g} for each of the K realizations of the virtual variables $\tilde{X}^{(k)}$, which would be time-consuming; see [52] for a more general discussion of computationally efficient implementations of the CRT. Further, inverting the CRT p-values based on the above statistics approximately yields confidence intervals.

Theorem A2. *Assume the partially linear model in (10) holds and \mathcal{H}_δ in (11) is true, for some fixed $\boldsymbol{\delta} = \boldsymbol{\tau} = \tau_* \mathbf{1}$ and $\tau_* \in \mathbb{R}$. For any $\alpha \in (0, 1)$, let $\hat{\mathcal{S}}_n(\alpha)$ be the set in (14) calculated with the statistics in (A32). Suppose this is evaluated from n samples, in the limit of $K \rightarrow \infty$; i.e., $\hat{p}_{\boldsymbol{\delta}}^{\text{CRT}}$ in (13) is replaced by*

$$\hat{p}_{\boldsymbol{\delta}}^{\text{CRT}, \infty} = \mathbb{P} \left[\bar{t}(\tilde{\mathbf{X}}^{(k)}, \mathbf{Z}, \mathbf{Y} - \mathbf{X} \odot \boldsymbol{\delta}) \geq \bar{t}(\mathbf{X}, \mathbf{Y}, \mathbf{Z} - \mathbf{X} \odot \boldsymbol{\delta}) \mid \mathbf{Z}, \mathbf{Y}, \mathbf{X} \right].$$

Assume also X is a.s. bounded and $\rho_j^2 = \mathbb{E}[\text{Var}[X_j | X_{-j}]] > 0$. Then, $\exists c > 0$ such that, for any $\epsilon > 0$,

$$\mathbb{P} \left[\hat{\mathcal{S}}_n^{\text{int}} \left(\alpha + \frac{\epsilon}{n} \right) \subseteq \hat{\mathcal{S}}_n(\alpha) \subseteq \hat{\mathcal{S}}_n^{\text{int}} \left(\alpha - \frac{\epsilon}{n} \right) \right] \geq 1 - 24 \frac{n}{\epsilon} \exp \left\{ - \frac{n(\rho_j^4 \wedge \rho_j^8)}{c} \right\},$$

where $\hat{\mathcal{S}}_n^{\text{int}}(\alpha + \epsilon/n)$ and $\hat{\mathcal{S}}_n^{\text{int}}(\alpha - \epsilon/n)$ are random intervals containing the true τ_* with probability at least $1 - (\alpha + \epsilon/n)$ and $1 - (\alpha - \epsilon/n)$, respectively.

In other words, inverting the CRT based on the statistics in (A32) leads to valid confidence sets that can be made convex (by expanding or shrinking them) with only a very small change in coverage, as long as K and the sample size n are sufficiently large. It is worth emphasizing the result is informative in a high-dimensional setting because the sample size only needs to be large with respect to constant one (as well as to $1/\alpha$ and $1/\rho_j^2$), not relative to the number of covariates in Z , which may be arbitrary. The above confidence intervals can also be proved to be consistent under some mild additional assumptions, in the sense that they will asymptotically shrink at rate $n^{-1/2}$ around the true parameter $\boldsymbol{\tau}$ as n increases.

Theorem A3. *Assume partially linear model in (10) and suppose \mathcal{H}_δ in (11) is true, for some fixed $\boldsymbol{\delta} = \boldsymbol{\tau} = \tau_* \mathbf{1}$ and $\tau_* \in \mathbb{R}$. For any $\alpha \in (0, 1)$, let $\hat{\mathcal{S}}_n(\alpha)$ denote the confidence set in (14) with the statistics in (A32), evaluated after letting $K \rightarrow \infty$, as in Theorem A2 (making the dependence on n explicit). Assume X is almost surely bounded within an interval of width $c_1 > 0$, and Y, \hat{g} in (10) are a.s. bounded within an interval of width $c_2 > 0$. Assume also $\rho_j^2 = \mathbb{E}[\text{Var}[X_j | X_{-j}]] > 0$. Then, for any real-valued sequence τ_n such that $|\tau_* - \tau_n| \geq n^{-1/2} (\log n)^{3/2}$, if n is large enough, then*

$$\mathbb{P} \left[\tau_n \in \hat{\mathcal{S}}_n(\alpha) \right] \lesssim \frac{14}{\alpha} \exp \left\{ - \frac{\rho_j^2 \log n}{4c_1^2 c_2^2} \right\}.$$

Above, the symbol \lesssim is defined such that $x_n \lesssim y_n$ means $x_n < y_n + o(y_n)$. In particular, this means the confidence intervals are approximately \sqrt{n} -consistent, in the sense that, for any real-valued sequence τ_n such that $|\tau_* - \tau_n| \geq n^{-1/2} (\log n)^{3/2}$,

$$\lim_{n \rightarrow \infty} \mathbb{P} \left[\tau_n \in \hat{\mathcal{S}}_n(\alpha) \right] = 0.$$

In other words, this establishes the asymptotic consistency of the CRT confidence intervals under no assumptions about the data-generating process other than the partially linear model in (10) with homogeneous effects. In particular, this result holds regardless of the unknown form of the nuisance function g or of the consistency (or lack thereof) of the machine-learning estimator \hat{g} . In fact, g and \hat{g} are only assumed to be bounded within some finite range (it may be possible to replace this last assumption with suitable tail bounds, e.g., sub-Gaussian tails, although we did not explore that direction). Thus, this consistency result is stronger than the double robustness property enjoyed by other methods for estimating individual effects in partially linear models, such as double machine learning [78]. Of course, such relative strength is unsurprising given that our model-X framework assumes $P_{X|Z}$ is known, unlike [78].

A1.5 Upper confidence bound for a quantile of individual linear effects

Algorithm A2: QCRT upper confidence bounds for a quantile of individual linear effects

Input: data $\mathbf{X}, \mathbf{Y}, \mathbf{Z}$, distribution of $P_{X|Z}$, target quantile level q , decreasing sequence $\{\lambda_k\}_{k=1}^K$, confidence level $\alpha \in (0, 1)$;
 Compute $E = \sum_{i=1}^n \mathbb{P} [X^i = 1 \mid Z^i]$;
if $E < n/2$ **then**
 | Define $\mathbf{X}' = \mathbf{1} - \mathbf{X}$, $\mathbf{Y}' = \mathbf{Y}$;
else
 | Define $\mathbf{X}' = \mathbf{X}$, $\mathbf{Y}' = -\mathbf{Y}$;
end
 Fit an estimate \hat{g} of g in (10), using the data in \mathbf{Y}', \mathbf{Z}' ;
 Initialize $U^{(1)}$ to a sufficiently small value ensuring $U^{(1)} > \tau_{(q)}$;
 Compute $T = t(\mathbf{X}', \mathbf{Y} - \hat{g}(\mathbf{Z}; \mathbf{Z}, \mathbf{Y}'))$;
for $k = 1, \dots, K - 1$ **do**
 | Define $\boldsymbol{\eta}^{(k)}$ as in (19), using $c = -U^{(k)}$;
 | Sample the knockoffs $\tilde{\mathbf{X}}'^{(k)}$ given the observed \mathbf{Z} based on $P_{X'|Z}$;
 | Compute $\tilde{T}^{(k)} = t(\tilde{\mathbf{X}}'^{(k)}, \mathbf{Y}' - \hat{g}(\mathbf{Z}; \mathbf{Z}, \mathbf{Y}') - (\mathbf{X}' - \tilde{\mathbf{X}}'^{(k)}) \odot \boldsymbol{\eta}^{(k)})$;
 | **if** $\tilde{T}^{(k)} \leq T$ **then**
 | | Update $U^{(k+1)} \leftarrow U^{(k)} - \lambda_k \alpha$;
 | **else**
 | | Update $U^{(k+1)} \leftarrow U^{(k)} + \lambda_k (1 - \alpha)$;
 | **end**
end
Output: $\hat{U}_q(\alpha) = -U^{(K+1)}$.

A2 Additional results from numerical experiments

A2.1 Lack of robustness of sharp randomization confidence intervals

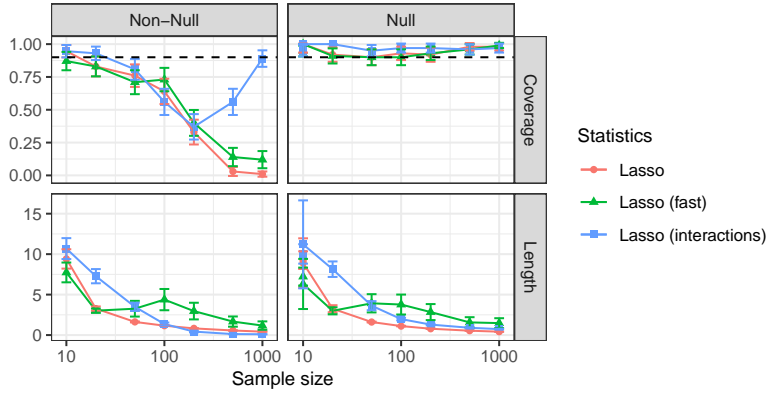


Figure A4: Performance of naive confidence intervals for average linear effects obtained by inverting the standard CRT for sharp hypotheses, on synthetic data following a partially linear model with one interaction per variable. Other details are as in Figure 4.

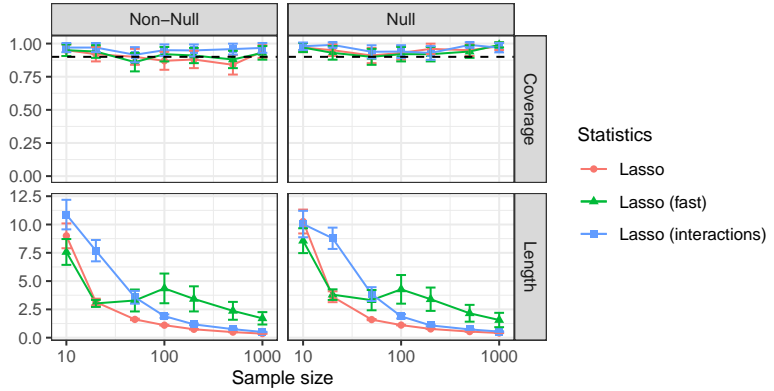


Figure A5: Performance of naive confidence intervals for average linear effects obtained by inverting the standard CRT for sharp hypotheses, on synthetic data following a partially linear model without interactions. Other details are as in Figure 4.

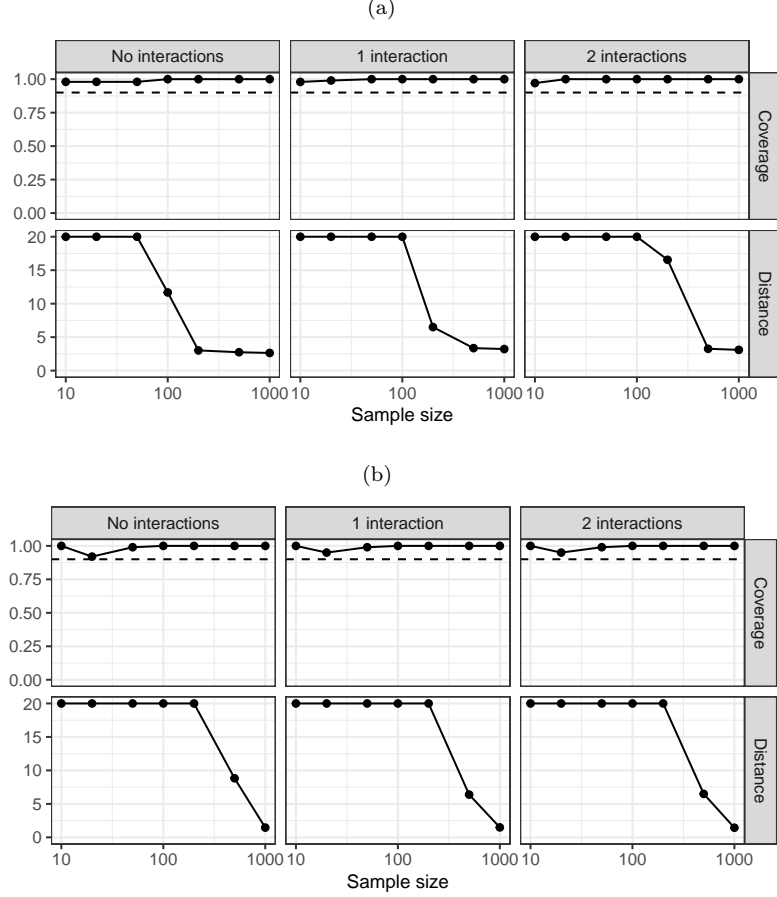


Figure A6: Performance of the confidence bounds for the quantiles of the individual effects obtained with the QCRT from Section 3, in the same numerical experiments as in Figures 4 and A4–A5. (a): Lower confidence bound for the 90% quantile of the individual effects for a non-null variable. (b): Upper confidence bound for the 10% quantile of the individual effects for a null variable. The performance of our method is quantified in terms of average coverage and absolute distance from the true quantile of interest. Other details are as in Figure 4.

A2.2 Inferences about quantiles of individual linear effects

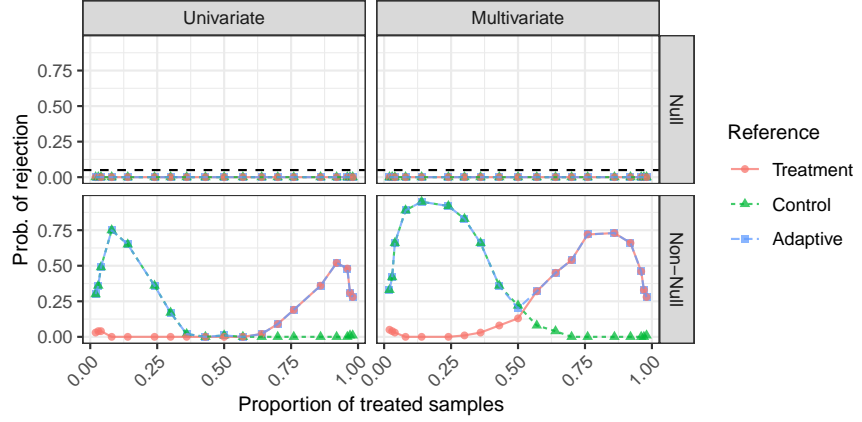


Figure A7: Rejection probability for the univariate and multivariate QCRT in simulations with synthetic data, as a function of the proportion of samples with $X = 1$. The tested hypothesis is that the 90% quantile of individuals effects is below 2. The sample size is 1000. Other details are as in Figure 5.

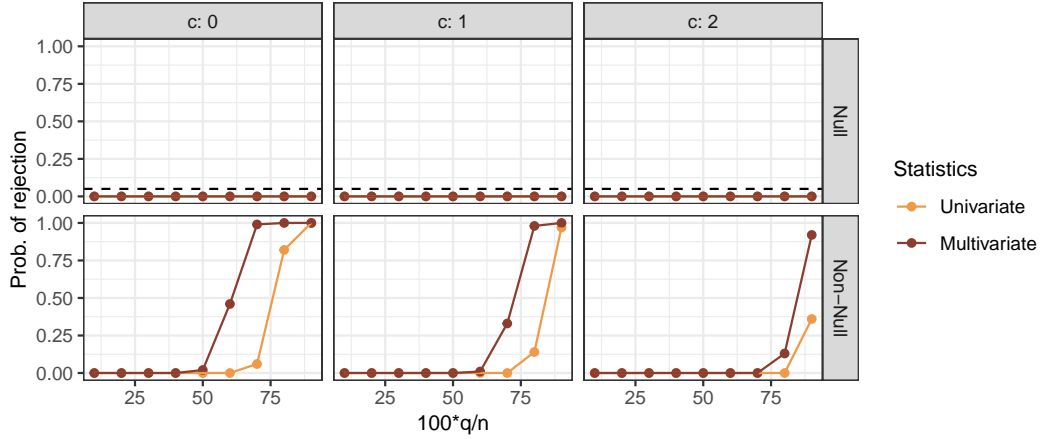


Figure A8: Rejection probability for the QCRT in simulations with synthetic data, as a function of the tested quantile q , for different values of the target constant bound c in (15). Other details are as in Figure A7.

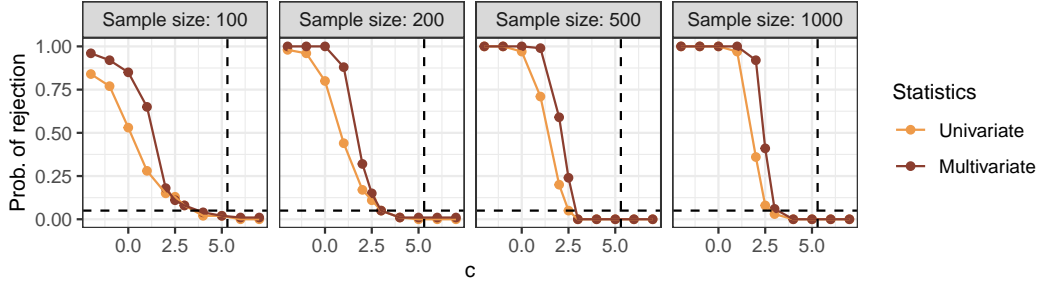


Figure A9: Rejection probability for the QCRT in simulations with synthetic data, as a function of the target constant bound c in (15), for different sample sizes. The tested quantile is the 90% one. Other details are as in Figure A7.

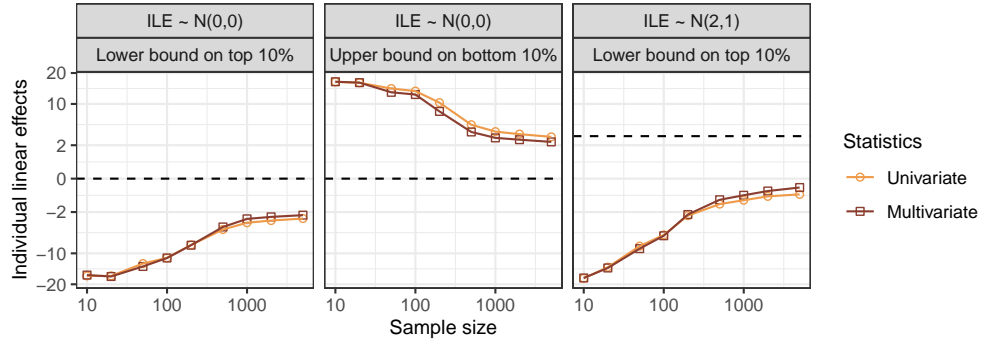


Figure A10: Bounds at confidence level 90% for quantiles of individual effects computed by inverting the QCRT in simulations with synthetic data. The proportion of samples with $X = 1$ is 0.76. Other details are as in Figure 6.

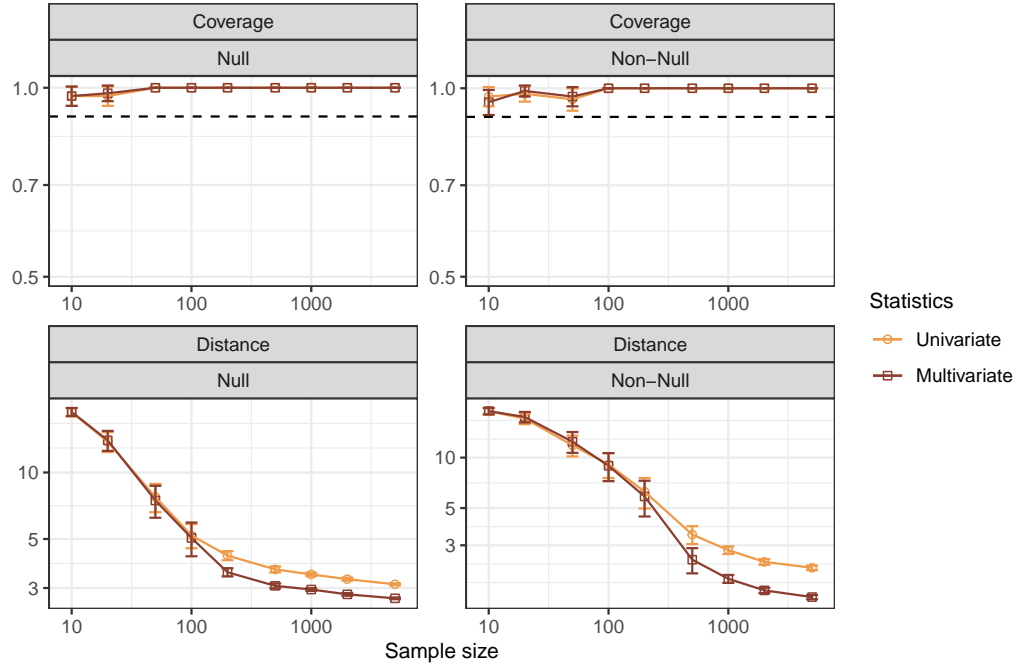


Figure A11: Performance of confidence bounds for quantiles of individual linear effects computed by inverting the QCRT in simulations with synthetic data. The target of inference is a lower bound for the 90% quantile of individual effects. The performance is measured in terms of the empirical coverage and average distance from the true target quantile. Left: null variable. Right: non-null variable. The dashed horizontal lines indicate the nominal 90% coverage level. The proportion of individuals with $X = 1$ is 24%. Other details are as in Figure 6.

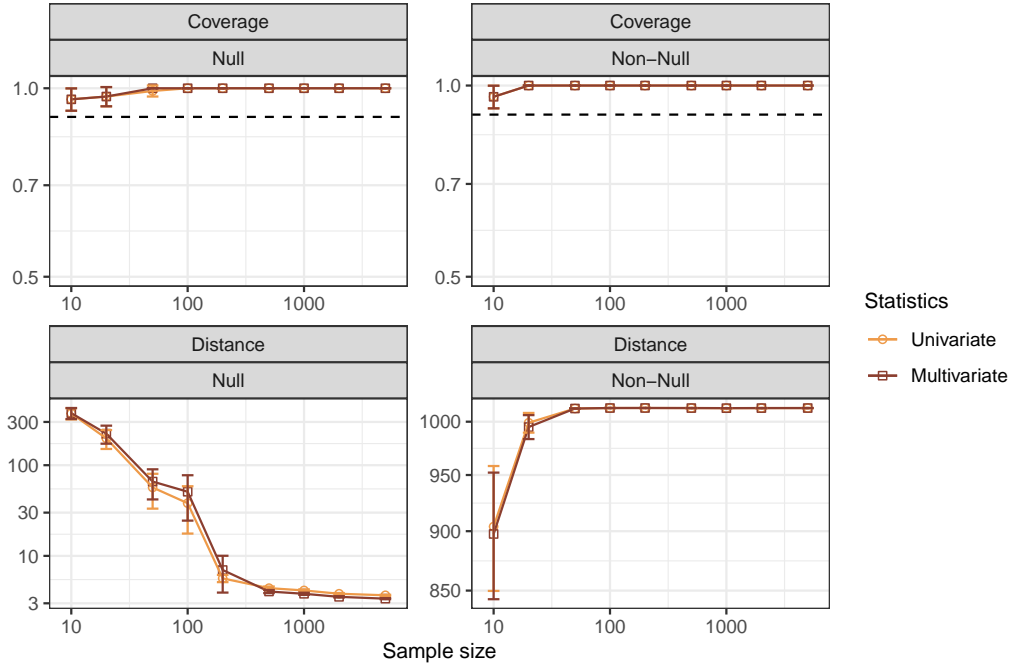


Figure A12: Performance of confidence bounds for quantiles of individual linear effects computed by inverting the QCRT in simulations with synthetic data. The proportion of individuals with $X = 1$ is 76%. Other details are as in Figure A11.

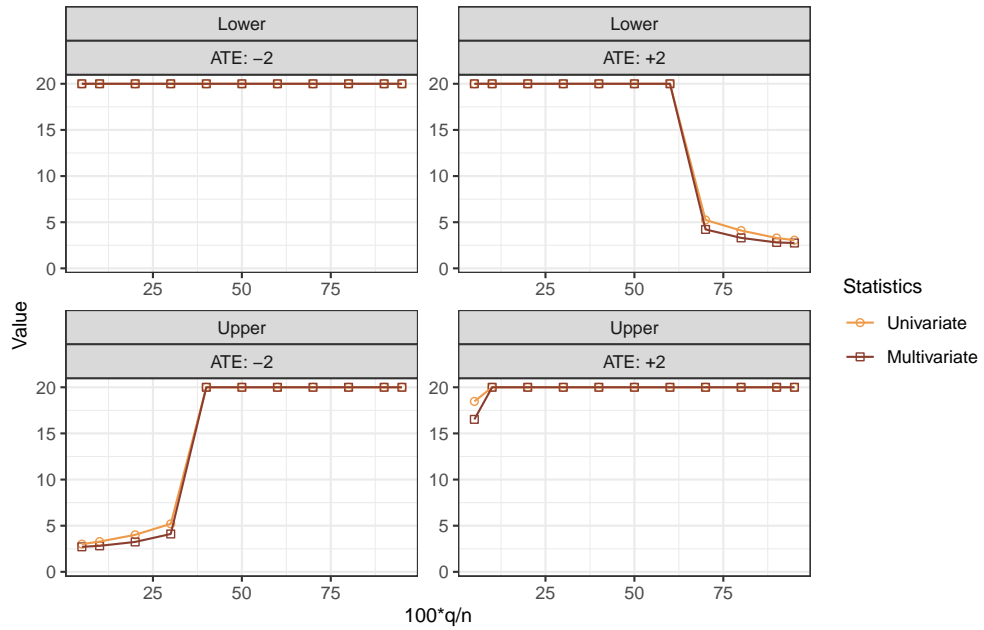


Figure A13: Performance of confidence bounds for quantiles of individual linear effects computed by inverting the QCRT in simulations with synthetic data. The target of inference is a lower bound for the 90% quantile of individual effects. Left: non-null variable with average linear effect equal to -2. Right: non-null variable with average linear effect equal to +2. The proportion of individuals with $X = 1$ is 24%. Other details are as in Figure 6.

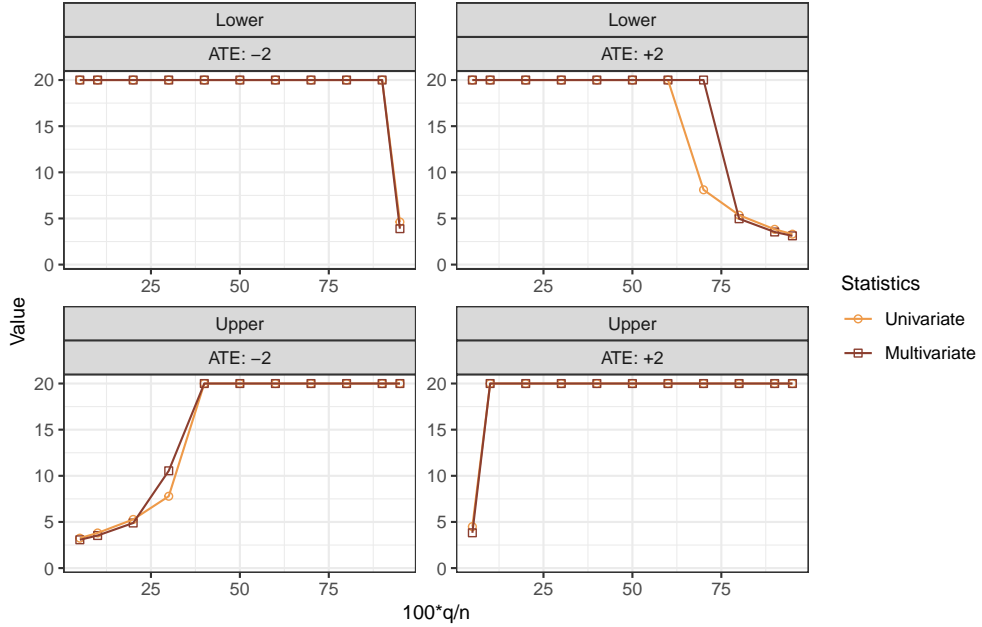


Figure A14: Performance of confidence bounds for quantiles of individual linear effects computed by inverting the QCRT in simulations with synthetic data. The proportion of individuals with $X = 1$ is 76%. Other details are as in Figure A13.

A3 Additional data analysis details

A3.1 Knockoffs for blood donation treatments

Table A1: Goodness-of-fit-diagnostics for knockoff treatments, for the blood donation data. The means and standard deviations of the knockoffs approximately match those of the corresponding true treatments.

	Treatments					Knockoffs				
	X_1	X_2	X_3	X_4	X_5	\tilde{X}_1	\tilde{X}_2	\tilde{X}_3	\tilde{X}_4	\tilde{X}_5
Mean	0.825	0.412	0.550	0.138	0.138	0.822	0.411	0.549	0.139	0.140
Standard deviation	0.380	0.492	0.497	0.344	0.344	0.382	0.492	0.498	0.346	0.347

Table A2: Goodness-of-fit-diagnostics for knockoff treatments, for the blood donation data. The pairwise correlations between different treatments approximately match those of the corresponding knockoffs, as well as those between treatments and knockoffs. Smaller values of the diagonal correlation terms in the upper-right block of the correlation matrix (in red) tend to correspond to higher power for the knockoff filter.

Treatments					Knockoffs					
X_1	X_2	X_3	X_4	X_5	\tilde{X}_1	\tilde{X}_2	\tilde{X}_3	\tilde{X}_4	\tilde{X}_5	
X_1	1	0.386	0.509	0.184	0.184	0.701	0.385	0.508	0.185	0.186
X_2	0.386	1	0.197	-0.335	0.477	0.389	0.607	0.197	-0.337	0.481
X_3	0.509	0.197	1	0.361	0.361	0.514	0.197	0.612	0.364	0.365
X_4	0.184	-0.335	0.361	1	-0.159	0.186	-0.334	0.362	0.622	-0.161
X_5	0.184	0.477	0.361	-0.159	1	0.186	0.478	0.362	-0.161	0.639
\tilde{X}_1						1	0.371	0.496	0.187	0.187
\tilde{X}_2						0.371	1	0.189	-0.319	0.464
\tilde{X}_3						0.496	0.189	1	0.347	0.347
\tilde{X}_4						0.187	-0.319	0.347	1	-0.162
\tilde{X}_5						0.187	0.464	0.347	-0.162	1

A3.2 Design of semi-synthetic experiments with blood donation data

The logistic model used to generate the imaginary binary outcomes in Section 5.3 is:

$$\text{logit}(\mathbb{P}[Y = 1 | X, Z]) = \varphi(X, Z),$$

with

$$\begin{aligned} \varphi(X, Z) = & -c + \\ & -b \cdot \mathbb{1}[\text{male}] + b \cdot \mathbb{1}[\text{married}] + b \cdot \mathbb{1}[\text{resident}] - b \cdot \mathbb{1}[\text{age} < 25] + \\ & -b \cdot \mathbb{1}[\text{student}] - b \cdot \mathbb{1}[\text{education} < 16] + b \cdot \mathbb{1}[\text{Rh}^-] - b \cdot \mathbb{1}[\text{blood type} \neq \text{O}] + \\ & + a \cdot X_1 [(1 - \mathbb{1}[\text{resident}]) + (1 - \mathbb{1}[\text{donation within 12 months}])] + \\ & + a \cdot X_2 [\mathbb{1}[\text{student}] + \mathbb{1}[\text{student}] \cdot \mathbb{1}[\text{male}]] + \\ & + a \cdot X_3 [(1 - \mathbb{1}[\text{male}]) + (1 - \mathbb{1}[\text{student}])] + \\ & + a \cdot X_4 [\mathbb{1}[\text{student}] + \mathbb{1}[\text{male}]] + \\ & + a \cdot X_5 [(1 - \mathbb{1}[\text{education} < 16])]. \end{aligned} \tag{A33}$$

Above, the coefficients are set as $a = 0.4$, $b = 0.2$, while c is such that half of the individuals in the data set on average receive a simulated $Y = 1$.

The linear model used to generate the imaginary continuous outcomes in Section 5.3 has Gaussian errors with standard deviation 0.2 and conditional mean equal to:

$$\mathbb{E}[Y | X, Z] = \varphi(X, Z),$$

with the same $\varphi(X, Z)$ as in (A33). Here, $a = 1$ and $b = 0.5$, while c is such that the sample mean of Y is 0.

A3.3 Additional figures from semi-synthetic experiments

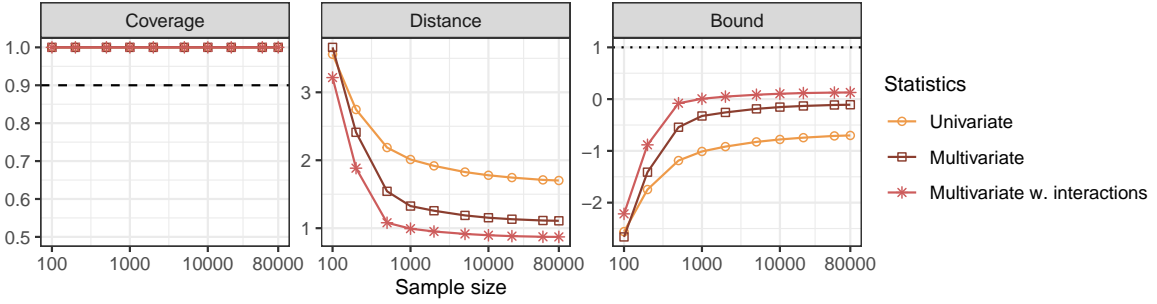


Figure A15: Quantile estimation of individual linear effects with the QCRT in a simulation based on real covariates and treatments from the randomized blood donation field experiment in Table 2. The fifth treatment from Table 3 is analyzed here. Other details are as in Figure 8.

A4 Mathematical proofs

A4.1 Individualized conditional testing with the SKF

Proof of Proposition A1. The proof is analogous to that of Proposition 1 in [10]. Suppose $\mathcal{H}_{0,j}^* : Y \perp\!\!\!\perp X_j \mid Z, X_{-j}, C$ is true. Then, it follows from $C \perp\!\!\!\perp X_j \mid Z, X_{-j}$ that $(Y, C) \perp\!\!\!\perp X_j \mid Z, X_{-j}$. Therefore, $\mathcal{H}_{0,j}$ must also be true. \square

Lemma A1. For any subset $\mathcal{S} \subseteq \{1, \dots, \hat{G}\}$ of true null hypotheses $\mathcal{H}_{0,j}^{(g_j)}$ in (5),

$$[\mathbf{X}, \tilde{\mathbf{X}}]_{\text{swap}(\mathcal{S})} \mid [\mathbf{X}, \tilde{\mathbf{X}}]_{\text{swap}(\mathbf{V})}, \mathbf{Y}, \mathbf{Z} \stackrel{d}{=} [\mathbf{X}, \tilde{\mathbf{X}}] \mid [\mathbf{X}, \tilde{\mathbf{X}}]_{\text{swap}(\mathbf{V})}, \mathbf{Y}, \mathbf{Z},$$

where \mathbf{V} is the random matrix used to define $\hat{\psi}$.

Proof of Theorem 1. It suffices to prove the “flip-sign” property in (9), as the subsequent result about false discovery rate control follows from there immediately as in [7]. In fact, the sign-flip property in (9) is analogous to the standard one from [7] and it holds conditional on $\hat{\psi}$, which fully defines the hypotheses.

Conditional on any $[\mathbf{X}, \tilde{\mathbf{X}}]_{\text{swap}(\mathbf{V})}, \mathbf{Y}, \mathbf{Z}, \hat{\phi}$ and \hat{G} are fixed. By construction, \mathbf{W} must satisfy (7), and therefore for any $\mathbf{U} \in \{\pm 1\}^{\hat{G} \times p}$

$$\mathbf{W}([\mathbf{X}, \tilde{\mathbf{X}}]_{\text{swap}(\mathbf{U})}, \mathbf{Y}, \mathbf{Z}) \mid [\mathbf{X}, \tilde{\mathbf{X}}]_{\text{swap}(\mathbf{V})}, \mathbf{Y}, \mathbf{Z} \stackrel{d}{=} \mathbf{U} \odot \mathbf{W}([\mathbf{X}, \tilde{\mathbf{X}}], \mathbf{Y}, \mathbf{Z}) \mid [\mathbf{X}, \tilde{\mathbf{X}}]_{\text{swap}(\mathbf{V})}, \mathbf{Y}, \mathbf{Z}.$$

Note that, above, $\hat{\psi}$ is fixed by $[\mathbf{X}, \tilde{\mathbf{X}}]_{\text{swap}(\mathbf{V})}, \mathbf{Y}, \mathbf{Z}$, and so is the number of rows \hat{G} of \mathbf{W} . Further, it follows from Lemma A1 that

$$\mathbf{W}([\mathbf{X}, \tilde{\mathbf{X}}]_{\text{swap}(\mathbf{U})}, \mathbf{Y}, \mathbf{Z}) \mid [\mathbf{X}, \tilde{\mathbf{X}}]_{\text{swap}(\mathbf{V})}, \mathbf{Y}, \mathbf{Z} \stackrel{d}{=} \mathbf{W}([\mathbf{X}, \tilde{\mathbf{X}}], \mathbf{Y}, \mathbf{Z}) \mid [\mathbf{X}, \tilde{\mathbf{X}}]_{\text{swap}(\mathbf{V})}, \mathbf{Y}, \mathbf{Z},$$

which, combined with the previous result, gives:

$$\mathbf{W} \odot \mathbf{U} \mid [\mathbf{X}, \tilde{\mathbf{X}}]_{\text{swap}(\mathbf{V})}, \mathbf{Y}, \mathbf{Z} \stackrel{d}{=} \mathbf{W} \mid [\mathbf{X}, \tilde{\mathbf{X}}]_{\text{swap}(\mathbf{V})}, \mathbf{Y}, \mathbf{Z}.$$

This implies the desired result because $\hat{\psi}$ is a function of $[\mathbf{X}, \tilde{\mathbf{X}}]_{\text{swap}(\mathbf{V})}, \mathbf{Y}, \mathbf{Z}$. \square

Proof of Lemma A1. We prove the following stronger equality in joint distribution:

$$\left([\mathbf{X}, \tilde{\mathbf{X}}]_{\text{swap}(\mathcal{S})}, [\mathbf{X}, \tilde{\mathbf{X}}]_{\text{swap}(\mathbf{V})}, \mathbf{Y}, \mathbf{Z}\right) \stackrel{d}{=} \left([\mathbf{X}, \tilde{\mathbf{X}}], [\mathbf{X}, \tilde{\mathbf{X}}]_{\text{swap}(\mathbf{V})}, \mathbf{Y}, \mathbf{Z}\right).$$

By independence, it suffices to establish the above result for a single row of the data matrices:

$$\left((X, \tilde{X})_{\text{swap}(s)}, Z, Y, (X, \tilde{X})_{\text{swap}(v)}\right) \stackrel{d}{=} \left((X, \tilde{X}), Z, Y, (X, \tilde{X})_{\text{swap}(v)}\right).$$

By construction of the knockoffs \tilde{X} , we know that

$$(X, \tilde{X})_{\text{swap}(s)} \mid Z \stackrel{d}{=} (X, \tilde{X}) \mid Z. \quad (\text{A34})$$

Further, for any fixed swap s and random swap v it holds that $v \odot s \stackrel{d}{=} v$, which implies

$$(X, \tilde{X})_{\text{swap}(s)} \mid (X, \tilde{X})_{\text{swap}(v)}, Z \stackrel{d}{=} (X, \tilde{X}) \mid (X, \tilde{X})_{\text{swap}(v)}, Z. \quad (\text{A35})$$

Combining (A34) and (A35) yields:

$$\left((X, \tilde{X})_{\text{swap}(s)}, (X, \tilde{X})_{\text{swap}(v)}, Z\right) \stackrel{d}{=} \left((X, \tilde{X}), (X, \tilde{X})_{\text{swap}(v)}, Z\right). \quad (\text{A36})$$

Now, recall that $Y \perp\!\!\!\perp \tilde{X} \mid Z, X$. Further, $Y \perp\!\!\!\perp X_s \mid Z, X_{-s}$ for all X_s swapped by s because the latter only involves null variables. Therefore, by the same argument as in the proof of Lemma 3.2 in [7],

$$Y \mid Z, (X, \tilde{X})_{\text{swap}(s)}, (X, \tilde{X})_{\text{swap}(v)} \stackrel{d}{=} Y \mid Z, (X, \tilde{X}), (X, \tilde{X})_{\text{swap}(v)}. \quad (\text{A37})$$

Finally, combining (A36) with (A37) gives the desired result. \square

Proof of Theorem A1. This result follows immediately from Theorem 1 in [41] with a simple extension of Proposition 5 therein. The original statement of Proposition 5 in [41] assumed the statistics \mathbf{W} to be computed using data collected from separate and a-priori fixed experimental settings (or *environments*), but it is easy to see that their proof only requires the flip-sign property (9) established by our Theorem 1. \square

A4.2 Quantile estimation of individual linear effects

Proof of Proposition 1. The proof is similar to that of the original CRT result from [7]. Under the null hypothesis \mathcal{H}_δ , we know $\mathbf{Y} - \mathbf{X} \odot \delta = g(\mathbf{Z}, \mathbf{C})$, and hence the CRT p-value in (13) becomes:

$$\begin{aligned} \hat{p}_\delta^{\text{CRT}}(\mathbf{X}, \mathbf{Y}, \mathbf{Z} - \mathbf{X} \odot \delta) &= \frac{1 + \sum_{k=1}^K \mathbb{1} \left[\bar{t}(\tilde{\mathbf{X}}^{(k)}, \mathbf{Z}, \mathbf{Y} - \mathbf{X} \odot \delta) \geq \bar{t}(\mathbf{X}, \mathbf{Y}, \mathbf{Z} - \mathbf{X} \odot \delta) \right]}{1 + K} \\ &= \frac{1 + \sum_{k=1}^K \mathbb{1} \left[\bar{t}(\tilde{\mathbf{X}}^{(k)}, \mathbf{Z}, g(\mathbf{Z}, \mathbf{C})) \geq \bar{t}(\mathbf{X}, \mathbf{Z}, g(\mathbf{Z}, \mathbf{C})) \right]}{1 + K}. \end{aligned}$$

Now, note that, conditional on \mathbf{Y} , \mathbf{Z} and \mathbf{C} (which is assumed to be independent of $X \mid Z$), the $K + 1$ vectors in $\{\tilde{\mathbf{X}}^{(k)}\}_{k=1}^K \cup \{\mathbf{X}\}$ are exchangeable with one another, as they are independent and identically distributed random samples from $P_{X|Z}$. Therefore, $\hat{p}_\delta^{\text{CRT}}(\mathbf{X}, \mathbf{Y}, \mathbf{Z})$ is uniformly distributed on $\{1/(K + 1), 2/(K + 1), \dots, 1\}$, by the same argument as in [7]. \square

Proposition A2. *Fix any $\delta \in \mathbb{R}^n$ and assume the partially linear model in (10) holds. If the sharp null hypothesis \mathcal{H}_δ in (11) is true, then, for any $\alpha \in (0, 1)$, the CRT p-value $\hat{p}_\delta(\mathbf{X}, \mathbf{Y}, \mathbf{Z})$ in (18) satisfies*

$$\mathbb{P}[\hat{p}_\delta(\mathbf{X}, \mathbf{Y}, \mathbf{Z}) \leq \alpha \mid \mathbf{Z}, \mathbf{Y}] \leq \alpha.$$

Proof of Proposition A2. This proof is very similar to that of Proposition 1. We begin by establishing the result for the special case in which $\hat{g}(z; \mathbf{Z}, \mathbf{Y}) = 0$ for all z . In this case, the CRT p-value can be written as:

$$\begin{aligned}\hat{p}_{\boldsymbol{\delta}}(\mathbf{X}, \mathbf{Y}, \mathbf{Z}) &= \frac{1 + \sum_{k=1}^K \mathbb{1} \left[t(\tilde{\mathbf{X}}^{(k)}, \mathbf{Y} - (\mathbf{X} - \tilde{\mathbf{X}}^{(k)}) \odot \boldsymbol{\delta}) \geq t(\mathbf{X}, \mathbf{Y}) \right]}{1 + K} \\ &= \frac{1 + \sum_{k=1}^K \mathbb{1} \left[t(\tilde{\mathbf{X}}^{(k)}, g(\mathbf{Z}, \mathbf{V}) + \tilde{\mathbf{X}}^{(k)} \odot \boldsymbol{\delta}) \geq t(\mathbf{X}, g(\mathbf{Z}, \mathbf{V}) + \mathbf{X} \odot \boldsymbol{\delta}) \right]}{1 + K},\end{aligned}$$

because $\mathbf{Y} = g(\mathbf{Z}, \mathbf{V}) + \mathbf{X} \odot \boldsymbol{\delta}$. Now, note that, conditional on \mathbf{Z} , \mathbf{Y} , and \mathbf{V} , the $K + 1$ random vectors in $\{\tilde{\mathbf{Z}}^{(k)}\}_{k=1}^K \cup \{\mathbf{Z}\}$ are exchangeable with one another (they are independent and identically distributed), and therefore $\hat{p}_{\boldsymbol{\delta}}(\mathbf{X}, \mathbf{Y}, \mathbf{Z})$ is uniformly distributed on $\{1/(K + 1), 2/(K + 1), \dots, 1\}$, as in the proof of Proposition 1.

For the second part of the proof, note that the residuals $Y^i - \hat{g}(Z^i; \mathbf{Z}, \mathbf{Y})$ can be written as:

$$\begin{aligned}Y^i - \hat{g}(Z^i; \mathbf{Z}, \mathbf{Y}) &= g(Z^i, V^i) - \hat{g}(Z^i; \mathbf{Z}, \mathbf{Y}) + \tau^i X^i \\ &= \Delta g(Z^i, V^i; \mathbf{Z}, \mathbf{Y}) + \tau^i X^i.\end{aligned}$$

Therefore, the residuals still obey a partially linear model in the form of (10) with the same variables and effects as in the original model, and with the only difference that the function $g(Z^i, V^i)$ is replaced by $\Delta g(Z^i, V^i; \mathbf{Z}, \mathbf{Y}) = g(Z^i, V^i) - \hat{g}(Z^i; \mathbf{Z}, \mathbf{Y})$. Given that the first part of the result proved above treats \mathbf{Z} , \mathbf{V} and \mathbf{Y} as fixed, while making no assumptions about the functional form of g , the remaining part of the proof follows immediately. \square

Proof of Theorem 2. We already know from Proposition A2 that, for any $\alpha \in (0, 1)$,

$$\mathbb{P}[\hat{p}_{\boldsymbol{\tau}}(\mathbf{X}, \mathbf{Y}, \mathbf{Z}) \leq \alpha | \mathbf{Z}, \mathbf{Y}] \leq \alpha.$$

Therefore, it suffices to show that $\hat{p}_{\boldsymbol{\delta}}(\mathbf{X}, \mathbf{Y}, \mathbf{Z}) \geq \hat{p}_{\boldsymbol{\tau}}(\mathbf{X}, \mathbf{Y}, \mathbf{Z})$ almost surely, which can be established by noting that $\mathcal{H}_{\leq \boldsymbol{\delta}}$ implies $\boldsymbol{\delta} \geq \boldsymbol{\tau}$ and $\hat{p}_{\boldsymbol{\delta}}(\mathbf{X}, \mathbf{Y}, \mathbf{Z})$ is element-wise monotone increasing in $\boldsymbol{\delta}$ (Lemma A2). \square

Lemma A2. *The CRT p-value $\hat{p}_{\boldsymbol{\delta}}(\mathbf{X}, \mathbf{Y}, \mathbf{Z})$ defined in (18) is monotone increasing in $\boldsymbol{\delta}$ (element-wise) if the statistic t in (18) is effect-increasing.*

Proof of Lemma A2. To simplify the notation, for any $\mathbf{a} \in \mathbb{R}^{n \times 1}$, define $\mathbf{Y}_{\mathbf{Z}, \boldsymbol{\delta}}(\mathbf{a})$ as

$$\mathbf{Y}_{\mathbf{X}, \boldsymbol{\delta}}(\mathbf{a}) = \mathbf{Y} - \mathbf{X} \odot \boldsymbol{\delta} + \mathbf{a} \odot \boldsymbol{\delta}.$$

For any $\tilde{\mathbf{X}} \in \mathbb{R}^{n \times 1}$ and $\bar{\boldsymbol{\delta}} \geq \boldsymbol{\delta}$, we can write

$$\begin{aligned}t(\tilde{\mathbf{X}}, \mathbf{Y} - \mathbf{X} \odot \bar{\boldsymbol{\delta}} + \tilde{\mathbf{X}} \odot \bar{\boldsymbol{\delta}}) &= t(\tilde{\mathbf{X}}, \mathbf{Y}_{\mathbf{X}, \bar{\boldsymbol{\delta}}}(\tilde{\mathbf{X}})) \\ &= t(\tilde{\mathbf{X}}, \mathbf{Y}_{\mathbf{X}, \boldsymbol{\delta}}(\tilde{\mathbf{X}}) + \mathbf{Y}_{\mathbf{X}, \bar{\boldsymbol{\delta}}}(\tilde{\mathbf{X}}) - \mathbf{Y}_{\mathbf{X}, \boldsymbol{\delta}}(\tilde{\mathbf{X}})).\end{aligned}$$

Then, note that

$$\begin{aligned}\mathbf{Y}_{\mathbf{X}, \bar{\boldsymbol{\delta}}}(\mathbf{a}) - \mathbf{Y}_{\mathbf{X}, \boldsymbol{\delta}}(\mathbf{a}) &= \mathbf{a} \odot \mathbf{Y}_{\mathbf{X}, \bar{\boldsymbol{\delta}}}(\mathbf{1}) + (\mathbf{1} - \mathbf{a}) \odot \mathbf{Y}_{\mathbf{X}, \bar{\boldsymbol{\delta}}}(\mathbf{0}) - [\mathbf{a} \odot \mathbf{Y}_{\mathbf{X}, \boldsymbol{\delta}}(\mathbf{1}) + (\mathbf{1} - \mathbf{a}) \odot \mathbf{Y}_{\mathbf{X}, \boldsymbol{\delta}}(\mathbf{0})] \\ &= \mathbf{a} \odot [\mathbf{Y}_{\mathbf{X}, \bar{\boldsymbol{\delta}}}(\mathbf{1}) - \mathbf{Y}_{\mathbf{X}, \boldsymbol{\delta}}(\mathbf{1})] + (\mathbf{1} - \mathbf{a}) \odot [\mathbf{Y}_{\mathbf{X}, \bar{\boldsymbol{\delta}}}(\mathbf{0}) - \mathbf{Y}_{\mathbf{X}, \boldsymbol{\delta}}(\mathbf{0})] \\ &= \mathbf{a} \odot \boldsymbol{\eta} + (\mathbf{1} - \mathbf{a}) \odot \boldsymbol{\xi},\end{aligned}$$

for some $\boldsymbol{\eta} \geq 0 \geq \boldsymbol{\xi}$. Therefore, by the effect-increasing property of t ,

$$\begin{aligned}t(\tilde{\mathbf{X}}, \mathbf{Y} - \mathbf{X} \odot \bar{\boldsymbol{\delta}} + \tilde{\mathbf{X}} \odot \bar{\boldsymbol{\delta}}) &= t(\tilde{\mathbf{X}}, \mathbf{Y}_{\mathbf{X}, \bar{\boldsymbol{\delta}}}(\tilde{\mathbf{X}})) \\ &= t(\tilde{\mathbf{X}}, \mathbf{Y}_{\mathbf{X}, \boldsymbol{\delta}}(\tilde{\mathbf{X}}) + \mathbf{Y}_{\mathbf{X}, \bar{\boldsymbol{\delta}}}(\tilde{\mathbf{X}}) - \mathbf{Y}_{\mathbf{X}, \boldsymbol{\delta}}(\tilde{\mathbf{X}})) \\ &= t(\tilde{\mathbf{X}}, \mathbf{Y}_{\mathbf{X}, \boldsymbol{\delta}}(\tilde{\mathbf{X}}) + \tilde{\mathbf{X}} \odot \boldsymbol{\eta} + (\mathbf{1} - \tilde{\mathbf{X}}) \odot \boldsymbol{\xi}) \\ &\geq t(\tilde{\mathbf{X}}, \mathbf{Y}_{\mathbf{X}, \boldsymbol{\delta}}(\tilde{\mathbf{X}})) \\ &= t(\tilde{\mathbf{X}}, \mathbf{Y} - \mathbf{X} \odot \boldsymbol{\delta} + \tilde{\mathbf{X}} \odot \boldsymbol{\delta}),\end{aligned}$$

since $\bar{\boldsymbol{\delta}} \geq \boldsymbol{\delta}$. And therefore $\hat{p}_{\bar{\boldsymbol{\delta}}}(\mathbf{X}, \mathbf{Y}, \mathbf{Z}) \geq \hat{p}_{\boldsymbol{\delta}}(\mathbf{X}, \mathbf{Y}, \mathbf{Z})$, by the definition of the CRT p-values in (18). \square

Proof of Theorem 3. By the same argument used in the proof of Proposition A2, it suffices to prove the result for the special case of $\hat{g} = 0$ in (20), because $\mathbf{Y} - \hat{g}(\mathbf{Z}; \mathbf{Z}, \mathbf{Y})$ still obeys a partially linear model in the form of (10) with the same variables and effects as in the original model. Therefore, we will simply assume $\hat{g} = 0$ hereafter. For any column vector $\boldsymbol{\delta} \in \mathbb{R}^n$, with a slight abuse of notation, we will write that $\boldsymbol{\delta} \in \mathcal{H}_{q, \leq, c}$ if and only if the q -th largest element of $\boldsymbol{\delta}$ is no greater than c . If the quantile null hypothesis $\mathcal{H}_{q, \leq, c}$ in (15) is true, then the vector $\boldsymbol{\tau}$ of true effects satisfies $\boldsymbol{\tau} \in \mathcal{H}_{q, \leq, c}$. Therefore,

$$\sup_{\boldsymbol{\delta} \in \mathcal{H}_{q, \leq, c}} \hat{p}_{\boldsymbol{\delta}}(\mathbf{X}, \mathbf{Y}, \mathbf{Z}) \geq \hat{p}_{\boldsymbol{\tau}}(\mathbf{X}, \mathbf{Y}, \mathbf{Z}),$$

and, for any $\alpha \in [0, 1]$,

$$\mathbb{P} \left[\sup_{\boldsymbol{\delta} \in \mathcal{H}_{q, \leq, c}} \hat{p}_{\boldsymbol{\delta}}(\mathbf{X}, \mathbf{Y}, \mathbf{Z}) \leq \alpha \mid \mathbf{Z}, \mathbf{Y} \right] \leq \mathbb{P} [\hat{p}_{\boldsymbol{\tau}}(\mathbf{X}, \mathbf{Y}, \mathbf{Z}) \leq \alpha \mid \mathbf{Z}, \mathbf{Y}] \leq \alpha,$$

where the second inequality follows from Proposition A2. This implies that $\sup_{\boldsymbol{\delta} \in \mathcal{H}_{q, \leq, c}} \hat{p}_{\boldsymbol{\delta}}(\mathbf{X}, \mathbf{Y}, \mathbf{Z})$ is a valid p-value for testing the quantile null hypothesis $\mathcal{H}_{q, \leq, c}$ in (15). The proof is then completed by applying Lemma A3, as that implies

$$\hat{p}_{q, c}(\mathbf{X}, \mathbf{Y}, \mathbf{Z}) \geq \sup_{\boldsymbol{\delta} \in \mathcal{H}_{q, \leq, c}} \hat{p}_{\boldsymbol{\delta}}(\mathbf{X}, \mathbf{Y}, \mathbf{Z}),$$

and therefore

$$\mathbb{P} [\hat{p}_{q, c}(\mathbf{X}, \mathbf{Y}, \mathbf{Z}) \leq \alpha \mid \mathbf{Z}, \mathbf{Y}] \leq \mathbb{P} \left[\sup_{\boldsymbol{\delta} \in \mathcal{H}_{q, \leq, c}} \hat{p}_{\boldsymbol{\delta}}(\mathbf{X}, \mathbf{Y}, \mathbf{Z}) \leq \alpha \mid \mathbf{Z}, \mathbf{Y} \right] \leq \alpha.$$

\square

Lemma A3. For any $\mathbf{Y}, \mathbf{X}, \tilde{\mathbf{X}}^{(k)} \in \mathbb{R}^n$ and $\mathbf{Z} \in \mathbb{R}^{n \times m}$, if $\boldsymbol{\eta}^{(k)}$ is defined as in (19) and t is an effect-increasing statistic, then

$$\sup_{\boldsymbol{\delta} \in \mathcal{H}_{q, \leq, c}} t(\tilde{\mathbf{X}}^{(k)}, \mathbf{Y} - (\mathbf{X} - \tilde{\mathbf{X}}^{(k)}) \odot \boldsymbol{\delta}) \leq t(\tilde{\mathbf{X}}^{(k)}, \mathbf{Y} - (\mathbf{X} - \tilde{\mathbf{X}}^{(k)}) \odot \boldsymbol{\eta}^{(k)}).$$

Proof of Lemma A3. We begin by considering the case of $c = 0$; then, the proof for $c \neq 0$ will follow easily.

Part I. Define the set $\tilde{\mathcal{T}}^{(k)} = \{i : \tilde{X}^{(k)i} = 1\}$, and let $\tilde{m}^{(k)} = |\tilde{\mathcal{T}}^{(k)}|$. Define $\tilde{l}^{(k)} = \min(\tilde{m}^{(k)}, n - q)$. For any $\boldsymbol{\delta} \in \mathcal{H}_{q, \leq, 0}$, let $\tilde{\mathcal{J}}^{(k)}$ be the set of indices for the $\tilde{l}^{(k)}$ largest coordinates of $\boldsymbol{\delta}$ among those in $\tilde{\mathcal{T}}^{(k)}$. Then, define a vector $\boldsymbol{\xi}^{(k)} \in \mathbb{R}^n$ such that

$$\xi^{(k)i} = \begin{cases} +\infty, & \text{if } i \in \tilde{\mathcal{J}}^{(k)}, \\ 0, & \text{otherwise.} \end{cases} \quad (\text{A38})$$

The first part of the proof consists of establishing that

$$t(\tilde{\mathbf{X}}, \mathbf{Y} + (\tilde{\mathbf{X}}^{(k)} - \mathbf{X}) \odot \boldsymbol{\delta}) \leq t(\tilde{\mathbf{X}}, \mathbf{Y} + (\tilde{\mathbf{X}}^{(k)} - \mathbf{X}) \odot \boldsymbol{\xi}^{(k)}). \quad (\text{A39})$$

Part II. The second part of the proof consists of establishing that

$$t(\tilde{\mathbf{X}}, \mathbf{Y} + (\tilde{\mathbf{X}}^{(k)} - \mathbf{X}) \odot \boldsymbol{\xi}^{(k)}) \leq t(\tilde{\mathbf{X}}, \mathbf{Y} + (\tilde{\mathbf{X}}^{(k)} - \mathbf{X}) \odot \boldsymbol{\eta}^{(k)}). \quad (\text{A40})$$

Wrapping up. Combining the results in (A39) and (A40), which are separately proved below, gives

$$t(\tilde{\mathbf{X}}, \mathbf{Y} + (\tilde{\mathbf{X}}^{(k)} - \mathbf{X}) \odot \boldsymbol{\delta}) \leq t(\tilde{\mathbf{X}}, \mathbf{Y} + (\tilde{\mathbf{X}}^{(k)} - \mathbf{X}) \odot \boldsymbol{\eta}^{(k)}),$$

which completes the proof for the special case of $c = 0$ because it implies

$$\sup_{\boldsymbol{\delta} \in \mathcal{H}_{q, \leq, 0}} t(\tilde{\mathbf{X}}^{(k)}, \mathbf{Y} - (\mathbf{X} - \tilde{\mathbf{X}}^{(k)}) \odot \boldsymbol{\delta}) \leq t(\tilde{\mathbf{X}}^{(k)}, \mathbf{Y} - (\mathbf{X} - \tilde{\mathbf{X}}^{(k)}) \odot \boldsymbol{\eta}^{(k)}). \quad (\text{A41})$$

In order to extend this result to the more general case of $c \neq 0$, note that $\mathcal{H}_{k,c} = \mathcal{H}_{k,0} + c\mathbf{1}$. Therefore,

$$\begin{aligned} & \sup_{\boldsymbol{\delta} \in \mathcal{H}_{k,c}} t(\tilde{\mathbf{X}}^{(k)}, \mathbf{Y} + (\tilde{\mathbf{X}}^{(k)} - \mathbf{X}) \odot \boldsymbol{\delta}) \\ &= \sup_{\boldsymbol{\delta} \in \mathcal{H}_{k,0}} t(\tilde{\mathbf{X}}^{(k)}, \mathbf{Y} + (\tilde{\mathbf{X}}^{(k)} - \mathbf{X}) \odot (\boldsymbol{\delta} + c\mathbf{1})) \\ &= \sup_{\boldsymbol{\delta} \in \mathcal{H}_{k,0}} t(\tilde{\mathbf{X}}^{(k)}, [\mathbf{Y} + (\tilde{\mathbf{X}}^{(k)} - \mathbf{X}) \odot c\mathbf{1}] + (\tilde{\mathbf{X}}^{(k)} - \mathbf{X}) \odot \boldsymbol{\delta})) \\ &\leq t(\tilde{\mathbf{X}}^{(k)}, \mathbf{Y} + (\tilde{\mathbf{X}}^{(k)} - \mathbf{X}) \odot (\boldsymbol{\eta}^{(0)} + c\mathbf{1})), \end{aligned}$$

where the inequality follows by applying (A41) with the modified outcome vector $\mathbf{Y} + (\tilde{\mathbf{X}}^{(k)} - \mathbf{X}) \odot (\boldsymbol{\eta} + c\mathbf{1})$ instead of \mathbf{Y} (this is allowed because (A41) holds for any \mathbf{Y}), and $\boldsymbol{\eta}^{(0)}$ is defined as:

$$\eta^i = \begin{cases} +\infty, & \text{if } i \in \tilde{\mathcal{I}}^{(k)}, \\ 0, & \text{otherwise.} \end{cases}$$

This completes the proof because the vector $\boldsymbol{\eta}$ defined in (19) is exactly given by $\boldsymbol{\eta} = \boldsymbol{\eta}^{(0)} + c\mathbf{1}$.

Part I: proof of (A39). Note that

$$\begin{aligned} t(\tilde{\mathbf{X}}, \mathbf{Y} + (\tilde{\mathbf{X}}^{(k)} - \mathbf{X}) \odot \boldsymbol{\xi}^{(k)}) &= t(\tilde{\mathbf{X}}, \mathbf{Y} + (\tilde{\mathbf{X}}^{(k)} - \mathbf{X}) \odot \boldsymbol{\delta} + (\tilde{\mathbf{X}}^{(k)} - \mathbf{X}) \odot (\boldsymbol{\xi}^{(k)} - \boldsymbol{\delta})) \\ &= t(\tilde{\mathbf{X}}, \mathbf{Y}_{\mathbf{X}, \boldsymbol{\delta}}(\tilde{\mathbf{X}}^{(k)}) + (\tilde{\mathbf{X}}^{(k)} - \mathbf{X}) \odot (\boldsymbol{\xi}^{(k)} - \boldsymbol{\delta})), \end{aligned}$$

where

$$\mathbf{Y}_{\mathbf{X}, \boldsymbol{\delta}}(\tilde{\mathbf{X}}^{(k)}) = \mathbf{Y} - \mathbf{X} \odot \boldsymbol{\delta} + \tilde{\mathbf{X}}^{(k)} \odot \boldsymbol{\delta}.$$

Let's look more closely at the $(\tilde{\mathbf{X}}^{(k)} - \mathbf{X}) \odot (\boldsymbol{\xi}^{(k)} - \boldsymbol{\delta})$ term. This can be written as:

$$\begin{aligned} (\tilde{\mathbf{X}}^{(k)} - \mathbf{X}) \odot (\boldsymbol{\xi}^{(k)} - \boldsymbol{\delta}) &= \tilde{\mathbf{X}}^{(k)} \odot (\tilde{\mathbf{X}}^{(k)} - \mathbf{X}) \odot (\boldsymbol{\xi}^{(k)} - \boldsymbol{\delta}) + (\mathbf{1} - \tilde{\mathbf{X}}^{(k)}) \odot (\tilde{\mathbf{X}}^{(k)} - \mathbf{X}) \odot (\boldsymbol{\xi}^{(k)} - \boldsymbol{\delta}) \\ &= \tilde{\mathbf{X}}^{(k)} \odot (\mathbf{1} - \mathbf{X}) \odot (\boldsymbol{\xi}^{(k)} - \boldsymbol{\delta}) + (\mathbf{1} - \tilde{\mathbf{X}}^{(k)}) \odot (-\mathbf{X}) \odot (\boldsymbol{\xi}^{(k)} - \boldsymbol{\delta}) \\ &= \tilde{\mathbf{X}}^{(k)} \odot \boldsymbol{\psi} + (\mathbf{1} - \tilde{\mathbf{X}}^{(k)}) \odot \boldsymbol{\omega}, \end{aligned}$$

for $\boldsymbol{\psi} = \tilde{\mathbf{X}}^{(k)} \odot (\mathbf{1} - \mathbf{X}) \odot (\boldsymbol{\xi}^{(k)} - \boldsymbol{\delta})$ and $\boldsymbol{\omega} = (\mathbf{1} - \tilde{\mathbf{X}}^{(k)}) \odot (-\mathbf{X}) \odot (\boldsymbol{\xi}^{(k)} - \boldsymbol{\delta})$. Recall that, by definition of $\mathcal{H}_{q, \leq, 0}$, it must be the case that $\delta^i \leq 0$ for all $i \in \tilde{\mathcal{T}}^{(k)} \setminus \tilde{\mathcal{J}}^{(k)}$. This implies $\delta^i \leq \xi^i = 0$ for all $i \in \tilde{\mathcal{T}}^{(k)} \setminus \tilde{\mathcal{J}}^{(k)}$. Further, $\delta^i \leq \xi^i = +\infty$ for all $i \in \tilde{\mathcal{J}}^{(k)}$. This means that $\delta^i \leq \xi^i$ for all $i \in \tilde{\mathcal{T}}^{(k)}$, and hence $\boldsymbol{\psi} \geq 0$. Further, it follows from the assumption that t is a monotone rank statistic that

$$\begin{aligned} t(\tilde{\mathbf{X}}, \mathbf{Y} + (\tilde{\mathbf{X}}^{(k)} - \mathbf{X}) \odot \boldsymbol{\xi}^{(k)}) &= t(\tilde{\mathbf{X}}, \mathbf{Y}_{\mathbf{X}, \boldsymbol{\delta}}(\tilde{\mathbf{X}}^{(k)}) + \tilde{\mathbf{X}}^{(k)} \odot \boldsymbol{\psi} + (\mathbf{1} - \tilde{\mathbf{X}}^{(k)}) \odot \boldsymbol{\omega}) \\ &= t(\tilde{\mathbf{X}}, \mathbf{Y}_{\mathbf{X}, \boldsymbol{\delta}}(\tilde{\mathbf{X}}^{(k)}) + \tilde{\mathbf{X}}^{(k)} \odot \boldsymbol{\psi}). \end{aligned}$$

Therefore, by the effect-increasing property of t ,

$$\begin{aligned} t(\tilde{\mathbf{X}}, \mathbf{Y} + (\tilde{\mathbf{X}}^{(k)} - \mathbf{X}) \odot \boldsymbol{\xi}^{(k)}) &= t(\tilde{\mathbf{X}}, \mathbf{Y}_{\mathbf{X}, \boldsymbol{\delta}}(\tilde{\mathbf{X}}^{(k)}) + \tilde{\mathbf{X}}^{(k)} \odot \boldsymbol{\psi}) \\ &\geq t(\tilde{\mathbf{X}}, \mathbf{Y}_{\mathbf{X}, \boldsymbol{\delta}}(\tilde{\mathbf{X}}^{(k)})) \\ &= t(\tilde{\mathbf{X}}, \mathbf{Y} + (\tilde{\mathbf{X}}^{(k)} - \mathbf{X}) \odot \boldsymbol{\delta}). \end{aligned}$$

This completes the proof of (A39).

Part II: proof of (A40). As in the proof of (A39), recall that $\tilde{\mathcal{T}}^{(k)} = \{i : \tilde{X}^{(k)i} = 1\}$, and $\tilde{m}^{(k)} = |\tilde{\mathcal{T}}^{(k)}|$. Define $\tilde{l}^{(k)} = \min(\tilde{m}^{(k)}, n - q)$. In order to simplify the notation hereafter we will omit the superscripts (k) and write m, l instead of $\tilde{m}^{(k)}, \tilde{l}^{(k)}$, whenever it does not create ambiguity. For any set $\mathcal{L} \subseteq \tilde{\mathcal{T}}$ of size l , i.e., $|\mathcal{L}| = l$, define a vector $\boldsymbol{\gamma} = \boldsymbol{\gamma}(\mathcal{L}) \in \mathbb{R}^n$ such that

$$\gamma^i = \begin{cases} +\infty, & \text{if } i \in \mathcal{L}, \\ 0, & \text{otherwise.} \end{cases} \quad (\text{A42})$$

In the following, we will study the value of $t(\tilde{\mathbf{X}}, \mathbf{Y} + (\tilde{\mathbf{X}} - \mathbf{X}) \odot \boldsymbol{\gamma})$.

Define $r_1 < r_2 < \dots < r_m$ as the ranks of Y^i for all $i \in \tilde{\mathcal{T}}$. Suppose $\{j_1, \dots, j_m\}$ is some permutation of $\{1, \dots, m\}$. Then, we can write as $r_{j_1} < r_{j_2} < \dots < r_{j_{m-l}}$ the ranks (in increasing order) of the outcomes Y^i with indices in $\tilde{\mathcal{T}} \setminus \mathcal{L}$, among those in $\tilde{\mathcal{T}}$, and $r_{j_{m-l+1}} < r_{j_{m-l+2}} < \dots < r_{j_m}$ be the analogous ranks of the outcomes Y^i with indices in \mathcal{L} . By definition of \mathcal{L} and $\boldsymbol{\gamma}$, we know that $Y^i + (\tilde{X}^i - X^i)\gamma^i = +\infty$ for $i \in \mathcal{L}$, and thus the ranks of $Y^i + (\tilde{X}^i - X^i)\gamma^i$ with $i \in \mathcal{L}$ must be $\{m-l+1, m-l+2, \dots, m\}$; that is,

$$\{r^i(\mathbf{Y} + (\tilde{\mathbf{X}} - \mathbf{X}) \odot \boldsymbol{\gamma}) : i \in \mathcal{L}\} = \{m-l+1, m-l+2, \dots, m\}. \quad (\text{A43})$$

For each $i \in \tilde{\mathcal{T}} \setminus \mathcal{L}$, there are $m - j_a$ indices i within $\tilde{\mathcal{T}}$ whose Y^i has larger rank than Y^i , because the rank of Y^i is r_{j_a} , for some appropriate $a : 1 \leq a \leq m-l$.

Given that $Y^i + (\tilde{X}^i - X^i)\gamma^i = Y^i$ for all $i \in \tilde{\mathcal{T}} \setminus \mathcal{L}$ because $\gamma^i = 0$ by definition, this also implies there are $l + (m - l - j_a) = m - j_a$ elements of $\mathbf{Y} + (\tilde{\mathbf{X}} - \mathbf{X}) \odot \boldsymbol{\gamma}$ with indices in $\tilde{\mathcal{T}} \setminus \mathcal{L}$ that are ranked higher than $Y^i + (\tilde{X}^i - X^i)\gamma^i = Y^i$. Therefore, the rank of $Y^i + (\tilde{X}^i - X^i)\gamma^i$ among $\mathbf{Y} + (\tilde{\mathbf{X}} - \mathbf{X}) \odot \boldsymbol{\gamma}$ is simply j_a . That is,

$$\{r^i(\mathbf{Y} + (\tilde{\mathbf{X}} - \mathbf{X}) \odot \boldsymbol{\gamma}) : i \in \tilde{\mathcal{T}} \setminus \mathcal{L}\} = \{j_1, j_2, \dots, j_{m-l}\}. \quad (\text{A44})$$

Combining (A43) and (A44) with the assumption that t is a monotone rank statistic, we find that the value of $t(\tilde{\mathbf{X}}, \mathbf{Y} + (\tilde{\mathbf{X}} - \mathbf{X}) \odot \boldsymbol{\gamma})$ can be written as:

$$\begin{aligned} t(\tilde{\mathbf{X}}, \mathbf{Y} + (\tilde{\mathbf{X}} - \mathbf{X}) \odot \boldsymbol{\gamma}) &= \sum_{i \in \tilde{\mathcal{T}}} \phi[r^i(\mathbf{Y} + (\tilde{\mathbf{X}} - \mathbf{X}) \odot \boldsymbol{\gamma})] \\ &= \sum_{i \in \mathcal{L}} \phi[r^i(\mathbf{Y} + (\tilde{\mathbf{X}} - \mathbf{X}) \odot \boldsymbol{\gamma})] + \sum_{i \in \tilde{\mathcal{T}} \setminus \mathcal{L}} \phi[r^i(\mathbf{Y} + (\tilde{\mathbf{X}} - \mathbf{X}) \odot \boldsymbol{\gamma})] \\ &= \sum_{i=1}^l \phi(m-l+i) + \sum_{a=1}^{m-l} \phi(j_a). \end{aligned}$$

We turn now to calculating $t(\tilde{\mathbf{X}}, \mathbf{Y} + (\tilde{\mathbf{X}} - \mathbf{X}) \odot \boldsymbol{\eta})$, which is a special case of the above with the generic $\boldsymbol{\gamma}$ replaced by the $\boldsymbol{\eta}$ defined as in (19) with $c = 0$; i.e.,

$$\eta^i = \begin{cases} +\infty, & \text{if } i \in \tilde{\mathcal{I}}, \\ 0, & \text{otherwise.} \end{cases}$$

Recall that $\tilde{\mathcal{I}}$ is the set of individuals with the smallest $l = \min(m, n - k)$ values of Y^i among those in $\tilde{\mathcal{T}}$, where m is the size of $\tilde{\mathcal{T}}$: the total number of individuals receiving a $\tilde{X} = 1$. Therefore, we know that in this case $j_a = l + a$ in (A44) and we can write

$$t(\tilde{\mathbf{X}}, \mathbf{Y} + (\tilde{\mathbf{X}} - \mathbf{X}) \odot \boldsymbol{\eta}) = \sum_{i=1}^l \phi(m-l+i) + \sum_{a=1}^{m-l} \phi(l+a).$$

By contrast, if γ is instead replaced by the ξ defined in (A38),

$$t(\tilde{\mathbf{X}}, \mathbf{Y} + (\tilde{\mathbf{X}} - \mathbf{X}) \odot \xi) = \sum_{i=1}^l \phi(m - l + i) + \sum_{a=1}^{m-l} \phi(j_a),$$

for some $j_a \leq l + a$. Therefore, we can conclude from the monotonicity of ϕ that

$$t(\tilde{\mathbf{X}}, \mathbf{Y} + (\tilde{\mathbf{X}} - \mathbf{X}) \odot \eta) - t(\tilde{\mathbf{X}}, \mathbf{Y} + (\tilde{\mathbf{X}} - \mathbf{X}) \odot \xi) = \sum_{a=1}^{m-l} \phi(l + a) - \sum_{a=1}^{m-l} \phi(j_a) \geq 0.$$

This completes the proof of (A40).

Proof of Proposition 2. Define $\mathbf{Y}' = -\mathbf{Y}$, $g' = -g$, and $c' = -c$. The assumption in (10) implies that \mathbf{Y}' follows a partially linear model in which the individual effects are $\tau' = -\tau$:

$$Y'^i = g'(Z^i, C^i, V^i) + \tau'^i X'^i. \quad (\text{A45})$$

Therefore, it Theorem 3 implies that the CRT p-value $\hat{p}_{q,c'}$ in (20), evaluated using the data in $(\mathbf{X}, \mathbf{Z}, \mathbf{Y}')$, is a valid p-value for testing whether $\tau'_{(q)} \leq c'$. The proof is completed by noting that $\tau'_{(q)} \leq c'$ is equivalent to $\tau_{(n-q)} \geq c$. \square

Proof of Proposition 3. Define $\mathbf{X}' = \mathbf{1} - \mathbf{X}$, $\mathbf{Y}' = -\mathbf{Y}$, and $g'(Z^i, C^i, V^i) = -g(Z^i, C^i, V^i) - \tau^i$. The assumption in (10) implies that \mathbf{Y}' also follows a partially linear model in which the X labels are swapped:

$$\begin{aligned} Y'^i &= -g(Z^i, C^i, V^i) - \tau^i X^i \\ &= -g(Z^i, C^i, V^i) + \tau^i (1 - X^i) - \tau^i \\ &= g'(Z^i, C^i, V^i) + \tau^i (1 - X^i) \\ &= g'(Z^i, C^i, V^i) + \tau^i X'^i. \end{aligned}$$

Therefore, it Theorem 3 implies that the CRT p-value $\hat{p}_{q,c'}$ in (20), evaluated using the data in $(\mathbf{X}', \mathbf{Z}, \mathbf{Y}')$, is a valid p-value for testing whether $\tau_{(q)} \leq c$. \square

\square

A4.3 Sharp confidence intervals from a specialized CRT

Proof of Theorem A2. Recall that $\mathbf{Y}' = \mathbf{Y} - \mathbf{X} \odot \delta$, where $\delta = \delta \mathbf{1}$ for some $\delta \in \mathbb{R}$. By the partially linear model (10), the statistics in (A32) can be written as

$$\bar{t}(\mathbf{X}', \mathbf{Z}, \mathbf{Y}') = (\tau - \delta) \frac{\sum_i (X^{(i)} - \bar{X})(X'^{(i)} - \bar{X}')} {\sum_i (X^{(i)} - \bar{X})^2} + \frac{1}{\sum_i (X^{(i)} - \bar{X})^2} \sum_i (X^{(i)} - \bar{X}) \left(g(Z^{(i)}, C^{(i)}) - \hat{g}(Z^{(i)}) \right).$$

When evaluated with the true variables (i.e., $\mathbf{X}' = \mathbf{X}$), these simplify to

$$\bar{t}(\mathbf{X}, \mathbf{Y}', \mathbf{Z}) = (\tau - \delta) + W_n,$$

where W_n is

$$W_n = \frac{1}{\sum_i (X^{(i)} - \bar{X})^2} \sum_i (X^{(i)} - \bar{X}) \left(g(Z^{(i)}, C^{(i)}) - \hat{g}(Z^{(i)}) \right).$$

When evaluated with the virtual variables (i.e., $\mathbf{X}' = \tilde{\mathbf{X}}$, omitting the superscript (k) which usually indicates the replicate number for the virtual variables), the statistics simplify to

$$\bar{t}(\tilde{\mathbf{X}}, \mathbf{Z}, \mathbf{Y}') = (\tau - \delta)A_n + \tilde{W}_n,$$

where we have defined

$$A_n = \frac{\Sigma_n}{\tilde{S}_n}, \quad \Sigma_n = \frac{1}{n} \sum_i (\tilde{X}^{(i)} - \bar{\tilde{X}})(X'^{(i)} - \bar{X}'), \quad \tilde{S}_n = \frac{1}{n} \sum_i (\tilde{X}^{(i)} - \bar{\tilde{X}})^2,$$

and

$$\tilde{W}_n = \frac{1}{\tilde{S}_n} \frac{1}{n} \sum_i (\tilde{X}^{(i)} - \bar{\tilde{X}}) (g(Z^{(i)}, C^{(i)}) - \hat{g}(Z^{(i)})).$$

Now, define the filtration \mathcal{F}_n as:

$$\mathcal{F}_n = \sigma \left(\left\{ X_j^{(i)}, Z^{(i)}, g(Z^{(i)}, C^{(i)}), \hat{g}(Z^{(i)}) \right\}_{i=1}^n \right),$$

which summarizes all available data and the random noise in Y , excluding only the virtual variables \tilde{X} . It is clear that, as $K \rightarrow \infty$, the CRT p-value $\hat{p}_{\delta}^{\text{CRT}}$ in (13) converges almost surely to

$$\hat{p}_{\delta}^{\text{CRT}, \infty} = \mathbb{P} \left[|\bar{t}(\tilde{\mathbf{X}}, \mathbf{Z}, \mathbf{Y}')| \geq |\bar{t}(\mathbf{X}, \mathbf{Y}', \mathbf{Z})| \mid \mathcal{F}_n \right].$$

Therefore, we will now focus on $\hat{p}_{\delta}^{\text{CRT}, \infty}$, sometimes referring to it simply as $\hat{p}(\delta)$ to lighten the notation. The specific form of the special CRT statistics derived above allows $\hat{p}(\delta)$ to be written more explicitly as

$$\hat{p}_n(\delta) = \mathbb{E} \left[\psi(\tau - \delta; W_n, \tilde{W}_n, A_n) \mid \mathcal{F}_n \right],$$

where, for any $\gamma \in \mathbb{R}$, $\psi(\gamma; W_n, \tilde{W}_n, A_n)$ is the indicator function of a set \mathbb{R}^m defined as follows:

$$\begin{aligned} \psi(\gamma; W_n, \tilde{W}_n, A_n) &= \mathbb{1} \left[\gamma \in \mathbb{R}^m(W_n, \tilde{W}_n, A_n) \right], \\ \mathbb{R}^m(W_n, \tilde{W}_n, A_n) &= \left\{ \gamma \in \mathbb{R} : (\gamma + W_n)^2 \leq (\gamma A_n + \tilde{W}_n)^2 \right\} \\ &= \left\{ \gamma \in \mathbb{R} : \gamma^2(1 - A_n^2) + 2\gamma(W_n - A_n \tilde{W}_n) + W_n^2 - \tilde{W}_n^2 \leq 0 \right\}. \end{aligned}$$

Let us now define

$$\begin{aligned} \hat{p}_n^{\text{int}}(\delta) &= \mathbb{E} \left[\psi(\tau - \delta; W_n, \tilde{W}_n, A_n) \mathbb{1} [|A_n| < 1] \mid \mathcal{F}_n \right], \\ \hat{\mathcal{S}}_n^{\text{int}}(\alpha) &= \{ \delta : \hat{p}_n^{\text{int}}(\delta) \geq \alpha \}. \end{aligned}$$

The set $\hat{\mathcal{S}}_n^{\text{int}}(\alpha)$ is convex because $\hat{p}_n^{\text{int}}(\delta)$ is a concave function of δ . To prove the last statement, it suffices to note that, for any $\omega > 0$ and $\delta_1, \delta_2 \in \mathbb{R}$,

$$\begin{aligned} \hat{p}_n^{\text{int}}(\omega\delta_1 + (1 - \omega)\delta_2) &= \mathbb{E} \left[\psi \left(\omega\gamma_1 + (1 - \omega)\gamma_2; W_n, \tilde{W}_n, A_n \right) \mathbb{1} [|A_n| < 1] \mid \mathcal{F}_n \right] \\ &\geq \mathbb{E} \left[\left[\omega\psi(\gamma_1; W_n, \tilde{W}_n, A_n) + (1 - \omega)\psi(\gamma_2; W_n, \tilde{W}_n, A_n) \right] \mathbb{1} [|A_n| < 1] \mid \mathcal{F}_n \right] \\ &= \omega \cdot \hat{p}_n^{\text{int}}(\delta_1) + (1 - \omega) \cdot \hat{p}_n^{\text{int}}(\delta_2), \end{aligned}$$

where $\gamma_1 = \tau - \delta_1$ and $\gamma_2 = \tau - \delta_2$. Above, the inequality simply follows from the fact that ψ is almost surely concave if $|A_n| < 1$. Therefore, the only thing that remains to be shown is that $\hat{\mathcal{S}}_n(\alpha)$ and $\hat{\mathcal{S}}_n^{\text{int}}(\alpha)$ are not too different from each other. The following lemma (proved below) helps us achieve this.

Lemma A4. *Under the assumptions of Theorem A2, there exist a constant $c > 0$ such that*

$$\mathbb{P}[|A_n| \geq 1] \leq 12 \exp \left\{ -\frac{n(\rho^4 \wedge \rho^8)}{c} \right\}.$$

Combining Lemma A4 with Markov's inequality gives us that, for any $\delta \in \mathbb{R}$ and $\epsilon > 0$,

$$\mathbb{P} \left[|\hat{p}_n(\delta) - \hat{p}_n^{\text{int}}(\delta)| \geq \frac{\epsilon}{2n} \right] \leq \frac{n}{2\epsilon} \mathbb{E} [|\hat{p}_n(\delta) - \hat{p}_n^{\text{int}}(\delta)|] \leq \frac{n}{2\epsilon} \mathbb{P}[|A_n| \geq 1] \leq \frac{n}{\epsilon} 24 \exp \left\{ -\frac{n(\rho^4 \wedge \rho^8)}{c} \right\}.$$

At this point the proof is almost complete. Note that, for any $\delta \notin \hat{\mathcal{S}}_n(\alpha)$, we have $\hat{p}_n(\delta) \leq \alpha$. Therefore, with high probability $\hat{p}_n^{\text{int}}(\delta) \leq \alpha + \epsilon/(2n)$, and hence $\delta \notin \hat{\mathcal{S}}_n^{\text{int}}(\alpha + \epsilon/(2n))$, which proves $\hat{\mathcal{S}}_n^{\text{int}}(\alpha + \epsilon/(2n)) \subseteq \hat{\mathcal{S}}_n(\alpha)$. The same argument also allows one to show that $\hat{\mathcal{S}}_n(\alpha + \epsilon/n) \subseteq \hat{\mathcal{S}}_n^{\text{int}}(\alpha - \epsilon/(2n))$. This completes the proof, as the inequalities on the other side are analogous. \square

Proof of Lemma A4. As $|A_n| = |\Sigma_n|/\tilde{S}_n$, we proceed by upper bounding the numerator and lower bounding the denominator. Define $\sigma^2 = \text{Var}[X]$ and $\xi = \sigma^2 - \rho^2 = \text{Var}[\mathbb{E}[X|Z]]$. Then, the following two lemmas will be useful.

Lemma A5. *Under the assumptions of Theorem A2, there exist a constant $c > 0$ such that, for any $\delta > 0$,*

$$\mathbb{P}[|\Sigma_n - \xi| \geq \delta] \leq 2 \exp \left\{ -\frac{2n\delta^4}{c^4} \right\} + 4 \exp \left\{ -\frac{2n\delta^2}{c^2} \right\}.$$

Lemma A6. *Under the assumptions of Theorem A2, if X is a.s. bounded within a finite interval of width $c > 0$, then for any $\delta > 0$,*

$$\mathbb{P} \left[\tilde{S}_n \leq \sigma^2 - (\delta + c\sqrt{\delta}) \right] \leq 3 \exp \left\{ -\frac{2n\delta}{c^2} \right\}.$$

Armed with Lemmas A5 and A6, we proceed as follows:

$$\begin{aligned} \mathbb{P}[|A_n| \geq 1] &= \mathbb{P}[|\Sigma_n| \geq \tilde{S}_n] \\ &\leq \mathbb{P}[|\Sigma_n| \geq \tilde{S}_n, \tilde{S}_n > \sigma^2 - (\delta + c\sqrt{\delta})] + \mathbb{P}[\tilde{S}_n \leq \sigma^2 - (\delta + c\sqrt{\delta})] \\ &\leq \mathbb{P}[|\Sigma_n| \geq \sigma^2 - (\delta + c\sqrt{\delta})] + \mathbb{P}[\tilde{S}_n \leq \sigma^2 - (\delta + c\sqrt{\delta})] \\ &= \mathbb{P}[|\Sigma_n| \geq \xi + \sigma^2 - \xi - (\delta + c\sqrt{\delta})] + \mathbb{P}[\tilde{S}_n \leq \sigma^2 - (\delta + c\sqrt{\delta})] \\ &= \mathbb{P}[|\Sigma_n| \geq \xi + \rho^2 - (\delta + c\sqrt{\delta})] + \mathbb{P}[\tilde{S}_n \leq \sigma^2 - (\delta + c\sqrt{\delta})] \\ &\leq \mathbb{P}[|\Sigma_n - \xi| + \xi \geq \xi + \rho^2 - (\delta + c\sqrt{\delta})] + \mathbb{P}[\tilde{S}_n \leq \sigma^2 - (\delta + c\sqrt{\delta})] \\ &= \mathbb{P}[|\Sigma_n - \xi| \geq \rho^2 - (\delta + c\sqrt{\delta})] + \mathbb{P}[\tilde{S}_n \leq \sigma^2 - (\delta + c\sqrt{\delta})]. \end{aligned}$$

Choosing the value of δ such that $\delta + c\sqrt{\delta} = \rho^2/2$ leads to

$$\mathbb{P}[|A_n| \geq 1] \leq 2 \exp \left\{ -\frac{2n[\rho^2/2]^4}{c^4} \right\} + 4 \exp \left\{ -\frac{2n[\rho^2/2]^2}{c^2} \right\} + 3 \exp \left\{ -\frac{2n\delta}{c^2} \right\}.$$

Furthermore, as long as the constant c is sufficiently large,

$$\begin{aligned}\mathbb{P}[|A_n| \geq 1] &\leq 6 \exp \left\{ -\frac{2n[\rho^2/2]^4}{c^4} \right\} + 3 \exp \left\{ -\frac{2n\delta}{c^2} \right\} \\ &\leq 6 \exp \left\{ -\frac{n\rho^8}{8c^4} \right\} + 6 \exp \left\{ -\frac{n\rho^4}{8c^4} \right\} \\ &\leq 12 \exp \left\{ -\frac{n(\rho^4 \wedge \rho^8)}{8c^4} \right\}.\end{aligned}$$

□

Proof of Lemma A5. Recall that Σ_n is defined as

$$\Sigma_n = \frac{1}{n} \sum_i (\tilde{X}^{(i)} - \bar{\tilde{X}})(X'^{(i)} - \bar{X}').$$

Therefore, if we define $\mu = \mathbb{E}[X]$ and

$$\begin{aligned}\Sigma'_n &= \frac{1}{n} \sum_i (\tilde{X}^{(i)} - \mu)(X'^{(i)} - \mu) \\ \Omega_n &= \left(\mu - \frac{1}{n} \sum_{i=1}^n X^{(i)} \right) \left(\mu - \frac{1}{n} \sum_{i=1}^n \tilde{X}^{(i)} \right),\end{aligned}$$

we can write

$$\Sigma_n = \Sigma'_n - \Omega_n.$$

This allows us to bound Σ_n by bounding Σ'_n and Ω_n separately, which is easier to do. For any $\delta > 0$,

$$\begin{aligned}\mathbb{P}[|\Sigma_n - \xi| \geq 2\delta^2] &= \mathbb{P}[|\Sigma'_n + \Omega_n - \xi| \geq 2\delta^2] \\ &\leq \mathbb{P}[|\Sigma'_n - \xi| + |\Omega_n| \geq 2\delta^2] \\ &\leq \mathbb{P}[|\Sigma'_n - \xi| + |\Omega_n| \geq 2\delta^2, |\Omega_n| < 2\delta^2] + \mathbb{P}[|\Omega_n| \geq \delta^2] \\ &\leq \mathbb{P}[|\Sigma'_n - \xi| \geq \delta^2] + \mathbb{P}[|\Omega_n| \geq \delta^2].\end{aligned}$$

To bound the first term above, note that Σ'_n is the sample average of n bounded and independent random variables $X^{(i)} = (\tilde{X}^{(i)} - \mu)(X'^{(i)} - \mu)$ with expected values equal to

$$\mathbb{E}[X^{(i)}] = \mathbb{E}[\mathbb{E}[X^{(i)} | \mathcal{F}_n]] = \mathbb{E}[(\mathbb{E}[X_j | Z] - \mu)^2] = \text{Var}[\mathbb{E}[X | Z]] = \xi.$$

Therefore, we can apply Hoeffding's inequality:

$$\mathbb{P}[|\Sigma'_n - \xi| \geq \delta^2] \leq 2 \exp \left\{ -\frac{2n\delta^4}{c^4} \right\}.$$

To bound the second term above, note that

$$\begin{aligned}\mathbb{P}[|\Omega_n| \geq t^2] &= \mathbb{P}\left[\left| \mu - \frac{1}{n} \sum_{i=1}^n X^{(i)} \right| \cdot \left| \mu - \frac{1}{n} \sum_{i=1}^n \tilde{X}^{(i)} \right| \geq \delta^2 \right] \\ &\leq 2 \cdot \mathbb{P}\left[\left| \mu - \frac{1}{n} \sum_{i=1}^n X^{(i)} \right| \geq \delta \right] \\ &\leq 4 \exp \left\{ -\frac{2n\delta^2}{c^2} \right\},\end{aligned}$$

where the second step above follows again from Hoeffding's inequality. Hence, we can conclude that

$$\mathbb{P} [|\Sigma_n - \xi| \geq 2\delta^2] \leq 2 \exp \left\{ -\frac{2n\delta^4}{c^4} \right\} + 4 \exp \left\{ -\frac{2n\delta^2}{c^2} \right\}.$$

□

Proof of Lemma A6. To simplify the notation, we prove the analogous bound in which S_n is replaced by

$$S_n = \frac{1}{n} \sum_{i=1}^n (X'^{(i)} - \bar{X}')^2.$$

In fact, S_n and \tilde{S}_n are identically distributed. After defining $\mu = \mathbb{E}[X]$, as before, one can rewrite S_n as

$$\begin{aligned} S_n &= \frac{1}{n} \sum_{i=1}^n (X'^{(i)} - \bar{X}')^2 = \frac{1}{n} \sum_{i=1}^n (X'^{(i)} - \mu + \mu - \bar{X}')^2 \\ &= \frac{1}{n} \sum_{i=1}^n (X'^{(i)} - \mu)^2 - (\mu - \bar{X}')^2. \end{aligned}$$

Following the same strategy as before, observe that, for any $t > 0$ and $0 < \delta < t$,

$$\begin{aligned} \mathbb{P}[S_n \leq \sigma^2 - t] &= \mathbb{P} \left[\frac{1}{n} \sum_{i=1}^n (X'^{(i)} - \mu)^2 - (\mu - \bar{X}')^2 \leq \sigma^2 - t \right] \\ &\leq \mathbb{P} \left[\frac{1}{n} \sum_{i=1}^n (X'^{(i)} - \mu)^2 \leq \sigma^2 - t + \delta \right] + \mathbb{P} [(\mu - \bar{X}')^2 > \delta]. \end{aligned}$$

To bound the first term above, remember that $\sigma^2 = \mathbb{E}[(X'^{(i)} - \mu)^2]$ and apply Hoeffding's inequality:

$$\mathbb{P} \left[\frac{1}{n} \sum_{i=1}^n (X'^{(i)} - \mu)^2 \leq \sigma^2 - (t - \delta) \right] \leq \exp \left\{ -\frac{2n(t - \delta)^2}{c^4} \right\}.$$

To bound the second term above, we can also use Hoeffding's inequality:

$$\mathbb{P} [(\mu - \bar{X}')^2 > \delta] = \mathbb{P} [|\mu - \bar{X}'| > \sqrt{\delta}] \leq 2 \exp \left\{ -\frac{2n\delta}{c^2} \right\},$$

Therefore, if we choose $t = \delta + c\sqrt{\delta}$, we obtain

$$\mathbb{P} [S_n \leq \sigma^2 - (\delta + c\sqrt{\delta})] \leq \exp \left\{ -\frac{2n(t - \delta)^2}{c^4} \right\} + 2 \exp \left\{ -\frac{2n\delta}{c^2} \right\} = 3 \exp \left\{ -\frac{2n\delta}{c^2} \right\}.$$

□

Proof of Theorem A3. Let us fix any $\delta \neq \tau$ and define $\gamma = \tau - \delta$. By Markov's inequality,

$$\mathbb{P} [\delta \in \hat{\mathcal{S}}_n(\alpha)] = \mathbb{P} [\hat{p}_n(\delta) > \alpha] \leq \frac{1}{\alpha} \mathbb{E} [\hat{p}_n(\delta)].$$

Furthermore, for any $\epsilon > 0$,

$$\begin{aligned} \mathbb{E} [\hat{p}_n(\delta)] &= \mathbb{E} [\psi(\gamma; W_n, \tilde{W}_n, A_n)] \\ &\leq \mathbb{E} [\psi(\gamma; W_n, \tilde{W}_n, A_n) \mathbb{1} [|W_n| < \epsilon, |\tilde{W}_n| < \epsilon, |A_n| < 1]] + \\ &\quad + \mathbb{P} [|W_n| \geq \epsilon] + \mathbb{P} [|\tilde{W}_n| \geq \epsilon] + \mathbb{P} [|A_n| \geq 1] \\ &= \mathbb{E} [\psi(\gamma; W_n, \tilde{W}_n, A_n) \mathbb{1} [|W_n| < \epsilon, |\tilde{W}_n| < \epsilon, |A_n| < 1]] + 2\mathbb{P} [|W_n| \geq \epsilon] + \mathbb{P} [|A_n| \geq 1], \end{aligned}$$

where the function ψ is defined as in the proof of Theorem A2. Our strategy is to separately bound each of the above terms, noting that Lemma A4 already takes care of the last one. Let us then look at the first term.

$$\begin{aligned}
& \mathbb{E} \left[\psi(\gamma; W_n, \tilde{W}_n, A_n) \mathbb{1} \left[|W_n| < \epsilon, |\tilde{W}_n| < \epsilon, |A_n| < 1 \right] \right] \\
&= \mathbb{E} \left[\mathbb{1} \left[\gamma^2(1 - A_n^2) + 2\gamma(W_n - A_n \tilde{W}_n) + W_n^2 - \tilde{W}_n^2 \leq 0 \right] \mathbb{1} \left[|W_n| < \epsilon, |\tilde{W}_n| < \epsilon, |A_n| < 1 \right] \right] \\
&\leq \mathbb{E} \left[\mathbb{1} \left[\gamma^2(1 - A_n^2) - 4|\gamma|\epsilon - 2\epsilon^2 \leq 0 \right] \mathbb{1} \left[|W_n| < \epsilon, |\tilde{W}_n| < \epsilon, |A_n| < 1 \right] \right] \\
&= \mathbb{E} \left[\mathbb{1} \left[A_n^2 \geq 1 - \frac{4|\gamma|\epsilon + 2\epsilon^2}{\gamma^2} \right] \mathbb{1} \left[|W_n| < \epsilon, |\tilde{W}_n| < \epsilon, |A_n| < 1 \right] \right] \\
&\leq \mathbb{P} \left[A_n^2 \geq 1 - \frac{4|\gamma|\epsilon + 2\epsilon^2}{\gamma^2} \right] \\
&\leq \mathbb{P} \left[A_n^2 \geq 1 - 2\frac{\epsilon^2}{\gamma^2} \right] \\
&= \mathbb{P} \left[|A_n| \geq \sqrt{1 - 2\frac{\epsilon^2}{\gamma^2}} \right] \\
&\leq \mathbb{P} \left[|A_n| \geq 1 - \frac{\epsilon^2}{\gamma^2} \right].
\end{aligned}$$

Lemma A7. *Let ϵ_n be a fixed sequence converging to 0 as $n \rightarrow \infty$. Under the assumptions of Theorem A3, there exist a constant $\tilde{c} > 0$ such that*

$$\mathbb{P} \left[|A_n| \geq 1 - \epsilon_n \frac{\rho^2}{\sigma^2} \right] \leq 6 \exp \left\{ -\frac{2n}{\tilde{c}} [(\rho^8 \vee \rho^4) - 8\epsilon_n] \right\} + 3 \exp \left\{ -\frac{n}{2\tilde{c}} \rho^4 \epsilon_n^2 \right\},$$

for any sufficiently large n .

Applying Lemma A7 to the inequality above leads to:

$$\begin{aligned}
\mathbb{E} [\hat{p}_n(\delta)] &\leq \mathbb{E} \left[\psi(\gamma; W_n, \tilde{W}_n, A_n) \mathbb{1} \left[|W_n| < \epsilon, |\tilde{W}_n| < \epsilon, |A_n| < 1 \right] \right] + 2\mathbb{P} [|W_n| \geq \epsilon] + \mathbb{P} [|A_n| \geq 1] \\
&\leq 2\mathbb{P} \left[|A_n| \geq 1 - \frac{\epsilon^2}{\gamma^2} \right] + 2\mathbb{P} [|W_n| \geq \epsilon] \\
&\leq 12 \exp \left\{ -\frac{2n}{\tilde{c}} \left[(\rho^8 \vee \rho^4) - 8\frac{\epsilon^2 \sigma^2}{\gamma^2 \rho^2} \right] \right\} + 6 \exp \left\{ -\frac{n}{2\tilde{c}} \rho^4 \frac{\epsilon^4}{\gamma^4} \frac{\sigma^4}{\rho^4} \right\} + 2\mathbb{P} [|W_n| \geq \epsilon] \\
&\leq 12 \exp \left\{ -\frac{2n}{\tilde{c}} \left[(\rho^8 \vee \rho^4) - 8\frac{\epsilon^2 \sigma^2}{\gamma^2 \rho^2} \right] \right\} + 6 \exp \left\{ -\frac{n}{2\tilde{c}} \frac{\epsilon^4}{\gamma^4} \rho^4 \right\} + 2\mathbb{P} [|W_n| \geq \epsilon],
\end{aligned}$$

as long as n is large enough and $\epsilon^2/\gamma^2 = o_n(1)$. Next, we need to bound $|W_n|$.

Lemma A8. *Under the assumptions of Theorem A3, if X is a.s. bounded within a finite interval of width $c > 0$ and Y, \hat{g} are a.s. bounded within an interval of width $d > 0$, then*

$$\mathbb{P} [|W_n| \geq \epsilon] \leq 7 \exp \left\{ -\frac{n\epsilon^2\sigma^2}{4c^2d^2} \right\}.$$

for any sufficiently large n , if $\epsilon = o_n(1)$.

It follows from Lemma A8 that

$$\begin{aligned}
\mathbb{E} [\hat{p}_n(\delta)] &\leq 12 \exp \left\{ -\frac{2n}{\tilde{c}} \left[(\rho^8 \vee \rho^4) - 8\frac{\epsilon^2 \sigma^2}{\gamma^2 \rho^2} \right] \right\} + 6 \exp \left\{ -\frac{n}{2\tilde{c}} \frac{\epsilon^4}{\gamma^4} \rho^4 \right\} + 14 \exp \left\{ -\frac{n\epsilon^2\sigma^2}{4c^2d^2} \right\} \\
&\leq 12 \exp \left\{ -\frac{2n}{\tilde{c}} \left[(\rho^8 \vee \rho^4) - 8\frac{\epsilon^2 \sigma^2}{\gamma^2 \rho^2} \right] \right\} + 6 \exp \left\{ -\frac{n}{2\tilde{c}} \frac{\epsilon^4}{\gamma^4} \rho^4 \right\} + 14 \exp \left\{ -\frac{n\epsilon^2\rho^2}{4c^2d^2} \right\},
\end{aligned}$$

for any sufficiently large n , if $\epsilon = o_n(1)$. Now, set $\epsilon = \gamma/(\log n)$, so that the inequality above becomes

$$\begin{aligned}\mathbb{E}[\hat{p}_n(\delta)] &\leq 12 \exp\left\{-\frac{2n}{\tilde{c}}\left[(\rho^8 \vee \rho^4) - \frac{8}{(\log n)^2} \frac{\sigma^2}{\rho^2}\right]\right\} + 6 \exp\left\{-\frac{n}{2\tilde{c}(\log n)^4} \rho^4\right\} + 14 \exp\left\{-\frac{n\gamma^2\rho^2}{4c^2d^2(\log n)^2}\right\} \\ &\leq 12 \exp\left\{-\frac{2n}{\tilde{c}}\left[(\rho^8 \vee \rho^4) - \frac{8}{(\log n)^2} \frac{\sigma^2}{\rho^2}\right]\right\} + 6 \exp\left\{-\frac{n}{2\tilde{c}(\log n)^4} \rho^4\right\} + 14 \exp\left\{-\frac{\rho^2 \log n}{4c^2d^2}\right\},\end{aligned}$$

where the second inequality above follows from the assumption that $\gamma = |\tau - \delta| \geq n^{-1/2} (\log n)^{3/2}$.

□

Proof of Lemma A7. Fix any $t^2 > 0$ and $\delta > 0$. Then,

$$\begin{aligned}\mathbb{P}[|A_n| \geq 1 - t^2] &= \mathbb{P}[|\Sigma_n| \geq (1 - t^2) S_n] \\ &\leq \mathbb{P}[|\Sigma_n| \geq (1 - t^2)(\sigma^2 - \delta)] + \mathbb{P}[S_n \leq \sigma^2 - \delta] \\ &\leq \mathbb{P}[|\Sigma_n| \geq \sigma^2 - t^2\sigma^2 - \delta] + \mathbb{P}[S_n \leq \sigma^2 - \delta] \\ &= \mathbb{P}[|\Sigma_n| \geq \xi + \rho^2 - (t^2\sigma^2 + \delta)] + \mathbb{P}[S_n \leq \sigma^2 - \delta] \\ &\leq \mathbb{P}[|\Sigma_n - \xi| \geq \rho^2 - (t^2\sigma^2 + \delta)] + \mathbb{P}[S_n \leq \sigma^2 - \delta].\end{aligned}$$

Setting $\delta = \sigma^2 t^2$ then gives:

$$\mathbb{P}[|A_n| \geq 1 - t^2] \leq \mathbb{P}[|\Sigma_n - \xi| \geq \rho^2 - 2\sigma^2 t^2] + \mathbb{P}[S_n \leq \sigma^2(1 - t^2)].$$

Assuming $\rho^2 > 2\sigma^2 t^2$, we can apply Lemmas A5 and A6 and obtain that there exist a constant \tilde{c} such that

$$\begin{aligned}\mathbb{P}[|A_n| \geq 1 - t^2] &\leq 2 \exp\left\{-\frac{2n}{\tilde{c}^4}(\rho^2 - 2\sigma^2 t^2)^4\right\} + 4 \exp\left\{-\frac{2n}{\tilde{c}^2}(\rho^2 - 2\sigma^2 t^2)^2\right\} + \\ &\quad + \exp\left\{-\frac{2n}{\tilde{c}^4} \frac{\sigma^4 t^4}{4}\right\} + 2 \exp\left\{-\frac{2n}{\tilde{c}^2} \frac{\sigma^2 t^2}{2}\right\} \\ &\leq 2 \exp\left\{-\frac{2n}{\tilde{c}^4} \left[\rho^8 - \frac{8}{\rho^2} t^2 \sigma^2\right]\right\} + 4 \exp\left\{-\frac{2n}{\tilde{c}^2} \left[\rho^4 - \frac{4}{\rho^2} t^2 \sigma^2\right]\right\} + \\ &\quad + \exp\left\{-\frac{n}{2\tilde{c}^4} (t^2 \sigma^2)^2\right\} + 2 \exp\left\{-\frac{n}{\tilde{c}^2} t^2 \sigma^2\right\} \\ &\leq 6 \exp\left\{-\frac{2n}{\tilde{c}^4} \left[(\rho^8 \vee \rho^4) - \frac{8}{\rho^2} t^2 \sigma^2\right]\right\} + \exp\left\{-\frac{n}{2\tilde{c}^4} (t^2 \sigma^2)^2\right\} + 2 \exp\left\{-\frac{n}{\tilde{c}^2} t^2 \sigma^2\right\}.\end{aligned}$$

As long as $t^2 < 2/\sigma^2$, it follows that

$$\mathbb{P}[|A_n| \geq 1 - t^2] \leq 6 \exp\left\{-\frac{2n}{\tilde{c}^4} \left[(\rho^8 \vee \rho^4) - \frac{8}{\rho^2} t^2 \sigma^2\right]\right\} + 3 \exp\left\{-\frac{n}{2\tilde{c}^4} (t^2 \sigma^2)^2\right\}.$$

To simplify the expression on the right-hand-side above, we can fix $\epsilon > 0$ and set $t^2 = \epsilon \rho^2 / \sigma^2$. Then,

$$\mathbb{P}[|A_n| \geq 1 - \epsilon \frac{\rho^2}{\sigma^2}] \leq 6 \exp\left\{-\frac{2n}{\tilde{c}^4} [(\rho^8 \vee \rho^4) - 8\epsilon]\right\} + 3 \exp\left\{-\frac{n}{2\tilde{c}^4} \rho^4 \epsilon^2\right\}.$$

□

Proof of Lemma A8. Recall that W_n is defined as

$$W_n = \frac{1}{\sum_i (X^{(i)} - \bar{X})^2} \sum_i (X^{(i)} - \bar{X}) \left(g(Z^{(i)}, C^{(i)}) - \hat{g}(Z^{(i)}) \right) = \frac{W'_n}{S_n},$$

where

$$W'_n = \frac{1}{n} \sum_i (X^{(i)} - \bar{X}) \left(g(Z^{(i)}, C^{(i)}) - \hat{g}(Z^{(i)}) \right).$$

Therefore, we will proceed with the usual strategy. For any $\epsilon > 0$ and $\delta > 0$,

$$\begin{aligned} \mathbb{P}[|W_n| \geq \epsilon] &= \mathbb{P}[|W'_n| \geq \epsilon(S_n - \sigma^2 + \sigma^2)] \\ &= \mathbb{P}[|W'_n| \geq \epsilon\sigma^2 + \epsilon(S_n - \sigma^2 + \delta) - \delta\epsilon] \\ &= \mathbb{P}[|W'_n| \geq \epsilon\sigma^2 + \epsilon(S_n - \sigma^2 - \delta) - \delta\epsilon, S_n - \sigma^2 - \delta > 0] + \mathbb{P}[S_n - \sigma - \delta \leq 0] \\ &\leq \mathbb{P}[|W'_n| \geq \epsilon(\sigma^2 - \delta)] + \mathbb{P}[S_n - \sigma - \delta \leq 0] \\ &\leq \mathbb{P}[|W'_n| \geq \epsilon(\sigma^2 - \delta - c\sqrt{\delta})] + 3 \exp\left\{-\frac{2n\delta}{c^2}\right\}, \end{aligned}$$

where the last inequality above follows from Lemma A6. Now we need to bound $|W'_n|$.

$$\begin{aligned} W'_n &= \frac{1}{n} \sum_i (X^{(i)} - \mu) \left(g(Z^{(i)}, C^{(i)}) - \hat{g}(Z^{(i)}) \right) + \frac{1}{n} \sum_i (\mu - \bar{X}) \left(g(Z^{(i)}, C^{(i)}) - \hat{g}(Z^{(i)}) \right) \\ &= \frac{1}{n} \sum_i (X^{(i)} - \mu) \left(g(Z^{(i)}, C^{(i)}) - \hat{g}(Z^{(i)}) \right) + (\mu - \bar{X}) \frac{1}{n} \sum_i \left(g(Z^{(i)}, C^{(i)}) - \hat{g}(Z^{(i)}) \right) \\ &= W''_n + (\mu - \bar{X}) \frac{1}{n} \sum_i \left(g(Z^{(i)}, C^{(i)}) - \hat{g}(Z^{(i)}) \right), \end{aligned}$$

where W''_n is defined as:

$$W''_n = \frac{1}{n} \sum_i (X^{(i)} - \mu) \left(g(Z^{(i)}, C^{(i)}) - \hat{g}(Z^{(i)}) \right).$$

At this point we need to use the assumption that Y and \hat{g} are bounded within an interval of width $d > 0$. Then, we can apply Hoeffding's inequality.

$$\begin{aligned} \mathbb{P}[|W'_n| \geq \epsilon] &\leq \mathbb{P}[|W''_n| + |\mu - \bar{X}|d \geq \epsilon] \\ &\leq \mathbb{P}[|W''_n| \geq \epsilon/2] + \mathbb{P}[|\mu - \bar{X}| \geq \epsilon/(2d)] \\ &\leq 2 \exp\left\{-\frac{2n(\epsilon/2)^2}{c^2 d^2}\right\} + 2 \exp\left\{-\frac{2n(\epsilon/2d)^2}{c^2}\right\} \\ &\leq 4 \exp\left\{-\frac{n\epsilon^2}{2c^2 d^2}\right\}. \end{aligned}$$

Therefore,

$$\begin{aligned} \mathbb{P}[|W_n| \geq \epsilon] &\leq 4 \exp\left\{-\frac{n\epsilon^2(\sigma^2 - \delta - c\sqrt{\delta})^2}{2c^2 d^2}\right\} + 3 \exp\left\{-\frac{2n\delta}{c^2}\right\} \\ &\leq 4 \exp\left\{-\frac{n\epsilon^2\sigma^2[\sigma^2 - 2(\delta + c\sqrt{\delta})]}{2c^2 d^2}\right\} + 3 \exp\left\{-\frac{2n\delta}{c^2}\right\} \\ &\leq 4 \exp\left\{-\frac{n\epsilon^2\sigma^4}{2c^2 d^2} + \frac{2n\epsilon^2 2(\delta + c\sqrt{\delta})}{2c^2 d^2}\right\} + 3 \exp\left\{-\frac{2n\delta}{c^2} + \frac{2n\epsilon^2 2(\delta + c\sqrt{\delta})}{2c^2 d^2}\right\} \end{aligned}$$

If we choose $\delta = \epsilon^2 \sigma^4 / (4d^2)$, we get

$$\begin{aligned}\mathbb{P}[|W_n| \geq \epsilon] &\leq 7 \exp \left\{ -\frac{2n\delta}{c^2} + \frac{2n\epsilon^2 2(\delta + c\sqrt{\delta})}{2c^2 d^2} \right\} \\ &\leq 7 \exp \left\{ -\frac{2n\epsilon^2 \sigma^4 / (4d^2)}{c^2} + \frac{2n\epsilon^2 2(\epsilon^2 \sigma^4 / (4d^2) + c(\epsilon \sigma^2 / (2d)))}{2c^2 d^2} \right\} \\ &\leq 7 \exp \left\{ -\frac{n\epsilon^2 \sigma^2}{2c^2 d^2} [1 - O(\epsilon)] \right\}.\end{aligned}$$

Therefore, as long as ϵ is small enough,

$$\mathbb{P}[|W_n| \geq \epsilon] \leq 7 \exp \left\{ -\frac{n\epsilon^2 \sigma^2}{4c^2 d^2} \right\}.$$

□